

*TUD-IKTP/97-03*  
*Herbstschule Maria Laach*  
*Sep. 1997*  
*revised 30.09.97*

# **Lectures on Flavour Oscillation and CP Asymmetry in $B$ Meson Decays**

*Roland Waldi*

*Institut für Kern- und Teilchenphysik*  
*Technische Universität Dresden*

---

**Contents**

1	<b>Introduction</b>	1
2	<b>Particle Anti-Particle Oscillations and CP Violation</b>	2
2.1	The Unitary CKM Matrix	2
2.1.1	Unitarity Triangles	4
2.1.2	Phases and Observables	7
2.2	Oscillation Phenomenology	9
2.2.1	Mechanical Analogon	13
2.2.2	Standard Model Predictions	13
2.2.3	Behaviour of the Four Neutral Meson Anti-Meson Systems	15
2.2.4	CP Eigenstates Versus Mass Eigenstates	20
2.2.5	Oscillation at the $\Upsilon(4S)$	23
2.2.6	Determination of the Mixing Parameters of $B$ Mesons	25
2.2.7	Predictions for $x_s$ , $y_s$ and $\delta_s$	27
2.3	CP Violation	28
2.3.1	CP Violation in $B$ Decays	29
2.3.2	CP Violation in Common Final States of $B^0$ and $\bar{B}^0$	31
2.3.2.1	The $B_s/\bar{B}_s$ Case	33
2.3.2.2	Final CP Eigenstates from $B^0$ or $B_s$ Decays	34
2.3.2.3	Mixtures of CP Eigenstates	37
2.3.2.4	Non-Eigenstates	38
2.3.2.5	The Total Decay Rate	39
2.3.2.6	CP Violation at the $\Upsilon(4S)$	40
2.3.3	CP Violation in $K$ Decays	43
3	<b>Measurement of CP Violation at <math>B</math> Meson Factories</b>	47
3.0.4	$B$ Production Cross Sections	49
3.0.5	$B$ Meson Fractions	50
3.1	Flavour Tagging	53
3.1.1	Observed Versus True Asymmetry	54
3.1.2	Statistical Tagging	57
3.2	Estimating the Performance	61
	<b>Acknowledgements</b>	62
	<b>References</b>	63

# 1. Introduction

Our understanding of physics in general and particle physics in particular has been mainly put forward by the discovery of **symmetries**. It is remarkable, that most of the symmetries discovered have, however, finally turned out to be only “almost-symmetries”, i. e. to be more or less broken.

The only unbroken symmetries so far discovered are the U(1) charge-phase symmetry and the SU(3) colour symmetry. The consequences are, that the electric and colour charges are exactly conserved in all observed reactions, and that the position in SU(3)-space cannot be determined, e. g. a “red” and a “blue” quark cannot be distinguished.

Each of the symmetries between leptons and quarks of different flavour is broken by the different masses and electro-weak charges of these particles, and is best approximated in strong interactions as isospin symmetry between the  $u$  and  $d$  quark due to their almost identical constituent mass.

Although physics laws are strictly symmetric under translation or rotation, space-time translational and rotational symmetry is broken through the solutions: The fact that matter is not distributed homogeneously throughout the universe introduces a locally asymmetric structure of space-time, or asymmetric boundary conditions to any microscopic system. The spatial symmetries are best approximated on a macroscopic scale—the universe—or for microscopic systems isolated from other matter by large distances.

Mirror symmetry (parity P) is broken in a more fundamental sense by weak interaction, which makes a maximal distinction between fermions of left and right chirality. First ideas of this unexpected behaviour emerged as a solution of the “ $\Theta$   $\tau$  puzzle”, the fact that the neutral kaon decays both to  $P = +1$  and  $P = -1$  eigenstates [1], and a direct observation as left-right-asymmetry in weak beta decays followed soon [2]. It is most pronounced in the massless neutrinos, which are produced in weak interactions only with lefthanded helicity, or righthanded in the case of anti-neutrinos, thus violating the charge-conjugation symmetry (C) at the same time.

The product of both discrete symmetries, CP, is almost intact, and seems to be conserved even in weak interaction processes. A small violation has first been observed in 1964 [3] in  $K^0$  decays, which are up to now the only system which does not respect CP symmetry completely. The explanation of this violation in the Standard Model will be briefly discussed in the next chapter. This is not the only possible description, but the one with no additional assumptions. At the same time, the Standard Model predicts CP violating effects in the decay of beauty mesons ( $B^0$ ,  $B_s$ ,  $B^+$ ), which should be even large in some rare decay channels.

## 2. Particle Anti-Particle Oscillations and CP Violation

Mesons are neither particles nor anti-particles in a strict sense, since they are composed of a quark and an anti-quark. This implies the existence of mesons with vacuum quantum numbers (e.g.  $f_0$ ). More important is the existence of pairs of charge-conjugate mesons, which can be transformed into each other via flavour changing weak interaction transitions. These are  $K^0/\bar{K}^0$  ( $\bar{s}d/s\bar{d}$ ),  $D^0/\bar{D}^0$  ( $c\bar{u}/\bar{c}u$ ),  $B^0/\bar{B}^0$  ( $\bar{b}d/b\bar{d}$ ), and  $B_s/\bar{B}_s$  ( $\bar{b}s/b\bar{s}$ ).

### 2.1 The Unitary CKM Matrix

The charged current weak interactions responsible for flavour changes are described by the couplings of the  $W$  boson to the current

$$J_\mu^{cc} = \begin{pmatrix} \bar{\nu}_e \\ \bar{\nu}_\mu \\ \bar{\nu}_\tau \end{pmatrix} \gamma_\mu \frac{1-\gamma_5}{2} \begin{pmatrix} e \\ \mu \\ \tau \end{pmatrix} + \sum_{r,g,b} \begin{pmatrix} \bar{u} \\ \bar{c} \\ \bar{t} \end{pmatrix} \gamma_\mu \frac{1-\gamma_5}{2} \mathbf{V} \cdot \begin{pmatrix} d \\ s \\ b \end{pmatrix} \quad (2.1)$$

with a non-trivial transformation matrix  $\mathbf{V}$  in the quark sector, the Cabibbo–Kobayashi–Maskawa (CKM) Matrix [4,5]:

$$\mathbf{V} = \begin{pmatrix} V_{ud} & V_{us} & V_{ub} \\ V_{cd} & V_{cs} & V_{cb} \\ V_{td} & V_{ts} & V_{tb} \end{pmatrix}$$

The quark flavours in (2.1) are defined as the mass eigenstates. A completely equivalent picture is to use the states ( $d', s', b'$ ) with  $\mathbf{V} \equiv \mathbf{1}$ , and define a non-diagonal mass matrix. Since mass generation is accomplished in the Standard Model via couplings to the Higgs field [6], this moves the question of the origin of the CKM matrix elements into the realm of mass generation, which belongs still to the more “mysterious” parts [7] of the Standard Model. The exploration of the Higgs sector is the main motivation for the LHC storage ring, which is built at CERN and will start operation around 2005 [8]. The Higgs-quark couplings alone involve 10 independent parameters of the Standard Model, the quark masses and the parameters of the CKM matrix, which are not related within the theory.

Local gauge invariance and baryon number conservation requires the CKM matrix to be unitary. If there were more than three quark families, this would not hold for the  $3 \times 3$  submatrix, but this possibility is unlikely, given the limit on neutrino flavours from LEP experiments, who find  $n_\nu = 2.991 \pm 0.016$  [9] for neutrinos with mass much below the  $Z^0$  mass. Thus, if a fourth generation exists, it must incorporate a massive neutrino which is more than a factor 1000 heavier than the tau neutrino, even if we assume the experimental upper limit for the latter.

From the 9 real parameters of a general unitary matrix, 5 can be absorbed in 1 global phase, 2 relative phases between  $u, c, t$  and 2 relative phases between  $d, s, b$  which are all subject to convention and in principle unobservable. If two quarks within one of these two groups were degenerate in mass, even the sixth phase could be removed by redefining the basis in their two-dimensional subspace.

Rephasing may be accomplished by applying a phase factor to every row and column:

$$V_{jk} \rightarrow e^{i(\phi_j - \phi_k)} V_{jk} \quad (2.2)$$

Note that  $j = u, c, t$ ,  $k = d, s, b$ , and the six numbers  $\phi_u, \phi_c, \phi_t, \phi_d, \phi_s, \phi_b$  represent only five independent phases in the CKM matrix, since different sets of  $\{\phi_j, \phi_k\}$  yield the same result. Any product where each row and column enters once as  $V_{ij}$  and once via a complex conjugate  $V_{kl}^*$  like  $V_{ij} V_{kl} V_{il}^* V_{kj}^*$  is **invariant**

under the transformation (2.2). This implies that observable phases must always correspond to similar products of CKM matrix elements with equal numbers of  $V$  and  $V^*$  factors and appropriate combination of indices.

Removing unphysical phases, the CKM matrix is described by **4 real parameters**, where only one is a phase parameter, while the other three are rotation angles in flavour space. The standard parametrization [9] (first proposed in [10], notation follows [11]) uses a choice of phases, that leave  $V_{ud}$  and  $V_{cb}$  real:

$$\begin{aligned} \mathbf{V} &= \begin{pmatrix} 1 & 0 & 0 \\ 0 & c_{23} & s_{23} \\ 0 & -s_{23} & c_{23} \end{pmatrix} \begin{pmatrix} c_{13} & 0 & s_{13}e^{-i\delta_{13}} \\ 0 & 1 & 0 \\ -s_{13}e^{i\delta_{13}} & 0 & c_{13} \end{pmatrix} \begin{pmatrix} c_{12} & s_{12} & 0 \\ -s_{12} & c_{12} & 0 \\ 0 & 0 & 1 \end{pmatrix} \\ &= \begin{pmatrix} c_{12}c_{13} & s_{12}c_{13} & s_{13}e^{-i\delta_{13}} \\ -s_{12}c_{23}-c_{12}s_{13}s_{23}e^{i\delta_{13}} & c_{12}c_{23}-s_{12}s_{13}s_{23}e^{i\delta_{13}} & c_{13}s_{23} \\ s_{12}s_{23}-c_{12}s_{13}c_{23}e^{i\delta_{13}} & -c_{12}s_{23}-s_{12}s_{13}c_{23}e^{i\delta_{13}} & c_{13}c_{23} \end{pmatrix} \end{aligned} \quad (2.3)$$

with  $c_{ij} = \cos\theta_{ij}$ ,  $s_{ij} = \sin\theta_{ij}$ , and  $s_{ij} > 0$ ,  $c_{ij} > 0$  ( $0 \leq \theta_{ij} \leq \pi/2$ ).

A convenient substitution<sup>1</sup> is  $s_{12} = \lambda$ ,  $s_{23} = A\lambda^2$ ,  $s_{13} \sin\delta_{13} = A\lambda^3\eta$ , and  $s_{13} \cos\delta_{13} = A\lambda^3\rho$ , which reflects the apparent hierarchy in the size of mixing angles via orders of a parameter  $\lambda$ . This leads to

$$\begin{aligned} \mathbf{V} &= \begin{pmatrix} 1 & 0 & 0 \\ 0 & \sqrt{1-A^2\lambda^4} & A\lambda^2 \\ 0 & -A\lambda^2 & \sqrt{1-A^2\lambda^4} \end{pmatrix} \cdot \\ &\cdot \begin{pmatrix} \sqrt{1-A^2\lambda^6(\rho^2+\eta^2)} & 0 & A\lambda^3(\rho-i\eta) \\ 0 & 1 & 0 \\ -A\lambda^3(\rho+i\eta) & 0 & \sqrt{1-A^2\lambda^6(\rho^2+\eta^2)} \end{pmatrix} \cdot \begin{pmatrix} \sqrt{1-\lambda^2} & \lambda & 0 \\ -\lambda & \sqrt{1-\lambda^2} & 0 \\ 0 & 0 & 1 \end{pmatrix} \\ &= \begin{pmatrix} 1-\frac{\lambda^2}{2}-\frac{\lambda^4}{8} & \lambda & A\lambda^3(\rho-i\eta) \\ -\lambda-A^2\lambda^5(\rho+i\eta-\frac{1}{2}) & 1-\frac{\lambda^2}{2}-\left(\frac{1}{8}+\frac{A}{2}\right)\lambda^4 & A\lambda^2 \\ A\lambda^3[1-(\rho+i\eta)(1-\frac{\lambda^2}{2})] & -A\lambda^2-A\lambda^4(\rho+i\eta-\frac{1}{2}) & 1-\frac{1}{2}A^2\lambda^4 \end{pmatrix} + \mathcal{O}(\lambda^6) \end{aligned} \quad (2.4)$$

and agrees to  $\mathcal{O}(\lambda^3)$  with the Wolfenstein approximation [12]:

$$\mathbf{V} = \begin{pmatrix} 1-\frac{\lambda^2}{2} & \lambda & A\lambda^3(\rho-i\eta+\frac{1}{2}\eta\lambda^2) \\ -\lambda & 1-\frac{\lambda^2}{2}-i\eta A^2\lambda^4 & A\lambda^2(1+i\eta\lambda^2) \\ A\lambda^3(1-\rho-i\eta) & -A\lambda^2 & 1 \end{pmatrix} \quad (2.5)$$

$$\approx \begin{pmatrix} 1-\frac{\lambda^2}{2} & \lambda & A\lambda^3(\rho-i\eta) \\ -\lambda & 1-\frac{\lambda^2}{2} & A\lambda^2 \\ A\lambda^3(1-\rho-i\eta) & -A\lambda^2 & 1 \end{pmatrix} \quad (2.6)$$

Equation (2.4) is more convenient [13] in higher orders than the original proposal of Wolfenstein, or an exact parametrization [14] using the Wolfenstein parameters.

Assuming a unitary  $3 \times 3$  matrix, from experimental information these parameters are [9]

$$\begin{aligned} \lambda &= 0.2205 \pm 0.0018 \\ A &= 0.80 \pm 0.08 \\ \sqrt{\rho^2 + \eta^2} &= 0.36 \pm 0.08 \end{aligned}$$

while the phase and therefore each individual value of  $\rho$  and  $\eta$  is still very uncertain. Inserting these parameters, equation (2.6) shows clearly the dominance of the diagonal matrix elements, indication that transitions between quarks of different families are suppressed. It is the unitarity constraint which

<sup>1</sup> An equivalent choice is  $\lambda = s_{12}c_{13}$  which leads to the same parametrization to  $\mathcal{O}(\lambda^5)$ .

makes  $V_{tb} = 0.9992 \pm 0.0002$  the best known matrix element. Experimental constraints on the magnitude (90%CL limits [9]) are:

$$\begin{pmatrix} 0.9745 \dots 0.9757 & 0.219 \dots 0.224 & 0.002 \dots 0.005 \\ 0.218 \dots 0.224 & 0.9736 \dots 0.9750 & 0.036 \dots 0.046 \\ 0.004 \dots 0.014 & 0.034 \dots 0.046 & 0.9989 \dots 0.9993 \end{pmatrix}$$

With already one more family of quarks, we have five additional real parameters, of which two are new non-trivial phases. Therefore, the measurement of all CKM matrix elements and their relative phases is an important test of the Standard Model.

### 2.1.1 Unitarity Triangles

If nature provides us with just these three families of fermions, unitarity requires the following 12 conditions to be fulfilled:

$$|V_{ud}|^2 + |V_{us}|^2 + |V_{ub}|^2 = 1 \quad (2.7a)$$

$$|V_{cd}|^2 + |V_{cs}|^2 + |V_{cb}|^2 = 1 \quad (2.7b)$$

$$|V_{td}|^2 + |V_{ts}|^2 + |V_{tb}|^2 = 1 \quad (2.7c)$$

$$|V_{ud}|^2 + |V_{cd}|^2 + |V_{td}|^2 = 1 \quad (2.7d)$$

$$|V_{us}|^2 + |V_{cs}|^2 + |V_{ts}|^2 = 1 \quad (2.7e)$$

$$|V_{ub}|^2 + |V_{cb}|^2 + |V_{tb}|^2 = 1 \quad (2.7f)$$

$$V_{ud}^* V_{cd} + V_{us}^* V_{cs} + V_{ub}^* V_{cb} = 0 \quad (2.7g)$$

$$V_{ud}^* V_{td} + V_{us}^* V_{ts} + V_{ub}^* V_{tb} = 0 \quad (2.7h)$$

$$V_{cd}^* V_{td} + V_{cs}^* V_{ts} + V_{cb}^* V_{tb} = 0 \quad (2.7i)$$

$$V_{ud} V_{us}^* + V_{cd} V_{cs}^* + V_{td} V_{ts}^* = 0 \quad (2.7j)$$

$$V_{ud} V_{ub}^* + V_{cd} V_{cb}^* + V_{td} V_{tb}^* = 0 \quad (2.7k)$$

$$V_{us} V_{ub}^* + V_{cs} V_{cb}^* + V_{ts} V_{tb}^* = 0 \quad (2.7l)$$

An arbitrary phase for the whole matrix cancels in  $\mathbf{V}^+ \mathbf{V}$ . A phase common to all elements in a line (column), corresponding to arbitrary phases between  $u, c, t$  ( $d, s, b$ ) will vanish in eqns. 2.7j-l (2.7g-i) and become a common factor in eqns. 2.7g-i (2.7j-l).

Dividing (2.7k) by  $A\lambda^3 \approx -V_{cd}V_{cb}^*$  yields the unitarity triangle<sup>2</sup> as shown in figure 2.1a. In the Wolfenstein approximation, it corresponds to

$$(\rho + i\eta) - 1 + (1 - \rho - i\eta) = 0 \quad (2.8)$$

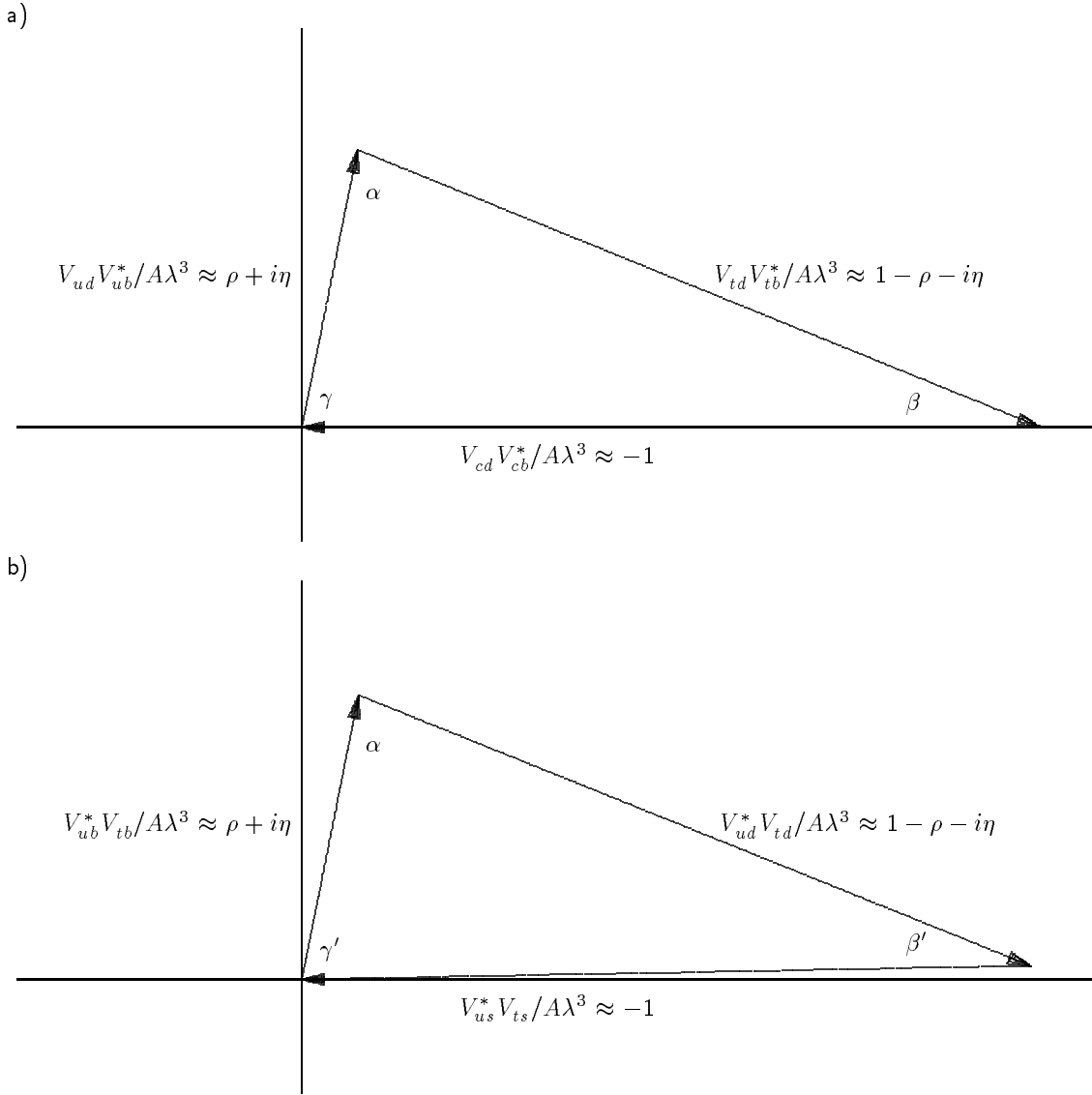
A second one from (2.7h) is shown in figure 2.1b. Dividing by  $A\lambda^3 \approx -V_{us}^*V_{ts}$  and using the approximation  $V_{ud} \approx 1$  gives the same triangle (2.8). A closer look, however, reveals slightly different lengths and angles to  $\mathcal{O}(\lambda^2)$ .

The angles<sup>3</sup> of the unitarity triangles (2.7k and h) in figure 2.1 are defined by

$$\begin{aligned} e^{i\alpha} &= -\frac{V_{td}V_{ub}V_{ud}^*V_{tb}^*}{|V_{td}V_{ub}V_{ud}V_{tb}|} \\ e^{i\beta} &= -\frac{V_{td}^*V_{cb}^*V_{cd}V_{tb}}{|V_{td}V_{cb}V_{cd}V_{tb}|} \approx e^{i\beta'} = -\frac{V_{td}^*V_{us}^*V_{ts}V_{ud}}{|V_{td}V_{us}V_{ts}V_{ud}|} \\ e^{i\gamma} &= -\frac{V_{ub}^*V_{cd}^*V_{cb}V_{ud}}{|V_{ub}V_{cd}V_{cb}V_{ud}|} \approx e^{i\gamma'} = -\frac{V_{ub}^*V_{ts}^*V_{us}V_{tb}}{|V_{ub}V_{ts}V_{us}V_{tb}|} \end{aligned}$$

<sup>2</sup> this geometric interpretation has been pointed out by Bjorken  $\sim$  1986; its first documentation in printed form is in ref. 15 and more general in ref. 16.

<sup>3</sup> in the complex plane, the angle  $\alpha - \beta$  between two vectors  $A = ae^{i\alpha}$  and  $B = be^{i\beta}$  is defined by  $e^{i(\alpha-\beta)} = AB^*/|AB|$  and  $\sin(\alpha - \beta) = \mathcal{I}m(AB^*)/|AB| = (AB^* - A^*B)/(2i|AB|)$ .



**Fig. 2.1** Unitarity triangles in the complex plane, corresponding to **a**:(2.7k) and **b**:(2.7h). Up to corrections of  $\mathcal{O}(\lambda^4)$  the top points are  $(\rho, \eta)$  in **(b)**, but  $([1 - \frac{\lambda^2}{2}]\rho, [1 - \frac{\lambda^2}{2}]\eta)$  in **(a)**, and the rightmost points are  $(1, 0)$  in **(a)**, but  $(1 - \lambda^2[\frac{1}{2} - \rho], \lambda^2 \eta)$  in **(b)**. The angles are related via  $\gamma - \gamma' = \beta' - \beta \approx \lambda^2 \eta$ .

These are rephasing invariant expressions, hence the angles resemble physical quantities independent of the CKM parametrization. It was first emphasized by Jarlskog [17], that CP violation can be described via a rephasing invariant quantity

$$J = \pm \mathcal{I}m V_{ij} V_{kl} V_{il}^* V_{kj}^* \approx A^2 \lambda^6 \eta$$

which is up to a sign independent of  $i, j, k, l$ , provided  $i \neq k, j \neq l$ .

$$\begin{aligned} J &= \mathcal{I}m(V_{ud} V_{cs} V_{us}^* V_{cd}^*) = \mathcal{I}m(V_{ud} V_{cb} V_{ub}^* V_{cd}^*) = \mathcal{I}m(V_{ud} V_{ts} V_{us}^* V_{td}^*) = \mathcal{I}m(V_{ud} V_{tb} V_{ub}^* V_{td}^*) \\ &= -\mathcal{I}m(V_{us} V_{cd} V_{ud}^* V_{cs}^*) = \mathcal{I}m(V_{us} V_{cb} V_{ub}^* V_{cs}^*) = -\mathcal{I}m(V_{us} V_{td} V_{ud}^* V_{ts}^*) = \mathcal{I}m(V_{us} V_{tb} V_{ub}^* V_{ts}^*) \\ &= -\mathcal{I}m(V_{ub} V_{cd} V_{ud}^* V_{cb}^*) = -\mathcal{I}m(V_{ub} V_{cs} V_{us}^* V_{cb}^*) = -\mathcal{I}m(V_{ub} V_{td} V_{ud}^* V_{tb}^*) = -\mathcal{I}m(V_{ub} V_{ts} V_{us}^* V_{tb}^*) \\ &= \mathcal{I}m(V_{cd} V_{ts} V_{cs}^* V_{td}^*) = \mathcal{I}m(V_{cd} V_{tb} V_{cb}^* V_{td}^*) = -\mathcal{I}m(V_{cs} V_{td} V_{cd}^* V_{ts}^*) = \mathcal{I}m(V_{cs} V_{tb} V_{cb}^* V_{ts}^*) \\ &= -\mathcal{I}m(V_{cb} V_{td} V_{cd}^* V_{tb}^*) = -\mathcal{I}m(V_{cb} V_{ts} V_{cs}^* V_{tb}^*) \end{aligned}$$

These terms are all products of the type  $\mathcal{I}m AB^* = |A||B|\mathcal{I}m e^{i(\arg A - \arg B)} = |A||B|\sin(\arg A - \arg B)$ , which is twice the area of a triangle with sides  $A$  and  $B$ , and  $A$  and  $B$  are sides of a unitarity triangle. The areas of all six unitarity triangles are equal and have the value  $J/2$ . As will be shown below, CP violating observables are typically proportional to the sine of the angles in unitarity triangles, like

$$\sin \gamma = \mathcal{I}m e^{i\gamma} = -\frac{\mathcal{I}m(V_{ub}^* V_{cd}^* V_{cb} V_{ud})}{|V_{ub} V_{cd} V_{cb} V_{ud}|} = -\frac{J}{|V_{ub} V_{cd} V_{cb} V_{ud}|}$$

and vanish for  $J = 0$ , i.e. if all triangles collapse into lines. If the non-trivial phase is 0 or  $\pi$ , the parameter  $\eta$  is 0 and hence  $J = 0$ . This would also be the case if two quarks of a given charge had the same mass, since then a rotation between these two flavours could be chosen that removes the phase factors, as can be seen in (2.3) where  $\theta_{13} = 0$  would remove all terms with the phase  $\delta_{13}$ .

The area of all triangles defined by (2.7g-l) is  $J/2$ . This corresponds to an area  $\approx \eta/2$  for the ones in figure 2.1, since their sides have been reduced by the factor  $A\lambda^3$ . If  $J = 0$ , also the area of the unitarity triangles would shrink to zero.

The angles of all six triangles (2.7g-l) can be determined using the standard parametrization (2.3) in a rewritten form

$$\mathbf{V} = \begin{pmatrix} |V_{ud}| & |V_{us}| & |V_{ub}|e^{-i\tilde{\gamma}} \\ -|V_{cd}|e^{i\phi_4} & |V_{cs}|e^{-i\phi_6} & |V_{cb}| \\ |V_{td}|e^{-i\tilde{\beta}} & -|V_{ts}|e^{i\phi_2} & |V_{tb}| \end{pmatrix} \quad (2.9)$$

with  $\tilde{\gamma} \equiv \delta_{13}$ . Here, absolute values and phases are given as separate factors. The angles  $\phi_2 \approx \eta\lambda^2$ ,  $\phi_4 \approx \eta A^2 \lambda^4$ , and  $\phi_6 \approx \eta A^2 \lambda^6$  are all positive and very small and their subscript indicates the order in  $\lambda$  of their magnitude. The unitarity triangles in figure 2.1 have angles

$$\begin{aligned} \beta &= \tilde{\beta} + \phi_4 \\ \beta' &= \tilde{\beta} + \phi_2 \\ \gamma &= \tilde{\gamma} - \phi_4 \\ \gamma' &= \tilde{\gamma} - \phi_2 \\ \alpha &= \pi - \tilde{\beta} - \tilde{\gamma} \end{aligned}$$

In the Wolfenstein approximation, the unitarity relations read (all terms given to order  $\lambda^3$  or, if this is still 0, [in brackets] to leading order)

$$-\lambda + \frac{1}{2}\lambda^3 + \lambda - \frac{1}{2}\lambda^3 + [A^2\lambda^5(\rho + i\eta)] = 0 \quad (2.7g')$$

$$A\lambda^3(1 - \rho - i\eta) - A\lambda^3 + A\lambda^3(\rho + i\eta) = 0 \quad (2.7h')$$

$$[-A\lambda^4(1 - \rho - i\eta)] - A\lambda^2 + A\lambda^2 = 0 \quad (2.7i')$$

$$\lambda - \frac{1}{2}\lambda^3 - \lambda + \frac{1}{2}\lambda^3 - [A^2\lambda^5(1 - \rho - i\eta)] = 0 \quad (2.7j')$$

$$A\lambda^3(\rho + i\eta) - A\lambda^3 + A\lambda^3(1 - \rho - i\eta) = 0 \quad (2.7k')$$

$$[A\lambda^4(\rho + i\eta)] + A\lambda^2 - A\lambda^2 = 0 \quad (2.7l')$$

and define three pairs of unitarity triangles, 6 in total:

- (2.7h') and (2.7k') are the ones shown in figure 2.1 with three sides of similar length, all of order  $A\lambda^3$ . This is “**the unitarity triangle**”. The other ones are quite flat, and it will require very high precision to prove experimentally that they are not degenerate to a line.
- (2.7i') and (2.7l') have two sides of length  $A\lambda^2$  and one much shorter of order  $A\lambda^4$ . This limits the small angles, which are  $\phi_2 + \phi_6$  and  $\phi_2 - \phi_6$ , respectively. They are close to the differences of angles in the large triangles  $\gamma - \gamma' = \beta' - \beta = \phi_2 - \phi_4$ .
- (2.7g') and (2.7j') have two sides of length  $\lambda$  and one very much shorter of order  $A^2\lambda^5$ , with a small angle  $\phi_4 - \phi_6$  and  $\phi_4 + \phi_6$ , respectively. Both are of order  $\lambda^4$ .



Tiny differences between the two standard unitarity triangles are  $\mathcal{O}(\lambda^2)$  corrections,

$$A\lambda^3(1 - \rho - i\eta) + \frac{-A\lambda^3}{+A\lambda^5(\rho + i\eta - \frac{1}{2}) + \mathcal{O}(\lambda^7)} + \frac{A\lambda^3(\rho + i\eta)}{+ \mathcal{O}(\lambda^7)} = 0 \quad (2.7h'')$$

$$A\lambda^3(\rho + i\eta) + \frac{-A\lambda^3}{-\frac{1}{2}A\lambda^5(\rho + i\eta) + \mathcal{O}(\lambda^7)} + \frac{A\lambda^3(1 - \rho - i\eta)}{+ \frac{1}{2}A\lambda^5(\rho + i\eta) + \mathcal{O}(\lambda^7)} = 0 \quad (2.7k'')$$

The angles in these two triangles can be estimated from experimental constraints on a  $3 \times 3$  unitary CKM matrix, leading to 95%CL limits [18]

$$25^\circ \leq \alpha \leq 125^\circ$$

$$11^\circ \leq \beta \leq 35^\circ$$

$$40^\circ \leq \gamma \leq 145^\circ$$

All phase angles are only weakly constrained by these limits, and one of the aims of experiments designed to observe CP violation in  $B$  meson decays is a first measurement, and ultimately a precise determination of their values. However, deviations from or extensions to the Standard Model may imply that the two triangles are dissimilar, or even that they are no (closed) triangles at all. Therefore, it is important to distinguish measurements of different parameters, even if they are expected to have identical or close values within the three family Standard Model.

### 2.1.2 Phases and Observables

The fact that phases of quark fields are unobservable numbers has been used to show that some phases in the CKM matrix are not observables either, and there remains some arbitrariness in the parametrization for this matrix. The freedom to choose quark phases may be extended to antiquarks, with six more phases  $\bar{\phi}_u, \bar{\phi}_c, \bar{\phi}_t, \bar{\phi}_d, \bar{\phi}_s, \bar{\phi}_b$ . With the new quark states

$$q'_j = e^{i\phi_j} q, \quad \bar{q}'_j = e^{i\bar{\phi}_j} \bar{q}_j, \quad j = u, c, t, d, s, b$$

also the phase induced by the CP operation is changed. The transition

$$\text{CP} |q_j\rangle = e^{i\phi_{\text{CP}j}} |\bar{q}_j\rangle \quad \rightarrow \quad \text{CP} |q'_j\rangle = e^{i\phi'_{\text{CP}j}} |\bar{q}'_j\rangle$$

requires

$$\phi'_{\text{CP}j} = \phi_{\text{CP}j} + \phi_j - \bar{\phi}_j$$

This equation leaves  $\phi'_{\text{CP}j}$  still completely undefined, since all three phases on the right-hand side are not observable, and therefore subject to arbitrary changes. It becomes meaningful, however, if it is applied to observables, like CP eigenvalues. Two CP eigenstates constructed from a meson and anti-meson state with eigenvalues  $\pm 1$  are related accordingly:

$$|q_j \bar{q}_k\rangle \pm e^{i\phi_{\text{CP}jk}} |q_k \bar{q}_j\rangle = e^{-i(\phi_j + \bar{\phi}_k)} \left[ |q'_j \bar{q}'_k\rangle \pm e^{i\phi'_{\text{CP}jk}} |q'_k \bar{q}'_j\rangle \right]$$

The new states  $|q'_j \bar{q}'_k\rangle \pm e^{i\phi'_{\text{CP}jk}} |q'_k \bar{q}'_j\rangle$  have the same eigenvalues, and differ by an overall unobservable phase from the old ones.

The CP operation on a meson, e. g. the pseudoscalar  $B^0$  meson  $|\bar{b}d\rangle$ , is

$$\text{CP} |B^0\rangle = e^{i\phi_{\text{CP}B}} |\bar{B}^0\rangle \quad (2.10)$$

where the phase factor  $e^{i\phi_{\text{CP}B}} = \langle \bar{B}^0 | \text{CP} |B^0\rangle$  depends on the parity of the bound-state wave function, and the chosen quark and antiquark phase convention. It is thus an unobservable, arbitrary phase.

Quark phase changes can in principle be compensated by phase changes of the CKM matrix elements according to (2.2), leaving terms like

$$\langle q_j | V_{jk} | q_k \rangle$$

invariant. However, this is **not** a physical requirement, and in fact the CP transformed

$$e^{i\phi_{CPkj}} \langle \bar{q}_j | V_{jk}^* | \bar{q}_k \rangle \quad (2.11)$$

has a phase which changes with the quark phases. Since none of the two terms corresponds to an observable, the actual choice of phases in the CKM matrix parametrization can be made **independent** of the choice of quark phases.

The appearance of an additional phase factor in (2.11) can be avoided by the restriction  $\bar{\phi}_j = -\phi_j$  for quark phase changes, and an appropriate phase convention which makes terms related by a CPT transformation relatively real. If a choice of phases is possible where all CKM matrix elements can be made real, also charged current weak interactions would not violate CP symmetry.

Phase conventions will also enter into relations among decay amplitudes. An amplitude for a weak decay  $B^0 \rightarrow X$  via a single well defined process can be written as

$$A = \langle X | \mathbf{H} | B^0 \rangle = \langle X | \mathbf{O} V | B^0 \rangle \quad (2.12)$$

where  $V$  is a product of the appropriate CKM matrix elements and  $\mathbf{O}$  is an operator describing the rest of the weak and possibly also subsequent strong interaction processes involved in the transition. Since strong interaction and also weak interaction—except for nontrivial phases in  $V$ —are CP invariant, the charge conjugate mirror process  $\bar{B}^0 \rightarrow \bar{X}$  has an amplitude

$$\begin{aligned} \bar{A} &= \langle \bar{X} | \mathbf{H} | \bar{B}^0 \rangle = e^{i\phi_{CPX}} \langle X | \mathbf{C} P \mathbf{O} V \mathbf{C} P^+ e^{-i\phi_{CPB}} | B^0 \rangle \\ &= e^{i\phi_{CPX} - \phi_{CPB}} \langle X | \mathbf{O} V^* | B^0 \rangle \\ &= e^{i(\phi_{CPX} - \phi_{CPB})} \frac{V^*}{V} A \end{aligned} \quad (2.13)$$

where also

$$\frac{V^*}{V} = e^{-2i \arg V}$$

is just a phase. Especially, if  $X$  is a CP eigenstate with eigenvalue  $\eta_X = \pm 1$ ,

$$\bar{A} = \eta_X e^{-i(\phi_{CPB} + 2 \arg V)} A \quad (2.14)$$

relates the two amplitudes, and the ratio  $\bar{A}/A$  flips sign with the CP eigenvalue.

All physical observables must be independent of the choice of phases. This is the case if only absolute values of amplitudes are involved, but for interference terms the phase convention cancels often in a more subtle way. Some examples will be shown in the following chapters. On the other hand, expressions where the arbitrary phases are still present cannot be observables.

## 2.2 Oscillation Phenomenology

An unstable meson can be described by the non-relativistic Schrödinger equation  $i\partial_t\psi = (m - \frac{i}{2}\Gamma)\psi$ , with the solution

$$|\psi\rangle = |\psi_0\rangle e^{-imt} e^{-\frac{1}{2}\Gamma t} \quad (2.15)$$

which reproduces the exponential law of radioactive decay, since  $|\psi_0|\psi\rangle|^2 = e^{-\Gamma t}$ .

The four meson pairs  $K^0/\bar{K}^0$ ,  $D^0/\bar{D}^0$ ,  $B^0/\bar{B}^0$ , and  $B_s/\bar{B}_s$  can be described as decaying two-component quantum states obeying the Schrödinger equation

$$i\partial_t\psi = \mathbf{H}\psi$$

with a general Hamiltonian

$$\mathbf{H} = \mathbf{M} - \frac{i}{2}\mathbf{\Gamma} = \begin{pmatrix} m_{11} - \frac{i}{2}\Gamma_{11} & m_{12} - \frac{i}{2}\Gamma_{12} \\ m_{12}^* - \frac{i}{2}\Gamma_{12}^* & m_{22} - \frac{i}{2}\Gamma_{22} \end{pmatrix} \quad (2.16)$$

where  $\mathbf{M}$  and  $\mathbf{\Gamma}$  are **hermitian**, but  $\mathbf{H}$  is not [19]. If the  $B^0/\bar{B}^0$  system is taken as a representative to illustrate the behaviour of oscillating meson pairs, the indices 1 and 2 correspond to base vectors  $|B^0\rangle$  and  $|\bar{B}^0\rangle$ , respectively. These states are assumed to be normalized, i. e.  $\langle\bar{B}^0|\bar{B}^0\rangle = \langle B^0|B^0\rangle = 1$ .

CPT invariance requires  $m_{11} = m_{22} := m$  and  $\Gamma_{11} = \Gamma_{22} := \Gamma$ , reducing the number of real parameters of the Hamiltonian to six.

$$\mathbf{H} = \begin{pmatrix} H & H_{12} \\ H_{21} & H \end{pmatrix} = \begin{pmatrix} m - \frac{i}{2}\Gamma & m_{12} - \frac{i}{2}\Gamma_{12} \\ m_{12}^* - \frac{i}{2}\Gamma_{12}^* & m - \frac{i}{2}\Gamma \end{pmatrix} \quad (2.17)$$

CPT invariance is one of the indispensable premises of any relativistic field theory within or beyond the Standard Model [20]. The generalized phenomenology including CPT violation will therefore not be considered here, but can be found in textbooks [21].

The parametrization of the off diagonal elements is convenient for calculation, but it is still the most general case, since 4 real parameters suffice to describe any  $H_{12}$  and  $H_{21}$ :

$$\begin{aligned} m_{12} &= \frac{1}{2}(H_{12} + H_{21}^*) \\ \mathcal{R}e m_{12} &= \frac{1}{2}(\mathcal{R}e H_{12} + \mathcal{R}e H_{21}) \\ \mathcal{I}m m_{12} &= \frac{1}{2}(\mathcal{I}m H_{12} - \mathcal{I}m H_{21}) \\ \Gamma_{12} &= i(H_{12} - H_{21}^*) \\ \mathcal{R}e \Gamma_{12} &= \mathcal{I}m H_{12} + \mathcal{I}m H_{21} \\ \mathcal{I}m \Gamma_{12} &= \mathcal{R}e H_{12} - \mathcal{R}e H_{21} \\ \mathcal{R}e H_{12} &= \mathcal{R}e m_{12} + \frac{1}{2}\mathcal{I}m \Gamma_{12} \\ \mathcal{R}e H_{21} &= \mathcal{R}e m_{12} - \frac{1}{2}\mathcal{I}m \Gamma_{12} \\ \mathcal{I}m H_{12} &= \mathcal{I}m m_{12} - \frac{1}{2}\mathcal{R}e \Gamma_{12} \\ \mathcal{I}m H_{21} &= \mathcal{I}m m_{12} - \frac{1}{2}\mathcal{R}e \Gamma_{12} \end{aligned}$$

Solving the eigenvalue problem  $\det(\mathbf{H} - a \cdot \mathbf{1}) = (H - a)^2 - H_{12}H_{21} = 0$ , one obtains two eigenstates with eigenvalues  $a = H \pm \sqrt{H_{12}H_{21}}$ , explicitly

$$\begin{aligned} a_L &= m_L - \frac{i}{2}\Gamma_L = m - \frac{i}{2}\Gamma - \sqrt{\left(m_{12} - \frac{i}{2}\Gamma_{12}\right)\left(m_{12}^* - \frac{i}{2}\Gamma_{12}^*\right)} \\ a_H &= m_H - \frac{i}{2}\Gamma_H = m - \frac{i}{2}\Gamma + \sqrt{\left(m_{12} - \frac{i}{2}\Gamma_{12}\right)\left(m_{12}^* - \frac{i}{2}\Gamma_{12}^*\right)} \end{aligned} \quad (2.18)$$

where  $L, H$  stands for “light” and “heavy”. It is immediately seen that  $m$  and  $\Gamma$  are the average mass  $\frac{1}{2}(m_H + m_L)$  and width  $\frac{1}{2}(\Gamma_H + \Gamma_L)$ . The differences are

$$\begin{aligned}\frac{\Delta m}{2} &= \frac{m_H - m_L}{2} = \mathcal{R}e \sqrt{\left(m_{12} - \frac{i}{2}\Gamma_{12}\right) \left(m_{12}^* - \frac{i}{2}\Gamma_{12}^*\right)} \\ \frac{\Delta \Gamma}{2} &= \frac{\Gamma_H - \Gamma_L}{2} = -2\mathcal{I}m \sqrt{\left(m_{12} - \frac{i}{2}\Gamma_{12}\right) \left(m_{12}^* - \frac{i}{2}\Gamma_{12}^*\right)} \\ \frac{\Delta a}{2} &= \frac{a_H - a_L}{2} = \sqrt{\left(m_{12} - \frac{i}{2}\Gamma_{12}\right) \left(m_{12}^* - \frac{i}{2}\Gamma_{12}^*\right)} = \sqrt{|m_{12}|^2 - \frac{1}{4}|\Gamma_{12}|^2 - i\mathcal{R}e(m_{12}\Gamma_{12}^*)}\end{aligned}\quad (2.19)$$

The connection between mass and lifetime (width) differences and the off-diagonal elements in the mass matrix are showing up in these equations, especially  $\Delta m = 0$  if  $m_{12} = 0$  and  $\Delta \Gamma = 0$  if  $\Gamma_{12} = 0$ . Squaring the last line leads to the useful relation

$$\Delta m \cdot \Delta \Gamma = 4\mathcal{R}e(m_{12}\Gamma_{12}^*) \quad (2.20)$$

which relates the sign of  $\Delta m$  and  $\Delta \Gamma$  with the off-diagonal elements  $m_{12}$  and  $\Gamma_{12}$ . It is convenient to define the dimensionless parameters

$$x = \frac{\Delta m}{\Gamma}, \quad y = \frac{\Delta \Gamma}{2\Gamma} = \frac{\Gamma_H - \Gamma_L}{\Gamma_H + \Gamma_L} = \frac{\tau_L - \tau_H}{\tau_L + \tau_H} \quad (2.21)$$

where  $x$  is a non-negative real number, and  $y$  may only assume values between  $-1$  and  $1$ . It is an asymmetry parameter in the widths or, equivalently, in the lifetimes  $\tau_L, \tau_H$ .

The eigenvectors  $|B_{L,H}\rangle = \begin{pmatrix} p \\ \pm q \end{pmatrix}$  are found by inserting (2.18) into  $\mathbf{H}|B_{L,H}\rangle = a_{L,H}|B_{L,H}\rangle$ , giving the ratio

$$\eta_m := \frac{q}{p} = \frac{1 - \epsilon}{1 + \epsilon} = -\sqrt{\frac{H_{21}}{H_{12}}} = -2\frac{m_{12}^* - \frac{i}{2}\Gamma_{12}^*}{\Delta m - \frac{i}{2}\Delta \Gamma} \quad (2.22)$$

and

$$\epsilon = \frac{1 - \eta_m}{1 + \eta_m} = \frac{\sqrt{H_{12}} + \sqrt{H_{21}}}{\sqrt{H_{12}} - \sqrt{H_{21}}} = \frac{H_{12} - H_{21}}{H_{12} + H_{21} - 2\sqrt{H_{12}H_{21}}}$$

Normalization requires  $|p|^2 + |q|^2 = 1$ , i. e.

$$\begin{aligned}p &= \frac{1 + \epsilon}{\sqrt{2(1 + |\epsilon|^2)}} = \frac{1}{\sqrt{1 + |\eta_m|^2}} \\ q &= \frac{1 - \epsilon}{\sqrt{2(1 + |\epsilon|^2)}} = \frac{\eta_m}{\sqrt{1 + |\eta_m|^2}}\end{aligned}$$

and single particle eigenstates are described by one complex parameter  $\eta_m$ . This parameter<sup>4</sup> is defined only up to an arbitrary phase, and only  $|\eta_m|$  is a measurable quantity. The value of the phase depends on conventions, one of them is the definition of the phase  $\phi_{\text{CP}B} = \arg\langle \bar{B}^0 | \text{CP} | B^0 \rangle$ . This makes also  $\epsilon$  (sometimes also denoted  $\bar{\epsilon}$ , e. g. in [23]) an arbitrary quantity. The standard choice of the CKM matrix (2.3) and  $\phi_{\text{CP}K} = 0$  make  $|\epsilon|$  small in the  $K^0/\bar{K}^0$  system, but a consistent convention  $\phi_{\text{CP}B} = 0$  leaves it at  $\mathcal{O}(0.1 \dots 1)$  in the  $B^0/\bar{B}^0$  system. A different definition of  $\epsilon$  for the kaon system given in [22] is independent of arbitrary phases. In general, convention independent parameters can be defined if decays are involved. They can usually be expressed via the unitarity angles (see fig. 2.1) and will be given for the  $B$  and  $K$  systems at the appropriate places below.

<sup>4</sup>  $\eta_m$  or  $-\eta_m$  is sometimes called  $\alpha$  in the literature, e. g. in [22,23].

The original Hamiltonian can be rewritten using the parameter  $\eta_m$  as

$$\mathbf{H} = \begin{pmatrix} m - \frac{i}{2}\Gamma & -\frac{\Delta m - \frac{i}{2}\Delta\Gamma}{2\eta_m} \\ -\eta_m \frac{\Delta m - \frac{i}{2}\Delta\Gamma}{2} & m - \frac{i}{2}\Gamma \end{pmatrix} = \begin{pmatrix} m - \frac{i}{2}\Gamma & -\frac{\Gamma}{2} \frac{1}{\eta_m} (x - iy) \\ -\frac{\Gamma}{2} \eta_m (x - iy) & m - \frac{i}{2}\Gamma \end{pmatrix} \quad (2.23)$$

and the mass and flavour eigenstates are related by the equations

$$|B_L\rangle = p|B^0\rangle + q|\bar{B}^0\rangle$$

$$|B_H\rangle = p|B^0\rangle - q|\bar{B}^0\rangle$$

$$|B^0\rangle = \frac{1}{2p} (|B_L\rangle + |B_H\rangle)$$

$$|\bar{B}^0\rangle = \frac{1}{2q} (|B_L\rangle - |B_H\rangle)$$

The eigenstates for non-hermitian  $\mathbf{H}$ , i.e.  $\Gamma_{12} \neq 0$ , are **not orthogonal**:

$$\delta := \langle B_H | B_L \rangle = |p|^2 - |q|^2 = \frac{1 - |\eta_m|^2}{1 + |\eta_m|^2} = \frac{2 \mathcal{R}e \epsilon}{1 + |\epsilon|^2} \quad (2.24)$$

In contrast to  $\epsilon$  the real number  $\delta$  is an observable. The deviation of  $|\eta_m|$  from one (called  $d_\alpha$  in [22]) is

$$|\eta_m| - 1 = \sqrt{\frac{1 - \delta}{1 + \delta}} - 1 \approx -\delta$$

For an arbitrary initial state

$$|\psi(0)\rangle = b_H|B_H\rangle + b_L|B_L\rangle = a|B^0\rangle + \bar{a}|\bar{B}^0\rangle$$

where the amplitudes are related via

$$b_{L,H} = \frac{1}{2} \left( \frac{a}{p} \pm \frac{\bar{a}}{q} \right) = \frac{a \pm \bar{a}/\eta_m}{2p}$$

$$a = p(b_L + b_H), \quad \bar{a} = q(b_L - b_H)$$

its time evolution may be described using a scaled time variable

$$T := \Gamma t \quad (2.25)$$

where  $\Gamma$  is the average width of the eigenstates  $B_H$  and  $B_L$ . These states have a simple exponential development with time. Their masses  $m_{H,L} = m \pm x \frac{\Gamma}{2}$  and widths  $\Gamma_{H,L} = \Gamma(1 \pm y)$  can be expressed with the dimensionless parameters  $x$  and  $y$  defined in (2.21).

$$\begin{aligned} |\psi(t)\rangle &= b_H e^{-i(m_H - i\Gamma_H/2)t} |B_H\rangle + b_L e^{-i(m_L - i\Gamma_L/2)t} |B_L\rangle \\ &= e^{-imt - T/2} \frac{e^{i(x-iy)T/2} + e^{-i(x-iy)T/2}}{2} (a|B^0\rangle + \bar{a}|\bar{B}^0\rangle) \\ &\quad + e^{-imt - T/2} \frac{e^{i(x-iy)T/2} - e^{-i(x-iy)T/2}}{2} \left( \frac{\bar{a}}{\eta_m} |B^0\rangle + a\eta_m |\bar{B}^0\rangle \right) \end{aligned} \quad (2.26a)$$

$$= e^{-imt - T/2} \left[ (a|B^0\rangle + \bar{a}|\bar{B}^0\rangle) \cos(x-iy) \frac{T}{2} + i \left( \frac{\bar{a}}{\eta_m} |B^0\rangle + a\eta_m |\bar{B}^0\rangle \right) \sin(x-iy) \frac{T}{2} \right] \quad (2.26b)$$

Starting with pure  $B^0$  mesons at  $t = 0$  corresponds to  $\bar{a} = 0$  and

$$|\psi(t)\rangle = a e^{-imt - T/2} \left[ \cos(x-iy) \frac{T}{2} |B^0\rangle + i\eta_m \sin(x-iy) \frac{T}{2} |\bar{B}^0\rangle \right] \quad (2.27)$$

Starting with pure  $\bar{B}^0$  mesons at  $t = 0$  is described by replacing  $\eta_m \leftrightarrow 1/\eta_m$ . This case corresponds to  $a = 0$  and

$$|\psi(t)\rangle = \bar{a}e^{-imt-T/2} \left[ \cos(x-iy)\frac{T}{2}|\bar{B}^0\rangle + \frac{i}{\eta_m}\sin(x-iy)\frac{T}{2}|B^0\rangle \right] \quad (2.28)$$

The numbers of  $B^0$  and  $\bar{B}^0$  at time  $T$  for  $N_0$  pure  $B^0$  mesons at  $T = 0$  are<sup>5</sup>

$$\begin{aligned} N_{B^0}(t) &= N_0 |\langle B^0 | \psi(t, \bar{a} = 0, a = 1) \rangle|^2 = N_0 \frac{e^{-T}}{2} (\cosh yT + \cos xT) \\ N_{\bar{B}^0}(t) &= N_0 |\langle \bar{B}^0 | \psi(t, \bar{a} = 0, a = 1) \rangle|^2 = N_0 |\eta_m|^2 \frac{e^{-T}}{2} (\cosh yT - \cos xT) \end{aligned} \quad (2.29)$$

These numbers, however, can not be observed. What is accessible by experiment is only the rate of decays to flavour specific final states  $X$  and  $\bar{X}$  at a given time  $T$ . These decay modes are often called **tagging modes**, since they serve as a “tag” to indicate the flavour of the mother particle at decay time. The rates can be obtained from (2.27) by multiplying with  $\langle X | \mathbf{H}$  or  $\langle \bar{X} | \mathbf{H}$ , respectively, to obtain the amplitudes. They are converted into rates

$$\begin{aligned} \dot{N}_{B^0 \rightarrow X}(t) &= N_0 \int \text{dPS} |\langle X | \mathbf{H} | \psi(t, \bar{a} = 0) \rangle|^2 = \frac{1}{2} N_0 e^{-T} \Gamma_X (\cosh yT + \cos xT) \\ \dot{N}_{\bar{B}^0 \rightarrow \bar{X}}(t) &= N_0 \int \text{dPS} |\langle \bar{X} | \mathbf{H} | \psi(t, \bar{a} = 0) \rangle|^2 = \frac{1}{2} N_0 |\eta_m|^2 e^{-T} \Gamma_X (\cosh yT - \cos xT) \end{aligned} \quad (2.30)$$

where

$$\Gamma_X = \int \text{dPS} |\langle X | \mathbf{H} | B^0 \rangle|^2 = \int \text{dPS} |\langle \bar{X} | \mathbf{H} | \bar{B}^0 \rangle|^2$$

is the partial width for a non-oscillating meson. It agrees in value for the two CP conjugate processes if the amplitudes differ only by phases. Integrating over all times the total number of decays are

$$\begin{aligned} N_{B^0 \rightarrow X} &= \int_0^\infty \dot{N}_{B^0 \rightarrow X}(t) dt = N_0 \frac{\Gamma_X}{\Gamma} \left[ \frac{1}{2(1-y^2)} + \frac{1}{2(1+x^2)} \right] \\ N_{\bar{B}^0 \rightarrow \bar{X}} &= \int_0^\infty \dot{N}_{\bar{B}^0 \rightarrow \bar{X}}(t) dt = N_0 \frac{\Gamma_X}{\Gamma} \left[ \frac{|\eta_m|^2}{2(1-y^2)} - \frac{|\eta_m|^2}{2(1+x^2)} \right] \end{aligned}$$

The corresponding numbers for initial  $\bar{B}^0$  mesons are obtained with the replacement  $\eta_m \rightarrow 1/\eta_m$ . If we ignore CP violating effects in the oscillation, i. e. for  $|\eta_m| = 1$ , we can define a meaningful branching fraction as

$$\mathcal{B}(B^0 \rightarrow X) = \frac{1}{N_0} \int_0^\infty [\dot{N}_{B^0 \rightarrow X}(t) + \dot{N}_{\bar{B}^0 \rightarrow \bar{X}}(t)] dt = \frac{\Gamma_X}{\Gamma(1-y^2)} = \frac{1}{2} \frac{\Gamma_X}{\Gamma_H} + \frac{1}{2} \frac{\Gamma_X}{\Gamma_L}$$

which agrees with  $\mathcal{B}(\bar{B}^0 \rightarrow \bar{X})$  defined accordingly for the same number  $N_0$  of  $\bar{B}^0$  mesons at  $t = 0$ .

<sup>5</sup> for example,  $\cos u = \frac{1}{2}(e^{iu} + e^{-iu})$ ,  $(\cos u)^* = \frac{1}{2}(e^{iu^*} + e^{-iu^*})$ , therefore

$$|\cos u|^2 = \frac{1}{4} \left( e^{i(u+u^*)} + e^{i(u-u^*)} + e^{i(u^*-u)} + e^{-i(u+u^*)} \right) = \frac{1}{2} (\cos 2 \operatorname{Re} u + \cosh 2 \operatorname{Im} u)$$

### 2.2.1 Mechanical Analogon

Equation (2.17) characterizes also the mechanical system of two coupled pendula of the same length: Without coupling, they are both described by an oscillation frequency  $m$  and a damping constant  $\Gamma$ . They correspond to the meson  $X^0$  and its antiparticle  $\bar{X}^0$ .

If they are coupled by a spring whose elasticity is proportional to a **non-negative real** number  $m_{12}$ , and a **non-negative real** damping constant  $\Gamma_{12}$ , the solutions correspond to a “long-lived” (= low damping), “light” (= low frequency) eigenstate where the pendula oscillate strictly in phase, and a “short-lived” (= high damping), “heavy” (= high frequency) eigenstate where one pendulum oscillates as a mirror image of the other, i. e. with phase difference  $180^\circ$ . The differences in frequency and damping are  $\Delta m = 2m_{12}$  and  $\Delta\Gamma = 2\Gamma_{12}$ , respectively.

When one pendulum is excited, it will slowly transfer its energy to the other and back. This beating corresponds to the oscillation between a meson  $X^0$  and its antiparticle  $\bar{X}^0$ . The beat frequency is  $\Delta m$ . While the oscillating part  $e^{-imt}$  in (2.15) is an unobservable phase factor, in meson anti-meson oscillation a mass difference can actually be observed as a frequency!

Due to the restriction of  $m_{12}$  and  $\Gamma_{12}$  to non-negative real values, this system has always  $\Delta m \Delta\Gamma \geq 0$  (in contrast to the oscillating mesons), and can also not simulate CP violation since there are no non-trivial phases.

### 2.2.2 Standard Model Predictions

The Hamiltonian (2.17) can be obtained using

$$\mathbf{H} = \mathbf{H}_0 + \mathbf{H}_w$$

where  $\mathbf{H}_0$  is the strong and electromagnetic Hamiltonian

$$\mathbf{H}_0 = \begin{pmatrix} E_0 & 0 \\ 0 & E_0 \end{pmatrix}$$

which has the stable flavour eigenstates  $B^0$  and  $\bar{B}^0$ , and  $\mathbf{H}_w$  is the weak interaction perturbation. The Wigner-Weisskopf approximation for small  $\mathbf{H}_w$  leads to [24]

$$H_{jk} = H_{0jk} + \langle j | \mathbf{H}_w | k \rangle + \sum_X \mathcal{P} \int \text{dPS} \langle j | \mathbf{H}_w | X \rangle \langle X | \mathbf{H}_w | k \rangle \left[ \frac{1}{E_0 - E_X} - i\pi\delta(E_0 - E_X) \right] \quad (2.31)$$

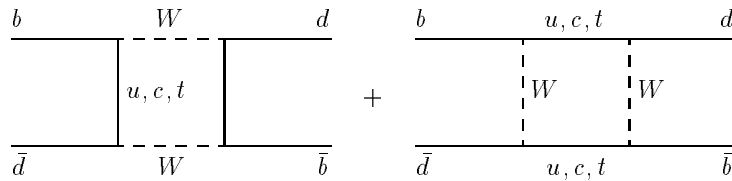
where the sum runs over all multiparticle states  $X$  which are eigenstates of  $\mathbf{H}_0$ , and  $\mathcal{P}$  denotes the principal value of the integral. The mass (hermitian) and decay (anti-hermitian) parts defined by (2.16) are

$$m_{jk} = \frac{1}{2}(H_{jk} + H_{kj}^*) = E_0 \delta_{jk} + \langle j | \mathbf{H}_w | k \rangle + \sum_X \mathcal{P} \int \text{dPS} \frac{\langle j | \mathbf{H}_w | X \rangle \langle X | \mathbf{H}_w | k \rangle}{E_0 - E_X}$$

and

$$\Gamma_{jk} = i(H_{jk} - H_{kj}^*) = 2\pi \sum_X \int \text{dPS} \langle j | \mathbf{H}_w | X \rangle \langle X | \mathbf{H}_w | k \rangle \delta(E_0 - E_X)$$

The off-diagonal elements  $H_{12,21}$  have non-zero contributions in the sum from states  $X$  which can be reached in weak decays of both  $B^0$  and  $\bar{B}^0$ . In contrast to the neutral kaon system, for  $B^0/\bar{B}^0$  these are only a small fraction of all  $B$  decays, and they contribute with alternating signs. Therefore  $H_{12,21}$  are dominated by the leading term  $\langle B^0 | \mathbf{H}_w | \bar{B}^0 \rangle$  which corresponds to the box diagrams



They give approximately [25]

$$H_{12} = \langle B^0 | \mathbf{H} | \bar{B}^0 \rangle \approx m_{12} = -\frac{G_F^2}{12\pi^2} e^{-i\phi_{CPB}} V_{tb}^2 V_{td}^{*2} m_W^2 m_B [f_B^2 B_B] \cdot [S(m_t^2/m_W^2) \cdot \eta_{\text{QCD}}] \quad (2.32)$$

The CP phase is introduced during the evaluation of the hadronic part of the matrix element. The Inami–Lim function

$$S(x) = x \left[ \frac{1}{4} + \frac{9}{4(1-x)} - \frac{3}{2(1-x)^2} - \frac{3x^2 \ln x}{2(1-x)^3} \right] \quad (2.33)$$

from the loop [26] is to lowest order a factor  $m_t^2/m_W^2$ . An evaluation of the product  $S(m_t^2/m_W^2)$  and  $\eta_{\text{QCD}}$  within a consistent renormalization scheme yields  $S \approx 2.3$ ,  $\eta_{\text{QCD}} \approx 0.55$  [27].

The hadronic part of the matrix element is approximated by

$$\langle B^0 | J_\mu J^\mu | \bar{B}^0 \rangle = \sum_X \langle B^0 | J_\mu | X \rangle \langle X | J^\mu | \bar{B}^0 \rangle = B_B \cdot \langle B^0 | J_\mu | 0 \rangle \langle 0 | J^\mu | \bar{B}^0 \rangle = B_B f_B^2 p_\mu p^\mu \quad (2.34)$$

where  $f_B$  is the  $B$  decay constant, and  $B_B$  accounts for the corrections to the vacuum insertion approximation. A big uncertainty is the product  $f_B^2 B_B$ , where the most reliable calculations now come from lattice gauge theory [28] with values around  $f_B \sqrt{B_B} \approx (200 \pm 40) \text{ MeV}$ .

In this approximation, we have for the  $B$  system

$$\Delta m = 2|m_{12}|$$

which can be used to determine  $|V_{td}|$  (since  $V_{tb} = 1$ ) from experimental results on  $B^0/\bar{B}^0$  mixing. The eigenstates are determined by

$$\eta_m = -\frac{m_{12}^*}{|m_{12}|} = e^{i\phi_{CPB}} \frac{V_{tb}^* V_{td}^2}{|V_{tb}^2 V_{td}^2|} = e^{i(\phi_{CPB} - 2\tilde{\beta})} \quad (2.35)$$

with  $-\tilde{\beta} = \arg V_{tb}^* V_{td}$ . This phase depends on the CKM parametrization and is—like the CP phase—not an observable. The arbitrariness cancels only in physical observables, which include decay amplitudes with further CKM elements and a CP phase. The corresponding

$$\epsilon = -i \frac{\sin \arg \eta_m}{1 + \cos \arg \eta_m}$$

is purely imaginary, i. e.  $\text{Re } \epsilon = 0$  and therefore  $\delta = 0$ . Within the same framework, for the  $B_s/\bar{B}_s$  system

$$\eta_{ms} = e^{i(\phi_{CPB_s} + 2\phi_2)} \quad (2.36)$$

It must be emphasized, however, that there exist common final states for all four meson pairs, and  $\Gamma_{12}$  never vanishes completely, leaving always a small  $\delta$ , and also a small  $\Delta\Gamma$ . Within the Standard Model  $\Gamma_{12}$  can be approximated by the absorptive part of the box diagram, corresponding to a quark representation of the final states. This is a poor approximation to light hadronic final states which are dominating in the  $K/\bar{K}$  system, and may still change the prediction for  $B/\bar{B}$  considerably. The box calculation yields [25]

$$\Gamma_{12} \approx -m_{12} \cdot \frac{3\pi}{2S(m_t^2/m_W^2)} \frac{m_b^2}{m_W^2} \left[ 1 + \frac{8}{3} \frac{m_c^2}{m_b^2} \frac{V_{cb} V_{cd}^*}{V_{tb} V_{td}^*} + \mathcal{O}\left(\frac{m_c^4}{m_b^4}\right) \right] \quad (2.37)$$

and  $\Delta\Gamma$  and  $\Delta m$  have **opposite signs**. The ratio can be estimated using (2.20) to be

$$\frac{\Delta\Gamma}{\Delta m} = \frac{2y}{x} \approx -\frac{3\pi}{2} \frac{m_b^2}{m_t^2} \sim -\frac{1}{250} \quad (2.38)$$



This ratio applies to both the  $B^0$  and  $B_s$  systems.

To leading order in  $\Gamma_{12}/m_{12}$  equation (2.22) yields

$$|\eta_m| - 1 = -\frac{1}{2} \mathcal{I}m \frac{\Gamma_{12}}{m_{12}} \approx \frac{2\pi}{S(m_t^2/m_W^2)} \frac{m_c^2}{m_W^2} \mathcal{I}m \frac{V_{cb} V_{cd}^*}{V_{tb} V_{td}^*} \quad (2.39)$$

from (2.37). This leads to a rough estimate of the convention-independent number

$$\delta \approx 1 - |\eta_m| \approx -2\pi \frac{m_c^2}{m_t^2} \frac{|V_{cb}| |V_{cd}|}{|V_{tb}| |V_{td}|} \sin \beta \sim -\frac{\sin \beta}{2000} \quad (2.40)$$

with  $|\delta| \ll 1$  where  $\beta$  is the CKM unitarity angle in figure 2.1a. Since this result is based on a leading order quark diagram, the number should be taken only as an order of magnitude. In particular, at this level of precision it can not be used to measure  $\beta$ .

### 2.2.3 Behaviour of the Four Neutral Meson Anti-Meson Systems

All four meson pairs  $K^0/\bar{K}^0$ ,  $D^0/\bar{D}^0$ ,  $B^0/\bar{B}^0$ , and  $B_s/\bar{B}_s$  show a different oscillation behaviour, since they have all different relations of  $\Gamma$ ,  $\Delta\Gamma$ , and  $\Delta m$ . The same symbols will be used for all four systems. Only when two specific systems shall be compared, their parameters will be distinguished by the subscripts  $K$ ,  $D$ ,  $d$ , and  $s$ , respectively. The dimensionless parameters  $x$  and  $y$  give the ratios of time constants involved:  $\tau = 1/\Gamma$  is the harmonic average of the lifetimes,  $t_{\text{osc}} = 2\pi/\Delta m = 2\pi\tau/x$  is the period of the oscillation, and  $t_{\text{rel}} = 2/\Delta\Gamma = \tau/y$  is the lifetime of the oscillation amplitude, i.e. the damping time constant of a relaxation process. Numerical values are summarized in table 2.1.

description	$K^0/\bar{K}^0$	$D^0/\bar{D}^0$	$B^0/\bar{B}^0$	$B_s/\bar{B}_s$
$\tau$ [ps]	$89.3 \pm 0.1; 51700 \pm 400$	$0.415 \pm .004$	$1.54 \pm 0.03$	$1.52 \pm 0.07$
$\Gamma$ [ $\text{s}^{-1}$ ]	$5.61 \cdot 10^9$	$2.4 \cdot 10^{12}$	$(6.41 \pm 0.16) \cdot 10^{11}$	$(6.2 \pm 0.4) \cdot 10^{11}$
$y = \Delta\Gamma/2\Gamma$	$-0.9966$	$ y  < 0.08$	$ y  \lesssim 0.01$	$-0.05 \dots -0.15^*$
$\Delta m$ [ $\text{s}^{-1}$ ]	$(5.30 \pm 0.02) \cdot 10^9$	$< 2 \cdot 10^{11}$	$(4.65 \pm 0.19) \cdot 10^{11}$	$> 7.8 \cdot 10^{12}$
$\Delta m$ [eV]	$(3.49 \pm 0.01) \cdot 10^{-6}$	$< 1.3 \cdot 10^{-4}$	$(3.1 \pm 0.1) \cdot 10^{-4}$	$> 5.1 \cdot 10^{-3}$
$x = \Delta m/\Gamma$	$0.945 \pm 0.002$	$< 0.09$	$0.72 \pm 0.03$	$11 \dots 40^*$
$\delta$	$(3.27 \pm 0.12) \cdot 10^{-3}$		$\sim -10^{-3}^*$	$ \delta  < 10^{-3}^*$
$ \eta_m ^2$	$0.99348 \pm 0.00024$	$\approx 1^*$	$1 \dots 1.002^*$	$\approx 1^*$

\* Standard Model expectation [29,18]

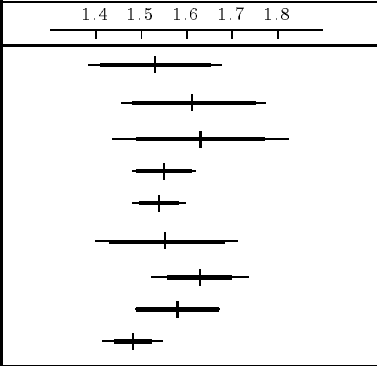
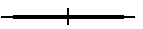
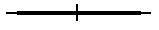



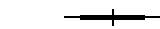

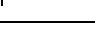

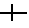
While the parameters of the  $K^0/\bar{K}^0$  system are well measured [9], theoretical assumptions enter into the  $B$  meson columns. Many precise lifetime measurements for neutral  $B$  mesons have become available last year. All lifetime measurements are summarized in table 2.2, and average to  $\tau_d = (1.54 \pm 0.03)$  ps.

Figures 2.2–2.5 show the number of mesons and anti-mesons as a function of the scaling lifetime variable  $T = t/\tau$  and the asymmetry

$$a(T) = \frac{\dot{N}(X \rightarrow X) - \dot{N}(X \rightarrow \bar{X})}{\dot{N}(X \rightarrow X) + \dot{N}(X \rightarrow \bar{X})} \Bigg|_T = \frac{(1 - |\eta_m|^2) \cosh yT + (1 + |\eta_m|^2) \cos xT}{(1 + |\eta_m|^2) \cosh yT + (1 - |\eta_m|^2) \cos xT} \quad (2.41)$$

for a meson produced at  $T = 0$  as a flavour eigenstate  $X$ , and decaying to a flavour-specific final state as  $X$  or  $\bar{X}$  at a later time  $T$ . Expressed via the small real parameter  $\delta$  instead of  $|\eta_m|$  this reads

$$a(T) = \frac{\cos xT + \delta \cosh yT}{\cosh yT + \delta \cos xT} \quad (2.42)$$

Table 2.2 $B^0$ lifetime measurements. Measurements which have been replaced by more recent ones are not included.		
	$\tau_d$ [ps]	experiment
	$1.53 \pm 0.12 \pm 0.08$	OPAL 95 [30]
	$1.61 \pm_{0.13}^{0.14} \pm 0.08$	DELPHI 95 [31]
	$1.63 \pm 0.14 \pm 0.13$	DELPHI 95 [32]
	$1.55 \pm 0.06 \pm 0.03$	ALEPH 96 [33]
	$1.537 \pm 0.041 \pm 0.039$	DELPHI 96 [34]
	$1.55 \pm_{0.12}^{0.13} \pm 0.09$	SLD 96 prel. [35]
	$1.63 \pm 0.07 \pm 0.08$	SLD 96 prel. [36]
	$1.58 \pm 0.09 \pm 0.02$	CDF 96 [37]
	$1.48 \pm 0.04 \pm 0.05$	CDF 96 [37]
	$1.54 \pm 0.03$	average

For an anti-meson produced at  $T = 0$  as a flavour eigenstate  $\bar{X}$ , and decaying to a flavour-specific final state as  $X$  or  $\bar{X}$  at time  $T$ , we obtain a similar expression, where only the  $\cos xT$  part changes sign:

$$\bar{a}(T) = \frac{\dot{N}(\bar{X} \rightarrow X) - \dot{N}(\bar{X} \rightarrow \bar{X})}{\dot{N}(\bar{X} \rightarrow X) + \dot{N}(\bar{X} \rightarrow \bar{X})} \Big|_T = -\frac{\cos xT - \delta \cosh yT}{\cosh yT - \delta \cos xT}$$

The approximation  $|\eta_m| = 1$  corresponding to  $\delta = 0$  leads to a simpler expression

$$a(T) = \frac{\cos xT}{\cosh yT} = -\bar{a}(T) \quad (2.43)$$

where  $x$  is clearly seen as the oscillation parameter, and  $y$  as the damping parameter.

The kaon has both  $x \approx 1$  and  $y \approx -1$ , i.e. the long-living state is the heavier mass eigenstate. With these parameters one half of a sample of kaons of either flavour decays rapidly, mainly into two pions with  $CP = +1$ , and the other half transforms to a sample of the long-living  $K_L^0$  states, which decay (aside from the small CP violation) to  $CP = -1$  eigenstates and to flavour-specific states. The ratio of lifetimes of the two states (table 2.1) is approximately 580. The time evolution of an initially pure  $K^0$  flavour eigenstate is shown in figure 2.2. The upper diagram shows the number of remaining  $K^0$  and  $\bar{K}^0$  after a scaled time  $T = \Gamma t$ , where  $\Gamma \approx \Gamma_S/2 = 1/(2\tau_S)$  is the average width of the short- and long-living state. The decay rate into flavour-specific final states is proportional to these numbers, while the dominant decays to CP eigenstates follow different evolution functions due to CP violation, and will be discussed below.

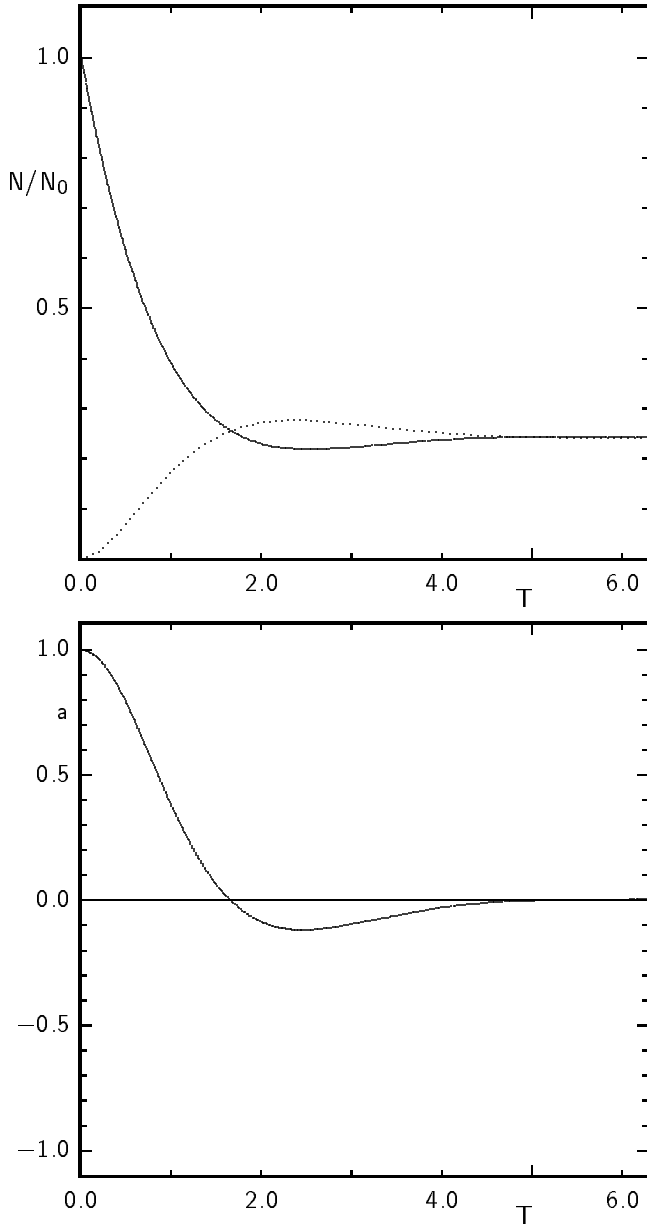
The  $D^0$  meson decays mainly to flavour specific states with well defined strangeness, with only a few decays to  $CP = +1$  eigenstates, as  $\pi\pi$ ,  $K\bar{K}$ ,  $K_L^0\pi^0$  and  $CP = -1$  states, as  $K_S^0\pi^0$  or  $K_S^0\omega$ . This leads to equal lifetimes for the two eigenstates, i.e.  $y \approx 0$ . The corresponding box graph has a  $b$  quark as the heaviest particle in the loop, which is accompanied by the small CKM elements  $V_{cb}$  and  $V_{ub}$ . The mass difference induced that way by the Standard Model is very small, corresponding to  $x \lesssim 0.002$ . Therefore, almost no asymmetry is visible in figure 2.3, although the number  $x = 0.02$  used for the plot is a factor 10 higher. The value  $x = 0.002$  corresponds to a total mixed fraction of initially pure  $D^0$  states given by

$$\chi = \frac{N_{\bar{D}^0 \rightarrow \bar{X}}}{N_{D^0 \rightarrow X} + N_{\bar{D}^0 \rightarrow \bar{X}}} = \frac{x^2}{2(1+x^2)} \quad (2.44)$$

as  $\chi \approx 2 \cdot 10^{-6}$ .

The parameters of the  $B^0/\bar{B}^0$  system have been introduced above. A good approximation is  $y = 0$  and  $\delta = 0$ , which leads for  $N_0$  pure  $B^0$  at  $t = 0$  to

$$\begin{aligned} N_{B^0}(T) &= \frac{1}{2}N_0 e^{-T} (1 + \cos xT) \\ N_{\bar{B}^0}(T) &= \frac{1}{2}N_0 e^{-T} (1 - \cos xT) \end{aligned} \quad (2.45)$$



**Fig. 2.2**  $K^0/\bar{K}^0$  mixing is determined by the parameters  $x = 0.95$ ,  $y = 0.996$ , and  $|\eta_m|^2 = 0.994$ .  $T = t/\bar{\tau}$  is the lifetime in units of  $\bar{\tau} \approx 2\tau_S$ , the inverse of the average width of  $K_L^0$  and  $K_S^0$ . The upper diagram shows the number of  $K^0$  (solid) and  $\bar{K}^0$  (dotted) as a function of  $T$  for a sample starting with 100%  $K^0$  mesons. The lower diagram shows the asymmetry  $a = (N_K - N_{\bar{K}})/(N_K + N_{\bar{K}})$ . The relaxation process soon dominates, leaving only  $K_L^0$  after not much more than one oscillation.

as shown in figure 2.4. The decay rate for flavour-specific final states (which are the majority of  $B^0$  decays) follows the same time evolution. The asymmetry function is simply

$$a(T) = \cos xT \quad (2.46)$$

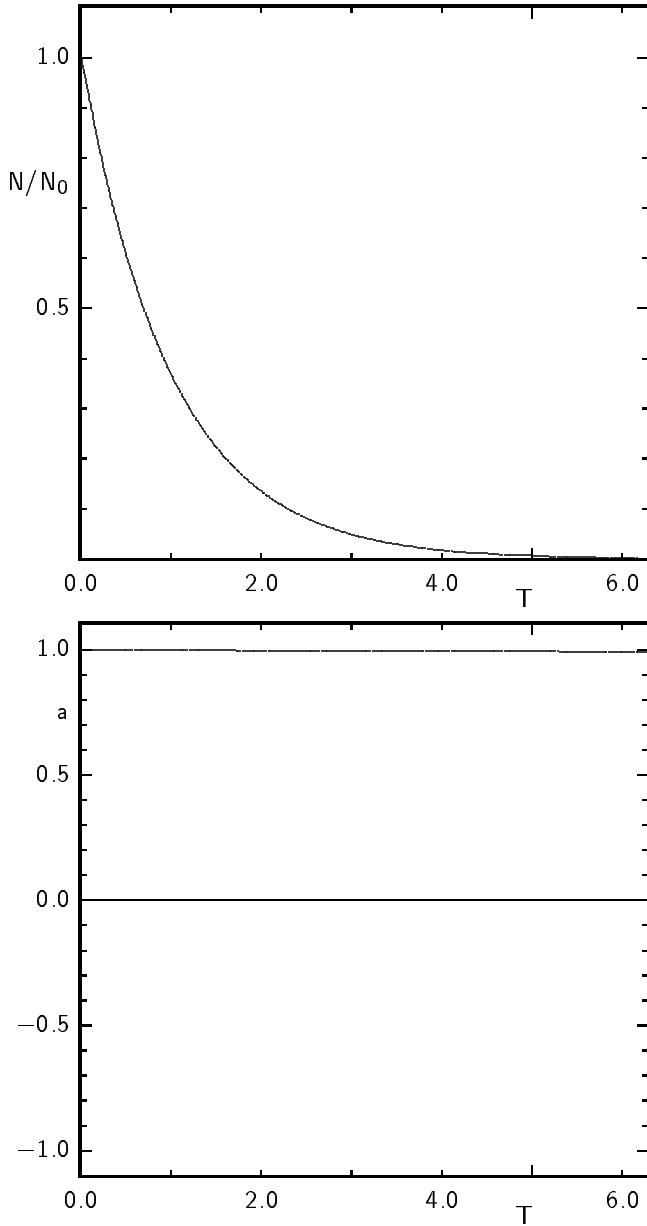
This asymmetry can be observed using a flavour-tagging decay, like  $B^0 \rightarrow D^- l^+ \nu$ . The rate of mesons decaying at time  $T$  into the channel  $X$  are given by (2.30) where  $y = 1$  makes  $\cosh yT = 1$  leading to the same asymmetry function  $a(T) = \cos xT$ . Integrating over all times, the observed numbers are

$$N_{B^0 \rightarrow X} = \int \dot{N}_{B^0 \rightarrow X}(T) dt = \frac{1}{2} N_0 \frac{\Gamma_X}{\Gamma} \frac{2 + x^2}{1 + x^2}$$

$$N_{\bar{B}^0 \rightarrow \bar{X}} = \int \dot{N}_{\bar{B}^0 \rightarrow \bar{X}}(T) dt = \frac{1}{2} N_0 \frac{\Gamma_X}{\Gamma} \frac{x^2}{1 + x^2}$$

Their asymmetry becomes

$$a_{\text{int}} = \frac{N_{\bar{B}^0 \rightarrow \bar{X}} - N_{B^0 \rightarrow X}}{N_{\bar{B}^0 \rightarrow \bar{X}} + N_{B^0 \rightarrow X}} = \frac{1}{1 + x^2}$$



**Fig. 2.3**  $D^0/\bar{D}^0$  oscillations have not yet been observed, and will be hardly visible even with  $x = 0.02$ , which is about 10 times the expected value. The other parameters in this plot are  $y = 0$  and  $|\eta_m| = 1$ .

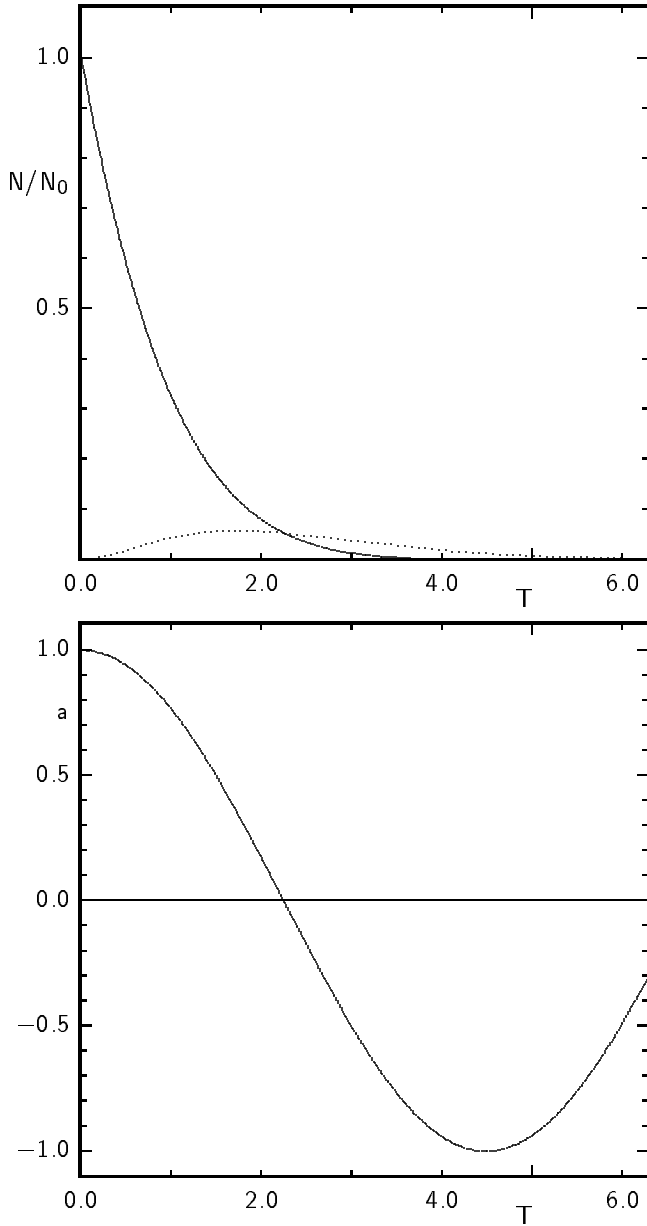
and the mixing probability is as in (2.44)

$$\chi = \frac{N_{\bar{B}^0 \rightarrow \bar{X}}}{N_{B^0 \rightarrow X} + N_{\bar{B}^0 \rightarrow \bar{X}}} = \frac{x^2}{2(1+x^2)} \quad (2.47)$$

It was this net effect which gave the first proof for a sizeable mixing parameter  $x \approx 0.7$  in the  $B^0$  meson system in 1987 [38]. The time-dependent particle anti-particle oscillations of the neutral  $B$  meson have been first seen six years later by experiments at LEP [39]. With  $x \approx 0.7$ , about one period is visible before most of the mesons are decayed.

If we assume the Standard Model predictions to be true, the  $B_s$  meson is a very interesting case. There will be a small  $y$  and a very large  $x$ . Figure 2.5 is plotted with  $x_s = 15$ , which is close to the lower limit of the theoretical range. The time-integrated mixing probability is for  $|\eta_m| = 1$

$$\chi = \frac{x^2 + y^2}{2(1+x^2)}$$



**Fig. 2.4**  $B^0/\bar{B}^0$  evolution is dominated by the oscillating part, with the parameters  $x = 0.70$ ,  $y = 0$ , and  $|\eta_m| = 1$ . The ratio of the areas under the dotted and solid curve in the upper plot is the mixing probability  $\chi$ . The zero transition in the asymmetry, which marks the crossover point in the upper plot, is at  $T = \frac{\pi}{2x}$ .

For large  $x_s \gg 1$ , this approaches its maximum value of 0.5, where a measurement of this quantity has no sensitivity on  $x$  any more. To observe the rapid oscillations, a very good lifetime resolution will be required. Experimentally, a lower limit  $x_s > 15$  has been found at LEP (see below).

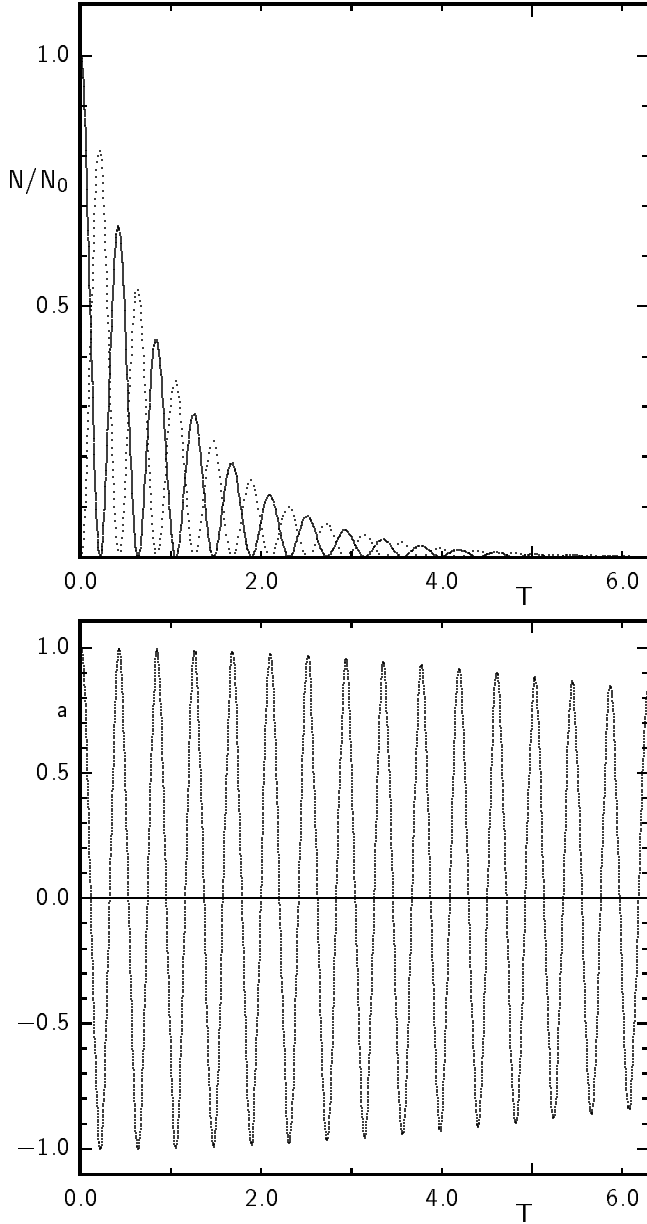
In the general case  $|\eta_m| \neq 1$ , the integrated mixing probability depends on the initial flavour. It is

$$\chi = \frac{|\eta_m|^2(x^2 + y^2)}{2 + x^2(1 + |\eta_m|^2) - y^2(1 - |\eta_m|^2)} = \frac{(1 - \delta)(x^2 + y^2)}{2[1 + x^2 + \delta(1 - y^2)]} \quad (2.48a)$$

for an initial  $B$  and

$$\bar{\chi} = \frac{(x^2 + y^2)}{2|\eta_m|^2 + x^2(1 + |\eta_m|^2) + y^2(1 - |\eta_m|^2)} = \frac{(1 + \delta)(x^2 + y^2)}{2[1 + x^2 - \delta(1 - y^2)]} \quad (2.48b)$$

for an initial  $\bar{B}$  (which is  $\chi$  with  $|\eta_m|$  replaced by  $1/|\eta_m|$  or  $\delta$  by  $-\delta$ ). This exhibits already CP violation, since the probabilities  $P(X \rightarrow \bar{X})$  and  $P(\bar{X} \rightarrow X)$  are different. It is also T violation, since the transition  $X \rightarrow \bar{X}$  is the time reversed process  $\bar{X} \rightarrow X$ .



**Fig. 2.5**  $B_s/\bar{B}_s$  is expected to be the most rapidly oscillating system, with a longer relaxation time. This plot assumes  $x_s = 15$ ,  $y_s = 0.10$ , and  $|\eta_m| = 1$ .

#### 2.2.4 CP Eigenstates Versus Mass Eigenstates

The following discussion will again use  $B^0/\bar{B}^0$  as an example, but is applicable to each of the four systems accordingly.

The standard phase convention requires all  $J^{PC} = 0^{-+}$  mesons to have  $\text{CP}|X\rangle = -|\bar{X}\rangle$ , fixing  $\phi_{\text{CP}B} = \pi$ . Independent of any convention, two orthogonal CP eigenstates

$$|B_+^0\rangle = \frac{1}{\sqrt{2}} (|B^0\rangle + \text{CP}|B^0\rangle), \quad |B_-^0\rangle = \frac{1}{\sqrt{2}} (|B^0\rangle - \text{CP}|B^0\rangle) \quad (2.49)$$

with  $\text{CP}|B_+^0\rangle = |B_+^0\rangle$  and  $\text{CP}|B_-^0\rangle = -|B_-^0\rangle$  can be defined. If a state agrees with one of these except for a phase factor, it will be a CP eigenstate.

The mass eigenstates of the  $B^0/\bar{B}^0$  system are not CP eigenstates. Using  $\text{CP}|B^0\rangle = e^{i\phi_{\text{CP}B}}|\bar{B}^0\rangle$ , they

are transformed by a CP operation as

$$\begin{aligned} \text{CP } |B_L\rangle &= \left( \frac{e^{i\phi_{\text{CPB}}}}{2\eta_m} + \frac{e^{-i\phi_{\text{CPB}}}\eta_m}{2} \right) |B_L\rangle - \left( \frac{e^{i\phi_{\text{CPB}}}}{2\eta_m} - \frac{e^{-i\phi_{\text{CPB}}}\eta_m}{2} \right) |B_H\rangle \\ &\approx \cos 2\tilde{\beta} |B_L\rangle - \sin 2\tilde{\beta} |B_H\rangle \\ \text{CP } |B_H\rangle &= - \left( \frac{e^{i\phi_{\text{CPB}}}}{2\eta_m} + \frac{e^{-i\phi_{\text{CPB}}}\eta_m}{2} \right) |B_H\rangle + \left( \frac{e^{i\phi_{\text{CPB}}}}{2\eta_m} - \frac{e^{-i\phi_{\text{CPB}}}\eta_m}{2} \right) |B_L\rangle \\ &\approx -\cos 2\tilde{\beta} |B_H\rangle + \sin 2\tilde{\beta} |B_L\rangle \end{aligned}$$

Where the approximation for the  $B^0/\bar{B}^0$  system depends on the phase convention for the CKM matrix which determines the angle  $\tilde{\beta}$ . If  $\tilde{\beta} = 0$  is chosen by an appropriate phase redefinition e.g. of the  $b$  field, these states would be eigenstates with  $\text{CP} = \pm 1$ , respectively. Still, there would be CP violation in their decay, and the CP eigenvalue of the final state would be different. Therefore, the question of which of the mass eigenstates is closest to which CP eigenstate has no convention independent answer. Only the CP eigenvalue of a decay product of one of these states is an observable, and the weak interaction does not conserve CP.

A meaningful question is which of  $B_H$  or  $B_L$  **decays** more often into  $\text{CP} = \pm 1$  eigenstates. In contrast to the neutral kaon system, most final states from  $B$  decays are flavour-specific, and both mass eigenstates decay into them via either their  $B^0$  or their  $\bar{B}^0$  component. The small fraction of states that can be reached both by  $B^0$  and  $\bar{B}^0$  includes the contribution from CP eigenstates which appear mainly through three processes. On the tree level, there are two main decay channels that can produce CP eigenstates:  $b \rightarrow c\bar{c}d$  with the  $c\bar{c}d\bar{d}$  final state, and  $b \rightarrow u\bar{u}d$  with the quark content  $u\bar{u}d\bar{d}$ . A state of the first kind will have decay amplitudes

$$A = \langle X_{c\bar{c}} | \mathbf{H} | B^0 \rangle = V_{cb}^* V_{cd} A_0, \quad \bar{A} = \langle X_{c\bar{c}} | \mathbf{H} | \bar{B}^0 \rangle = \eta_X e^{-i\phi_{\text{CPB}}} V_{cb} V_{cd}^* A_0$$

where  $\eta_X = \pm 1$  is the CP eigenvalue of the state. The corresponding decay amplitudes of  $B_H$  and  $B_L$  are

$$\begin{aligned} A_{L,H} &= \langle X_{c\bar{c}} | \mathbf{H} | B_{L,H} \rangle = pA \pm q\bar{A} \\ &= pA \left( 1 \pm \eta_m \eta_X e^{-i\phi_{\text{CPB}}} \frac{V_{cb} V_{cd}^*}{V_{cb}^* V_{cd}} \right) \\ &= pA (1 \pm |\eta_m| \eta_X e^{-2i\beta}) \end{aligned}$$

The decay ratio is then (in the approximation  $|\eta_m| = 1$ )

$$\frac{|A_H|^2}{|A_L|^2} = \frac{|1 - \eta_X e^{-2i\beta}|^2}{|1 + \eta_X e^{-2i\beta}|^2} = \frac{1 - \eta_X \cos 2\beta}{1 + \eta_X \cos 2\beta} \quad (2.50)$$

which is for  $\beta < \frac{\pi}{4}$  less than 1 for  $\eta_X = +1$  and *vice versa*. In this case, the heavier state  $B_H$  will decay more often into states with negative CP eigenvalue,  $\eta_X = -1$ .

Accordingly, for the  $u\bar{u}d\bar{d}$  states

$$A_{L,H} = \langle X_{u\bar{u}} | \mathbf{H} | B_{L,H} \rangle = pA (1 \pm |\eta_m| \eta_X e^{2i\alpha})$$

and the ratio

$$\frac{|A_H|^2}{|A_L|^2} = \frac{|1 - \eta_X e^{2i\alpha}|^2}{|1 + \eta_X e^{2i\alpha}|^2} = \frac{1 - \eta_X \cos 2\alpha}{1 + \eta_X \cos 2\alpha}$$

depends on the angle  $\alpha$ , which is likely to be larger than  $\frac{\pi}{4}$ . This would give the opposite answer, i.e. the heavier state  $B_H$  will decay more often into states with positive CP eigenvalue,  $\eta_X = +1$ .

Some decays with an intermediate state  $c\bar{c}d\bar{s}$  or  $c\bar{c}\bar{d}s$  proceed into  $K^0$  or  $\bar{K}^0$ , which finally result in  $c\bar{c}d\bar{d}$  via a  $K_L^0$  or  $K_S^0$  sequential decay. Among those is the gold-plated decay  $B^0 \rightarrow J/\psi K_S^0$ . The total decay chain involves almost the same CKM element phase factors as the direct  $b \rightarrow c\bar{c}d$  decay, leading to the same answers as for this decay mode (a more detailed discussion follows below in section 2.3).

For decays via  $W$  exchange, like  $b\bar{d} \rightarrow c\bar{c}$  or  $b\bar{d} \rightarrow u\bar{u}$ , the same CKM elements are involved, and the same arguments lead to the same answers as above. Also, the favoured penguin-type transition  $b \rightarrow s$  with subsequent hadronization into a  $K_L^0$  or  $K_S^0$  has a net phase close to  $\beta'$  leading to the ratio (2.50).

CP eigenstates with quark content  $d\bar{d}$  can be reached via CKM-suppressed penguin-type loops. Due to the top quark dominance the amplitudes are

$$A = \langle X_{d\bar{d}} | \mathbf{H} | B^0 \rangle \approx V_{tb}^* V_{td} A_0, \quad \bar{A} = \langle X_{d\bar{d}} | \mathbf{H} | \bar{B}^0 \rangle \approx \eta_X e^{-i\phi_{CPB}} V_{tb} V_{td}^* A_0$$

and the CKM element phases cancel, which gives

$$\frac{|A_H|}{|A_L|} = \frac{1 - \eta_X}{1 + \eta_X}$$

i. e.  $B_H$  decays exclusively into states with negative CP eigenvalue,  $\eta_X = -1$ , and  $B_L$  into states with  $\eta_X = +1$ .

All these results receive corrections from non-leading terms, like  $c$  quark loops in the last case, or  $b \rightarrow d$  penguin corrections to the  $b \rightarrow u$  transition final states. Since systems with a  $c\bar{c}$  pair probably constitute the major part for both CP eigenvalues, the heavy mass eigenstate can be said to be the one which decays more often into final states with CP = -1, and the light one into those with CP = +1, but both have also substantial branching fractions into final states with the opposite CP value. This is a consequence of the CP violating phase in the CKM matrix, but is not a CP violating decay, since none of the two  $B$  mass eigenstates was a CP eigenstate before it decayed.

The situation would be different for a purely real CKM matrix (up to phases that can be removed by quark phase changes). In this case, all unitarity triangles would be degenerate to lines, and their angles would be 0 or  $\pi$ . Therefore,  $\cos 2\alpha = \cos 2\beta = 1$ , and the heavier state would be the **only** to decay to CP = -1, while CP = +1 final states would be reached exclusively via decays of  $B_L$ . For decay products which are CP eigenstates this situation would correspond to a perfectly predictable CP eigenvalue corresponding to the mass eigenstate  $B_L$  or  $B_H$ . A natural choice of phases in this case would force all terms of the weak interaction Hamiltonian to be real, corresponding to  $\eta_m = e^{i\phi_{CPB}}$ . Then CP  $|B_L\rangle = +|B_L\rangle = |B_+\rangle$  and CP  $|B_H\rangle = -|B_H\rangle = -|B_-\rangle$ , and CP is conserved in decays where this quantum number is meaningful.

Exactly this situation is **almost** true for the  $K^0/\bar{K}^0$  system. The light  $K_S^0$  decays to about 99.9% into the CP = +1 eigenstates  $\pi^+\pi^-$  and  $\pi^0\pi^0$ , while the  $K_L^0$  decays to one third into a CP = -1 eigenstate with 3 pions, the rest being mainly flavour specific semileptonic decays, and only 0.3% are to the CP = +1 two pion state [9]. Therefore, a parametrization is chosen where  $K_S^0 \approx K_+$  and  $K_L^0 \approx K_-$ . If we have a  $K_S^0$  as decay product of the  $B$ , we are used to assign it a CP = +1 eigenvalue contribution to the whole final state. To be precise, this is only correct if the  $K_S^0$  decays into a CP = +1 final state. In this case also a  $K_L^0 \rightarrow \pi\pi$  will be assigned the same CP = +1 eigenvalue, i. e. the “ $K_S^0$ ” denotes its final state rather than the undecayed particle, and a  $K_S^0 \rightarrow \pi l\nu$  as a flavour specific state is not included in this use of the label  $K_S^0$ .



### 2.2.5 Oscillation at the $\Upsilon(4S)$

The  $B\bar{B}$  system from strong interaction  $\Upsilon(4S)$  decay is in an odd C and P eigenstate with angular momentum  $L = 1$ , retaining the quantum numbers  $J^{PC} = 1^{--}$  of the mother particle. This system has to be treated as a coherent quantum state. The time evolution of a state with odd symmetry is different from that of one with even symmetry. This is due to the fact, that only one anti-symmetric  $X\bar{X}$  state,

$$|\bar{X}(1)X(2)\rangle - |X(1)\bar{X}(2)\rangle$$

is possible, so it has to stay constant. There are, however, three symmetric states,

$$\begin{aligned} &|\bar{X}(1)X(2)\rangle + |X(1)\bar{X}(2)\rangle \\ &|X(1)X(2)\rangle \\ &|\bar{X}(1)\bar{X}(2)\rangle \end{aligned}$$

and their relative amplitudes may change with time. The quantum numbers characterizing the two different mesons, which are represented by (1) and (2) here, can be thought of as the spatial wave functions  $\psi(\mathbf{x})$  and  $\psi(-\mathbf{x})$  or alternatively the states in momentum space  $|\mathbf{p}\rangle$  and  $|\mathbf{-p}\rangle$ .

Explicitly, for initial  $B\bar{B}$  states of well defined symmetry,

$$\psi(0) = |B^0(1)\bar{B}^0(2)\rangle \pm |B^0(2)\bar{B}^0(1)\rangle$$

the time evolution from (2.26b) translates into

$$\begin{aligned} \psi(t) = e^{-2imt}e^{-T} & \left[ \left( c^2|B^0(1)\bar{B}^0(2)\rangle + i\eta_m sc|\bar{B}^0(1)\bar{B}^0(2)\rangle + \frac{i}{\eta_m}sc|B^0(1)B^0(2)\rangle - s^2|B^0(2)\bar{B}^0(1)\rangle \right) \right. \\ & \left. \pm \left( c^2|B^0(2)\bar{B}^0(1)\rangle + i\eta_m sc|\bar{B}^0(1)\bar{B}^0(2)\rangle + \frac{i}{\eta_m}sc|B^0(1)B^0(2)\rangle - s^2|B^0(1)\bar{B}^0(2)\rangle \right) \right] \end{aligned} \quad (2.51)$$

for  $-$ :

$$\psi_-(t) = e^{-2imt}e^{-T} [ |B^0(1)\bar{B}^0(2)\rangle - |B^0(2)\bar{B}^0(1)\rangle ] \quad (2.51a)$$

for  $+$ :

$$\begin{aligned} \psi_+(t) = e^{-2imt}e^{-T} & \left[ \cos(x - iy)T (|B^0(1)\bar{B}^0(2)\rangle + |B^0(2)\bar{B}^0(1)\rangle) \right. \\ & \left. + i \sin(x - iy)T \left( \frac{1}{\eta_m}|B^0(1)B^0(2)\rangle + \eta_m|\bar{B}^0(1)\bar{B}^0(2)\rangle \right) \right] \end{aligned} \quad (2.51b)$$

where the shorthand notation  $s = \sin(x - iy)T/2$ ,  $c = \cos(x - iy)T/2$  has been used in (2.51). This means, the anti-symmetric state stays always a 100% correlated  $B\bar{B}$ , as long as none of them has decayed. This is a typical example of a coherent quantum state, where both mesons always have exactly opposite flavour, although none of the single mesons is in a flavour eigenstate. Only when one decays into a state revealing its flavour (not necessarily the first one that decays) the state ‘‘collapses’’ and the second one continues as a one-particle state evolving in time according to (2.26).

The second case (2.51b) of an even wave function leads to a probability oscillating with twice the single- $B$  frequency between a like-sign ( $BB$  or  $\bar{B}\bar{B}$ ) and opposite-sign ( $B\bar{B}$ ) flavour state.

For different times  $T_1$  and  $T_2$  of  $B$  meson (1) and (2), e.g. the times of decay of the two  $B$  mesons, we have for the anti-symmetric state

$$\begin{aligned} |\psi_-(T_1, T_2)\rangle = e^{(-im/\Gamma + \frac{1}{2})(T_1+T_2)} & \left[ \cos(x - iy)\frac{T_1 - T_2}{2} (|B^0(1)\bar{B}^0(2)\rangle - |B^0(2)\bar{B}^0(1)\rangle) \right. \\ & \left. - i \sin(x - iy)\frac{T_1 - T_2}{2} \left( \frac{1}{\eta_m}|B^0(1)B^0(2)\rangle - \eta_m|\bar{B}^0(1)\bar{B}^0(2)\rangle \right) \right] \end{aligned} \quad (2.52a)$$

$$\begin{aligned} = \frac{e^{(-im/\Gamma + \frac{1}{2})(T_1+T_2)}}{2pq} & \left[ \cos(x - iy)\frac{T_1 - T_2}{2} (-|B_L(1)B_H(2)\rangle + |B_L(2)B_H(1)\rangle) \right. \\ & \left. - i \sin(x - iy)\frac{T_1 - T_2}{2} (|B_L(1)B_H(2)\rangle + |B_L(2)B_H(1)\rangle) \right] \end{aligned} \quad (2.52b)$$

Again it is seen that for  $T_1 = T_2$  only the anti-symmetric state is present, and mixed states, i. e. two final states indicating the same beauty flavour, will show up only at  $T_1 \neq T_2$ . The mixing probability ( $B$  and  $\bar{B}$  denote the flavour at decay time)

$$\frac{N(BB + \bar{B}\bar{B})}{N(BB + B\bar{B} + \bar{B}B + \bar{B}\bar{B})} = \chi \quad (2.53)$$

is identical to that for a single  $B$  meson. This can be understood from the fact that the second  $B$  meson is in a flavour eigenstate exactly when the first one decays into a tagging mode, and then evolves in time as a single oscillating  $B$  meson until it decays itself. The probability can also be obtained from equation (2.52a) using  $N(BB) = \mathcal{N} \int |\langle B^0(1)B^0(2)|\psi_-(T_1, T_2)\rangle|^2 dT_1 dT_2$ , and  $N(\bar{B}\bar{B})$ ,  $N(B\bar{B})$ ,  $N(\bar{B}B)$  accordingly. The normalization factor  $\mathcal{N}$  depends on the branching fractions into tagging modes and in general on the parameters  $y$ ,  $\delta$  and  $x$ , but cancels anyway in the ratio.

For incoherent  $B^0\bar{B}^0$  pair production, e.g. in  $b\bar{b}$  jet fragmentation, the integrated mixed-rate is determined by two independent mixing probabilities

$$\frac{N(BB + \bar{B}\bar{B})}{N(BB + B\bar{B} + \bar{B}B + \bar{B}\bar{B})} = 2\chi(1 - \chi)$$

Equation (2.52b) is an expansion in the two mass eigenstates. The anti-symmetric wave function is always composed of two different states, there will be never  $B_H B_H$  or  $B_L B_L$ , even at different decay times.

The question of CP eigenstates can only be answered after both  $B$  mesons have decayed. This involves the phases in decay amplitudes, and includes all effects of CP violation which will be discussed in detail below.

For the symmetric state, the wave function is

$$\begin{aligned} |\psi_+(T_1, T_2)\rangle &= e^{(-im/\Gamma + \frac{1}{2})(T_1 + T_2)} \left[ \cos(x - iy) \frac{T_1 + T_2}{2} (|B^0(1)\bar{B}^0(2)\rangle + |B^0(2)\bar{B}^0(1)\rangle) \right. \\ &\quad \left. + i \sin(x - iy) \frac{T_1 + T_2}{2} \left( \frac{1}{\eta_m} |B^0(1)B^0(2)\rangle + \eta_m |\bar{B}^0(1)\bar{B}^0(2)\rangle \right) \right] \\ &= \frac{e^{(-im/\Gamma + \frac{1}{2})(T_1 + T_2)}}{2pq} \left[ \cos(x - iy) \frac{T_1 + T_2}{2} (|B_L(1)B_L(2)\rangle - |B_H(1)B_H(2)\rangle) \right. \\ &\quad \left. + i \sin(x - iy) \frac{T_1 + T_2}{2} (|B_L(1)B_L(2)\rangle + |B_H(1)B_H(2)\rangle) \right] \quad (2.54) \end{aligned}$$

This is very similar to the function of an anti-symmetric state, but the oscillation is in the **sum** of the two lifetimes instead of the lifetime difference.

In the approximation  $|\eta_m| = 1$  and  $y = 0$ , the integrated mixed-rate is

$$\frac{N(BB + \bar{B}\bar{B})}{N(BB + B\bar{B} + \bar{B}B + \bar{B}\bar{B})} = \frac{x^2(3 + x^2)}{2(1 + x^2)^2} = \chi(3 - 4\chi)$$

In the general case, it is

$$\frac{N(BB + \bar{B}\bar{B})}{N(BB + B\bar{B} + \bar{B}B + \bar{B}\bar{B})} = \frac{(1 + \delta^2)(x^2 + y^2)[3 - y^2 + x^2(1 + y^2)]}{2[(1 + x^2)^2(1 + y^2) - \delta^2(1 - x^2)(1 - y^2)^2]}$$

but cannot be related to the mixing probabilities of single mesons  $\chi$  and  $\bar{\chi}$ .

The expansion in mass eigenstates shows, that the symmetric wave functions consists always of two eigenstates with the same mass, i. e.  $B_H B_H$  or  $B_L B_L$ .

### 2.2.6 Determination of the Mixing Parameters of $B$ Mesons

Only a small fraction of  $B$  meson decays has been fully reconstructed. However, the flavour of a  $B$  meson can be identified by various “tags”. The first observation of a then unexpected large  $B^0\bar{B}^0$  mixing by ARGUS in 1987 [38] used the best flavour tags available: In multihadron events on the  $\Upsilon(4S)$  resonance, 25 like-sign lepton pairs were observed which could not be attributed to other sources but semileptonic  $B$  decays. The charge of the lepton from  $\bar{b} \rightarrow l^+ \nu \bar{c}$  in these decays is identical to the beauty (or bottomness) quantum number of the meson, and these events had to be attributed to  $B^0 B^0$  and  $\bar{B}^0 \bar{B}^0$  final states from  $\Upsilon(4S)$  decays. The mixing probability  $\chi$  can be calculated from the number of like- and opposite-sign dilepton events as

$$\chi = \frac{[N(l^+l^+) + N(l^-l^-)] \cdot (1+f)}{N(l^+l^+) + N(l^-l^-) + N(l^+l^-)}$$

where the ratio of semileptonic branching fractions of neutral and charged  $B$  mesons and of their production rates enters as

$$f = \frac{[\mathcal{B}(B^+ \rightarrow l^+ \nu X)]^2 \cdot \mathcal{B}(\Upsilon(4S) \rightarrow B^+ B^-)}{[\mathcal{B}(B^0 \rightarrow l^+ \nu X)]^2 \cdot \mathcal{B}(\Upsilon(4S) \rightarrow B^0 \bar{B}^0)}$$

In addition, this observation was supported by four events with one fully reconstructed  $B$  meson plus a lepton of “wrong” sign, and one exclusive event  $\Upsilon(4S) \rightarrow B^0 B^0$  with both  $B^0$  mesons reconstructed.

Results on mixing obtained on the  $\Upsilon(4S)$  are summarized in table 2.3. In addition to leptons and fully reconstructed  $B$  mesons as flavour tags also fully reconstructed  $D^{*\pm}$  mesons, partially reconstructed  $D^{*\pm} \rightarrow (D^0/\bar{D}^0)\pi^\pm$ , partially reconstructed  $B^0 \rightarrow D^{*-}l^+\nu$ , and charged kaons have been used.

0.10      0.20      0.30	$\chi$	tags	experiment
	$0.16 \pm 0.05$	$ll$	ARGUS 87 [38]
	$0.144 \pm 0.036 \pm 0.036$		CLEO 89 [40]
	$0.180 \pm 0.050$	$ll, D^*l, B^0l$	ARGUS 92 [41] *
	$0.157 \pm 0.016 \pm 0.018 \pm \begin{smallmatrix} 0.028 \\ 0.021 \end{smallmatrix}$	$ll$	CLEO 93 [42] *
	$0.149 \pm 0.023 \pm 0.021$	$B^0l$	CLEO 93 [42] *
	$0.162 \pm 0.044 \pm 0.039$	$(D^*)ll$	ARGUS 93 [43] *
	$0.20 \pm 0.13 \pm 0.12$	$D^*K$	ARGUS 96 [44]
	$0.19 \pm 0.07 \pm 0.09$	$B^0K$	ARGUS 96 [44] *
	$0.159 \pm 0.020$		all (*) averaged

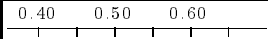

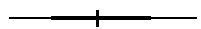



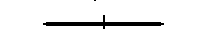




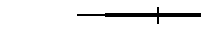





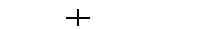
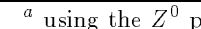

While only the integrated effect can be observed on the  $\Upsilon(4S)$  at presently existing symmetric colliders, an observation of the oscillating behaviour was possible at the  $Z^0$ , where the lifetime can be measured. This yields directly the frequency  $\Delta m$  from the asymmetry

$$a(t) = \frac{\dot{N}(B) - \dot{N}(\bar{B})}{\dot{N}(B) + \dot{N}(\bar{B})} \Big|_t = \cos \Delta m t$$

Results are summarized in table 2.4.

The mixing parameter  $x$  can be calculated from the mixing probability using (2.47) and from the oscillation frequency as  $x = \Delta m \tau$  which requires also precise knowledge on the average lifetime  $\tau_d = (1.54 \pm 0.03)$  ps of the  $B^0$  meson (table 2.2).

$$\begin{aligned} x &= \Delta m \tau = 0.729 \pm 0.027 && \text{LEP+SLD+CDF avg. 96} \\ x &= \sqrt{\frac{\chi}{\frac{1}{2} - \chi}} = 0.683 \pm 0.063 && \text{ARGUS, CLEO avg. 96} \\ x &= 0.722 \pm 0.025 && \text{common average} \end{aligned}$$

Table 2.4 $B^0/\bar{B}^0$ eigenstate mass difference from the oscillation frequency			
	$\Delta m$ [ $\text{ps}^{-1}$ ]	tags	experiment
	$0.52 \pm_{0.10}^{0.11} \pm_{0.03}^{0.04}$	$D^*l$	ALEPH 93 [39]
	$0.50 \pm_{0.06}^{0.07} \pm_{0.10}^{0.11}$	$ll$	ALEPH 94 [45]
	$0.436 \pm 0.026 \pm 0.020$	$D^*/l/\text{jet charge}$	ALEPH 96 [46] *
	$0.50 \pm 0.12 \pm 0.06$		DELPHI 94 [47]
	$0.531 \pm_{0.046}^{0.050} \pm 0.078$	$l/K/\text{jet charge}$	DELPHI 96 [48] *
	$0.496 \pm 0.034$	$D^*/l/\text{jet charge}$	DELPHI 97 [49] *
	$0.508 \pm 0.075 \pm 0.025$	jet charge	OPAL 94 [50]
	$0.548 \pm 0.050 \pm_{0.019}^{0.023}$	$D^*l$	OPAL 96 [51] *
	$0.444 \pm 0.029 \pm_{0.017}^{0.020}$	jet charge $l$	OPAL 97 [52] *
	$0.430 \pm 0.043 \pm_{0.030}^{0.028}$	$ll$	OPAL 97 [53] *
	$0.496 \pm_{0.051}^{0.055} \pm 0.043$	$ll$	L3 96 [54] *
	$0.58 \pm 0.07 \pm 0.08$	$K^a$	SLD 96 prel. [55] *
	$0.56 \pm 0.08 \pm 0.04$	jet charge $a$	SLD 96 prel. [55] *
	$0.520 \pm 0.072 \pm 0.035$	$l^a$	SLD 96 prel. [56] *
	$0.452 \pm 0.074 \pm 0.049$	jet charge $l^a$	SLD 96 prel. [57] *
	$0.446 \pm 0.057 \pm_{0.031}^{0.034}$	$(B\pi^+)$	CDF 96 [58] *
	$0.471 \pm_{0.068}^{0.078} \pm 0.034$	$\pi^+/Dl$	CDF 97 [59]
	$0.50 \pm 0.05 \pm 0.06$	$ll$	CDF 96 [60] *
	$0.474 \pm 0.015$		all (*) averaged

<sup>a</sup> using the  $Z^0$  polarization asymmetry at SLC

The two independent methods agree very well, and yield a common value of the scaled mass difference with 4% precision. A value  $x \approx 0.7$  compatible with the present best estimate will be used within this paper.

Table 2.5 $B_s/\bar{B}_s$ eigenstate mass difference from the oscillation frequency.	
$\Delta m$ [ $\text{ps}^{-1}$ ]	experiment
$> 1.8$ (95%CL)	ALEPH 94 [45]
$> 6.1$ (95%CL)	ALEPH 95 (jet charge $l$ ) [61]
$> 6.6$ (95%CL)	ALEPH 96 [62]
$> 3.1, \notin [5.0, 7.6]$ (95%CL)	OPAL 97 [52]
$> 7.8$ (95%CL)	ALEPH 96 [63]
$> 10.0$ (95%CL)	LEP combined 97 [64]

From average  $b/\bar{b}$  mixing at  $e^+e^-$  annihilation and  $Z^0$  decay, a value  $\chi_s \approx 0.5$  can be inferred with large errors ( $\gtrsim 0.2$  [9]) due to the small  $B_s$  fraction in  $b$  jets. Direct (non-) observations of the oscillation leads to more stringent limits on the frequency, summarized in table 2.5. For the  $B_s/\bar{B}_s$  system, using the latest lower limit on the oscillation frequency  $\Delta m_s > 7.8/\text{ps}$  and the  $B_s$  lifetime value  $\tau_s = (1.52 \pm 0.07)\text{ps}$  (table 2.6), the present lower limit is  $x_s > 15$ , which is already close to the lowest expected values. It corresponds to a mixing probability  $\chi_s > 0.496$ .

Table 2.6 $B_s$ lifetime measurements. Measurements which have been replaced by more recent ones are not included.		
1.2 1.3 1.4 1.5 1.6 1.7 1.8 1.9	$\tau_s$ [ps]	experiment
	$1.54 \pm^{0.25}_{0.21} \pm 0.06$	$D_s l$ , OPAL 95 [65]
	$1.37 \pm^{0.14}_{0.12} \pm 0.04$	$D_s l$ , CDF 96 [66]
	$1.34 \pm^{0.23}_{0.19} \pm 0.05$	$J/\psi \phi$ , CDF 96 [67]
	$1.65 \pm^{0.34}_{0.31} \pm 0.12$	$D_s h$ , DELPHI 96 [68]
	$1.60 \pm 0.26 \pm^{0.13}_{0.15}$	$D_s$ , DELPHI 96 [68]
	$1.76 \pm 0.20 \pm^{0.15}_{0.10}$	$\phi l$ , DELPHI 96 [68]
	$1.53 \pm^{0.17}_{0.15} \pm 0.07$	$D_s l$ , DELPHI 96 prel. [69]
	$1.61 \pm^{0.30}_{0.29} \pm^{0.18}_{0.16}$	$D_s h$ , ALEPH 96 [70]
	$1.54 \pm^{0.14}_{0.13} \pm 0.04$	$D_s l$ , ALEPH 96 [62]
	$1.72 \pm^{0.20}_{0.19} \pm^{0.18}_{0.17}$	$D_s$ , OPAL 97 [71]
	$1.52 \pm 0.07$	average

### 2.2.7 Predictions for $x_s$ , $y_s$ and $\delta_s$

Since the lifetimes of  $B^0$  and  $B_s$  agree within present precision, a first approximation using (2.32) is

$$\frac{x_s}{x_d} \sim \frac{|V_{ts}|^2}{|V_{td}|^2}$$

which gives an estimate of the expected  $x_s$  range between 3 and 100. It suffers from the poor knowledge on  $V_{td}$ , which has to be obtained from the measured  $x_d$ . With the top mass known and lattice calculations giving more reliable numbers for  $f_B$ ,  $f_{B_s}$ ,  $B_B$  and  $B_{B_s}$ , theoretical predictions for  $x_s$  become more precise. The Standard Model now favours numbers between 15 and 40. Recently reported ranges are  $13.4 \dots 27.8$  [18] and  $20.1 \pm^{11.6}_{9.7}$  [72].

The  $B_s$  meson eigenstates are expected to have also different widths. A value of  $2y_s = \Delta\Gamma/\Gamma \approx 0.18 \left(\frac{f_{B_s}}{200 \text{ MeV}}\right)^2$  is predicted from quark level QCD calculations [73], a similar number  $2y_s \approx 0.15$  is obtained using exclusive decay channels [74]. In the naive quark model a larger value around 0.20 is expected, and a recent QCD evaluation gives  $2y_s = 0.16 \pm^{0.11}_{0.09}$  [75].

The refined ratio (2.38) is

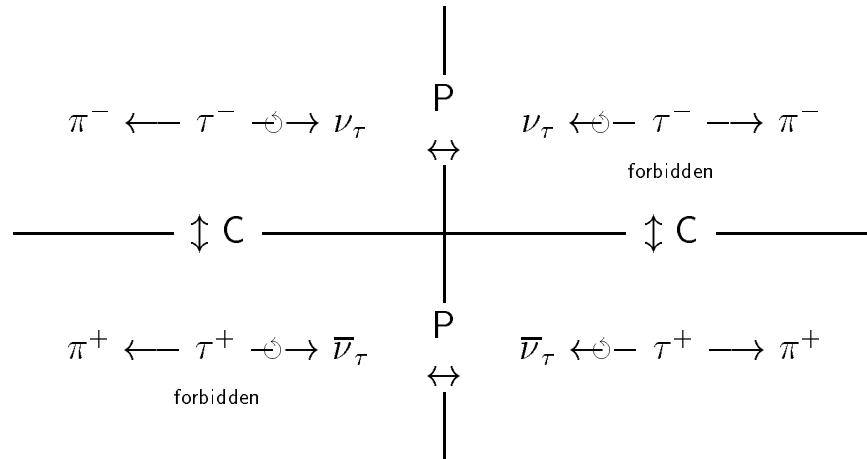
$$\frac{x_s}{2y_s} \approx -\frac{2 m_t^2}{\pi m_b^2} \frac{0.54 \pm 0.02}{3 - 8m_c^2/m_b^2} \approx -(200 \dots 250)$$

and corresponds to a lowest order estimate [76] neglecting QCD corrections. The range given reflects only a variation of quark masses.

Finally, replacing  $d$  with  $s$  equation (2.40) can be used to estimate  $\delta_s \sim \sin(\phi_2 + \phi_6)/2000 \sim 10^{-5}$ . Again, large corrections to this simple calculation may be expected.

## 2.3 CP Violation

Standard Model weak interactions are long known to violate parity and charge conjugation symmetries, in most cases even maximally. However, the combined symmetry operation CP leads generally to transitions identical to the original ones, i.e. CP symmetry is conserved. A typical example is the weak decay of a  $\tau$  lepton into  $\pi\nu_\tau$ , as shown in figure 2.6. While a  $\tau^-$  lepton can decay into a left-handed neutrino and a pion, the charge-conjugate decay of a  $\tau^+$  into a left-handed anti-neutrino is forbidden. However, if one looks at the mirror-image, i.e. one applies a parity transformation at the same time, the decay is allowed, and even more the amplitudes for both decays are equal. If we extend our definition of “anti-particle” to mean not only sign-flip of all charge-like quantities, but also of the spin, we have the CP operation and a perfect symmetry even for most weak-interaction processes. CP violation, on the contrary, is a true violation of particle anti-particle symmetry, which can not be restored by a mirror.



**Fig. 2.6** Parity (P) and charge conjugation (C) operations on  $\tau^- \rightarrow \pi^- \nu_\tau$ . The upper right and lower left processes are forbidden.

If all interactions were CP symmetric, we had no way to distinguish left-/right-handedness, positive/negative charge etc. Parity and C violation in weak interaction connects handedness with charge, but still does not allow a distinction between the two members of a pair. CP violating  $K^0$  decays, however, provide a different decay rate function of time for  $K^0$  and  $\bar{K}^0$ , which could be used to explicitly distinguish them by a dip or bump in this function.

Although we are presently not able to observe the difference of matter and anti-matter at far regions of the universe, the absence of regions of matter anti-matter annihilation boundaries suggests that the whole universe is made of matter, violating CP asymmetry to a large extent. Small asymmetries of the order  $10^{-10}$  at the early universe are sufficient to explain this present situation, however, it is difficult to create these from the CP violation in the Standard Model which has particle anti-particle asymmetry only in mesons, whereas baryon number violation is observed in the universe. If one assumes baryon number violating processes at phase boundaries of the early universe, e.g. at the symmetry breaking phase transition to the electroweak interaction in the Standard Model, still the CP asymmetry via the CKM phase is many orders of magnitude smaller than the observed number of baryons per background photon [77]. Thus, CP violating mechanisms beyond the Standard Model are likely to exist, and we will possibly observe them as small deviations from the Standard Model predictions.

The origin of CP violation in  $K$  and  $B$  mesons may be only within the Standard Model, but other possibilities are not ruled out. The observation of CP violation in  $B$  mesons may either yield a consistent picture with one set of Standard Model parameters, or produce contradictory results, making extensions or an alternative theory unavoidable.

Complementary searches for CP violation will give additional constraints: Only small CP violating effects are predicted by the Standard Model in weak decays of other particles, like  $D^0$  mesons or strange baryons [78]. CP asymmetries in the yet unobserved neutrino oscillations [79] or CP violation in lepton decay [80] are potential windows to alternative models. The search for magnetic monopoles or electric dipole moments [81] in pointlike or spherically symmetric particles, e. g. in leptons, quarks or the neutron, is another way to find non-standard CP violation. However, in contrast to CP violation in weak interaction, these would not be examples of broken symmetry between particles and anti-particles, but rather of mirror symmetry, while the charge conjugation symmetry is conserved. At present, only upper limits on these effects exist, and no glimpse beyond the Standard Model has been obtained.

### 2.3.1 CP Violation in $B$ Decays

The  $B^0/\bar{B}^0$  meson system has a simple description in the Standard Model: One parameter  $x$  is sufficient to parametrize the oscillation, since  $y = 0$  and  $|\eta_m| = 1$  are good approximations.

CP violation in  $B$  decays occurs always via interference, in three different ways:

- 1) Direct CP violation  $\Gamma(B \rightarrow X) \neq \Gamma(\bar{B} \rightarrow \bar{X})$  can be observed by final state counting experiments. An example is the  $B$  decay to  $K\pi$ , where an asymmetry

$$\frac{N(B^0 \rightarrow K^+\pi^-) - N(\bar{B}^0 \rightarrow K^-\pi^+)}{N(B^0 \rightarrow K^+\pi^-) + N(\bar{B}^0 \rightarrow K^-\pi^+)} \lesssim 0.1$$

is expected. Decays with CP asymmetries like this example require in the Standard Model (at least) two interfering channels with different CKM phase  $\phi_{1,2}$  and a strong phase difference  $\delta_{12} = \delta_2 - \delta_1$ . This defines the amplitudes

$$\begin{aligned} A(B^0 \rightarrow X) &= A_1 e^{i\phi_1} + A_2 e^{i\phi_2} e^{i\delta_{12}} \\ \bar{A}(\bar{B}^0 \rightarrow \bar{X}) &= A_1 e^{-i\phi_1} + A_2 e^{-i\phi_2} e^{i\delta_{12}} \end{aligned} \quad (2.55)$$

where  $A_1$  and  $A_2 e^{i\delta_{12}}$  is unchanged due to CP invariance of the strong interaction. They contribute to the rates as

$$\begin{aligned} |A|^2 &= |A_1|^2 + |A_2|^2 + 2 \mathcal{R}e(A_1 A_2^*) \cos(\phi_1 - \phi_2 - \delta_{12}) \\ |\bar{A}|^2 &= |A_1|^2 + |A_2|^2 + 2 \mathcal{R}e(A_1 A_2^*) \cos(\phi_2 - \phi_1 - \delta_{12}) \end{aligned}$$

which are different if  $\cos(\phi_1 - \phi_2 - \delta_{12}) \neq \cos(\phi_2 - \phi_1 - \delta_{12})$ . This is not the case if  $\delta_{12} = 0$  or if  $\phi_1 = \phi_2$ .

In the example  $B \rightarrow K\pi$ , the first amplitude is from a  $b \rightarrow s$  penguin diagram which has a dominant contribution from the  $t$  quark in the loop, with a CKM phase  $\arg(V_{tb}^* V_{ts})$  and a  $K\pi$  state with isospin  $\frac{1}{2}$ . The second amplitude occurs via a tree diagram  $b \rightarrow u + \bar{u}s$  transition, with  $\arg(V_{ub}^* V_{us})$  and isospin  $\frac{1}{2}$  and  $\frac{3}{2}$  amplitudes. The interference terms are proportional to  $\cos(\gamma' \pm \delta_{12})$ . Asymmetries of this type can also be observed in charged  $B$  decays, e. g.  $B^\pm \rightarrow K^\pm \pi^0$ .

CKM unitarity angles can be extracted from those asymmetries using flavour SU(3) and isospin relations to constrain the strong phase difference [82].

- 2) CP violation induces also a small asymmetry in the oscillation probability  $P(B^0 \rightarrow \bar{B}^0) \neq P(\bar{B}^0 \rightarrow B^0)$  due to  $|\eta_m| \neq 1$ . This is due to the interference of other amplitudes with the leading box diagram of  $B/\bar{B}$  mixing, with a  $t$  quark in the loop. The oscillation asymmetry (2.42) starting with an initial  $B^0$  meson can be expanded in  $\delta$  as

$$a(T) = \frac{\dot{N}(B) - \dot{N}(\bar{B})}{\dot{N}(B) + \dot{N}(\bar{B})} \Big|_T = \frac{\cos xT}{\cosh yT} + \delta \left( 1 - \frac{\cos^2 xT}{\cosh^2 yT} \right) + \mathcal{O}(\delta^2) \quad (2.56)$$

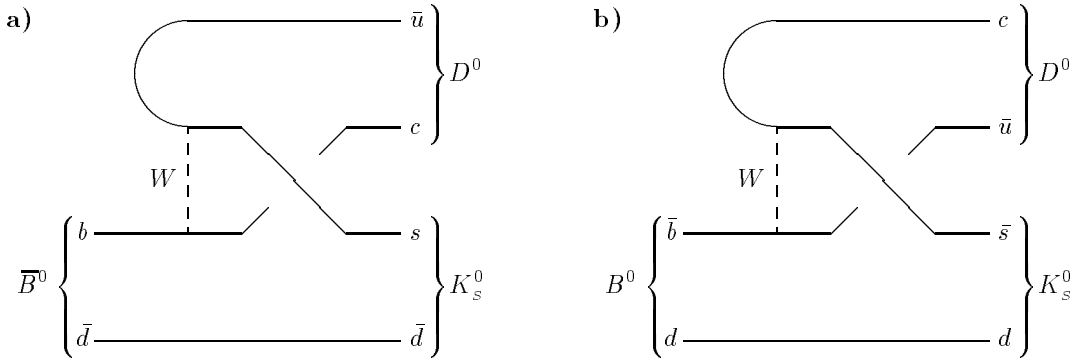


Fig. 2.7 Diagrams for  $\bar{B}^0 \rightarrow D^0 K_s^0$  (a) and  $B^0 \rightarrow D^0 K_s^0$  (b).

which is for  $y = 0$

$$a(T) \approx \cos xT + \delta \sin^2 xT = \cos xT + \frac{\delta}{2}(1 - \cos 2xT)$$

Starting with a  $\bar{B}^0$  at  $T = 0$  gives for the same asymmetry

$$\bar{a}(T) = \left. \frac{\dot{N}(B) - \dot{N}(\bar{B})}{N(B) + N(\bar{B})} \right|_T \approx -\cos xT + \frac{\delta}{2}(1 - \cos 2xT)$$

i. e. if  $\delta < 0$  as indicated by (2.40) there are always more  $B \rightarrow \bar{B}$  than  $\bar{B} \rightarrow B$  oscillations. Using leptons as flavour tag the net asymmetry can be observed at the  $\Upsilon(4S)$  as

$$\frac{N(B\bar{B} \rightarrow l^+l^+) - N(B\bar{B} \rightarrow l^-l^-)}{N(B\bar{B} \rightarrow l^+l^+) + N(B\bar{B} \rightarrow l^-l^-)} = \frac{1 - |\eta_m|^4}{1 + |\eta_m|^4} = \frac{2\delta}{1 + \delta^2}$$

and should be very small in the Standard Model, where (2.39) predicts  $|2\delta| \lesssim 10^{-3}$ . The first upper limit on this asymmetry of 0.18 (90%CL) [42] was still far above expectation. A recent measurement at LEP [52] gives a limit of 0.06 (90%CL) (assuming CPT symmetry).

- 3) The interference of oscillation and decay leads to lifetime dependent differences  $\Gamma(B^0|_{t=0} \rightarrow X|_t) \neq \Gamma(\bar{B}^0|_{t=0} \rightarrow X|_t)$  for a common final state of  $B$  and  $\bar{B}$  with asymmetry amplitude modulation  $\propto \sin \Delta m t$ .

The final state  $X$  can be a CP eigenstate, like  $J/\psi K_s^0$  (CP = -1) or  $\pi^+\pi^-$  (CP = +1), or a state that can be reached from both  $B^0$  mesons via different processes, like  $B^0 \rightarrow D^0 K_s^0$  and  $\bar{B}^0 \rightarrow D^0 K_s^0$  (figure 2.7).

In the Standard Model, CP violating interference can lead to almost maximum asymmetries. In many cases, large values are expected, and the time-dependence is a further handle to avoid misinterpretation of data. Therefore, all proposed experiments focus on these effects, which will be described in the next section.

A unique case of this interference can be observed in coherent anti-symmetric  $B\bar{B}$  states, i. e. in  $\Upsilon(4S) \rightarrow B^0\bar{B}^0$ , as a single event

$$\Upsilon(4S) \rightarrow B\bar{B} \rightarrow XY$$

with  $\text{CP}(XY) = \text{CP}(X)\text{CP}(Y)(-1)^L = -1 \neq \text{CP}(\Upsilon(4S)) = +1$ . Here  $X$  and  $Y$  must be CP eigenstates, and the expected rate for such events varies with the lifetime difference of the two  $B$  mesons.



### 2.3.2 CP Violation in Common Final States of $B^0$ and $\bar{B}^0$

The most pronounced manifestation of CP violation in the  $B^0/\bar{B}^0$  system is expected in interference of oscillation and decay to final states common to  $B^0$  and  $\bar{B}^0$  [83,84]. The effect is largest for CP eigenstates, but may occur at any final state where the amplitudes of the mixed and unmixed decay can interfere:

$$\begin{array}{ccc} & \bar{B}^0 & \\ & \nearrow \quad \searrow & \\ B^0 & \longrightarrow & X \end{array} \quad (2.57)$$

The simplest situation is the evolution of an isolated  $B^0$  meson produced (e.g. incoherently in  $b\bar{b}$  fragmentation) at  $t = 0$  as a flavour eigenstate. An unambiguous flavour tag for the state at production time may be a charged state from the second  $b$ , which cannot mix. The amplitude for  $B|_{t=0} \rightarrow X|_{t=T}$  is derived from (2.27) as

$$\mathcal{M}(B^0 \rightarrow X) = e^{-imt-T/2} A \left\{ \cos(x-iy) \frac{T}{2} - ir \sin(x-iy) \frac{T}{2} \right\}$$

using the ratio of the upper and lower path's amplitudes in (2.57)

$$r := \frac{\eta_m \bar{A}}{A}$$

where  $A = A(B^0 \rightarrow X)$  and  $\bar{A} = A(\bar{B}^0 \rightarrow X)$  are the decay amplitudes of the flavour eigenstates. The cos-term describes the lower path with pure  $b/\bar{b}$  oscillation, while the sin-term is a true interference term that vanishes if  $r = 0$ . The amplitude for  $\bar{B}|_{t=0} \rightarrow X|_{t=T}$  is

$$\bar{\mathcal{M}}(\bar{B}^0 \rightarrow X) = e^{-imt-T/2} \bar{A} \left\{ \cos(x-iy) \frac{T}{2} - \frac{i}{r} \sin(x-iy) \frac{T}{2} \right\}$$

If  $X$  is a CP eigenstate, the ratio  $\bar{A}/A$  is just a phase, which includes the sign of the CP eigenvalue of  $X$ . The phase of the product  $r$  is independent of conventions, and is in fact an observable, as will be shown below. More general,  $A$  and  $\bar{A}$  can have also different magnitudes. Figure 2.7 shows an example for this case, where the diagrams for  $\bar{B}^0 \rightarrow D^0 K_s^0$  and  $B^0 \rightarrow D^0 K_s^0$  are different. Another example is a mixture of CP eigenstates, as in the final state  $D^{*+} D^{*-}$  which is CP = -1 for  $L = 1$  and CP = +1 for  $L = 0$  or 2.

The corresponding decay rates are proportional to

$$\begin{aligned} |\mathcal{M}|^2 &= e^{-T} \left\{ |A|^2 \left| \cos(x-iy) \frac{T}{2} \right|^2 + |A|^2 |r|^2 \left| \sin(x-iy) \frac{T}{2} \right|^2 \right. \\ &\quad \left. + i \sin x \frac{T}{2} \cos x \frac{T}{2} (A^* \bar{A} \eta_m - A \bar{A}^* \eta_m^*) + \sinh y \frac{T}{2} \cosh y \frac{T}{2} (A^* \bar{A} \eta_m + A \bar{A}^* \eta_m^*) \right\} \end{aligned} \quad (2.58)$$

$$\begin{aligned} &= e^{-T} |A|^2 \left\{ \frac{1+|r|^2}{2} \cosh yT + \frac{1-|r|^2}{2} \cos xT + \cos(\arg r) \sinh yT - \sin(\arg r) \sin xT \right\} \\ &= e^{-T} |A|^2 \left\{ \frac{1+|r|^2}{2} \cosh yT + \frac{1-|r|^2}{2} \cos xT + \mathcal{R}e r \sinh yT - \mathcal{I}m r \sin xT \right\} \end{aligned} \quad (2.58a)$$

$$\begin{aligned} |\bar{\mathcal{M}}|^2 &= e^{-T} |\bar{A}|^2 \left\{ \frac{1+|r|^2}{2|r|^2} \cosh yT - \frac{1-|r|^2}{2|r|^2} \cos xT + \frac{\cos(\arg r)}{|r|} \sinh yT + \frac{\sin(\arg r)}{|r|} \sin xT \right\} \\ &= e^{-T} \frac{|A|^2}{|\eta_m|^2} \left\{ \frac{1+|r|^2}{2} \cosh yT - \frac{1-|r|^2}{2} \cos xT + \mathcal{R}e r \sinh yT + \mathcal{I}m r \sin xT \right\} \end{aligned} \quad (2.58b)$$

where the oscillating interference term is proportional to

$$\frac{1}{2} (A^* \bar{A} \eta_m - A \bar{A}^* \eta_m^*) = \mathcal{I}m(A^* \bar{A} \eta_m) = |A|^2 |r| \sin \arg r = |A|^2 \cdot \mathcal{I}m r$$

and the relaxation part of the interference is proportional to  $|r| \cos \arg r = \mathcal{R}e r$ . For decays to CP eigenstates,  $|r| = |\eta_m| \approx 1$  and the amplitude of the asymmetry oscillation is the sine of the phase angle  $\arg r$ . For decays like  $B^0/\bar{B}^0 \rightarrow D^0 K_s^0$  where  $|A| \neq |\bar{A}|$  and consequently  $|r| \neq 1$ , the asymmetry oscillation gets a physical dilution factor

$$D_P = \frac{2|r|}{1+|r|^2} = \frac{2|A||\bar{A}|}{|A|^2 + |\bar{A}|^2}$$

to the  $\sin xT$  term, and a mixing contribution as an additional  $\cos xT$  term.

In the approximation  $|\eta_m| = 1$  and  $y = 0$  the rates are given by

$$|\mathcal{M}|^2 = e^{-T} \left\{ \frac{|A|^2 + |\bar{A}|^2}{2} + \frac{|A|^2 - |\bar{A}|^2}{2} \cos xT - |A||\bar{A}| \sin(\arg r) \sin xT \right\} \quad (2.59)$$

$$|\bar{\mathcal{M}}|^2 = e^{-T} \left\{ \frac{|A|^2 + |\bar{A}|^2}{2} - \frac{|A|^2 - |\bar{A}|^2}{2} \cos xT + |A||\bar{A}| \sin(\arg r) \sin xT \right\}$$

This leads to an oscillating asymmetry as a function of the proper lifetime of the signal- $B$

$$a(T) = \frac{\dot{N}(\bar{B}^0 \rightarrow X) - \dot{N}(B^0 \rightarrow X)}{\dot{N}(\bar{B}^0 \rightarrow X) + \dot{N}(B^0 \rightarrow X)} \Big|_T = \Theta_0 \cos xT + A_0 \sin xT \quad (2.60)$$

where the  $B$  flavours are taken at  $T = 0$ , and the amplitudes are

$$\Theta_0 = \frac{|r|^2 - 1}{|r|^2 + 1}, \quad A_0 = \frac{2 \mathcal{I}m r}{1 + |r|^2} = D_P \sin \arg r$$

If in addition  $|A| = |\bar{A}|$ , especially if  $X$  is a CP eigenstate, this simplifies further to  $|r| = 1$ :

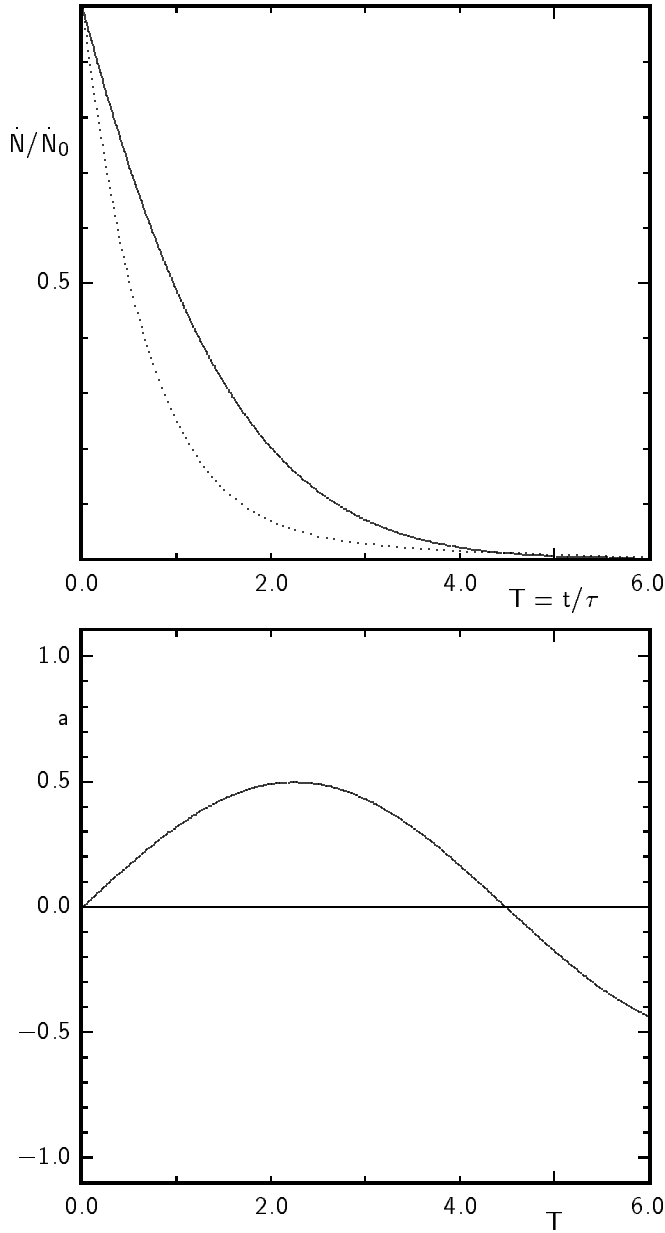
$$\begin{aligned} |\mathcal{M}|^2 &= e^{-T} |A|^2 \left\{ 1 - \sin(\arg r) \sin xT \right\} \\ |\bar{\mathcal{M}}|^2 &= e^{-T} |A|^2 \left\{ 1 + \sin(\arg r) \sin xT \right\} \end{aligned} \quad (2.61)$$

The corresponding rates  $\dot{N}(B^0|_{T=0} \rightarrow X) \propto |\mathcal{M}|^2$  and  $\dot{N}(\bar{B}^0|_{T=0} \rightarrow X) \propto |\bar{\mathcal{M}}|^2$  are illustrated in figure 2.8. They show a time-dependent asymmetry

$$a(T) = \frac{\dot{N}(\bar{B}^0 \rightarrow X) - \dot{N}(B^0 \rightarrow X)}{\dot{N}(\bar{B}^0 \rightarrow X) + \dot{N}(B^0 \rightarrow X)} \Big|_T = A_0 \sin xT \quad (2.62)$$

with  $A_0 = \sin \arg r$ .

The scaling time variable is  $T = t_s/\tau$  defined by the signal  $B$  lifetime  $t_s$  for incoherent  $b\bar{b}$  production. It has to be replaced by  $T = (t_s - t_t)/\tau$  for coherent  $B\bar{B}$  production on the  $\Upsilon(4S)$ , where  $t_t$  denotes the second  $B$  meson in the  $\Upsilon(4S)$  decay in a flavour tagging decay mode. This is in full analogy to the mixing situation described in section 2.2.5, and will be discussed in more detail below.



**Fig. 2.8** Time dependent rate of  $\bar{B}^0 \rightarrow J/\psi K_s^0$  (—) and  $B^0 \rightarrow J/\psi K_s^0$  (.....) for  $A_0 = \sin 2\beta = 0.5$  and  $x = 0.70$ . The lower plot shows the asymmetry  $a(T)$ .

### 2.3.2.1 The $B_s/\bar{B}_s$ Case

For the  $B_s$  meson,  $y$  is not negligible, and the asymmetry (2.60) is modulated,

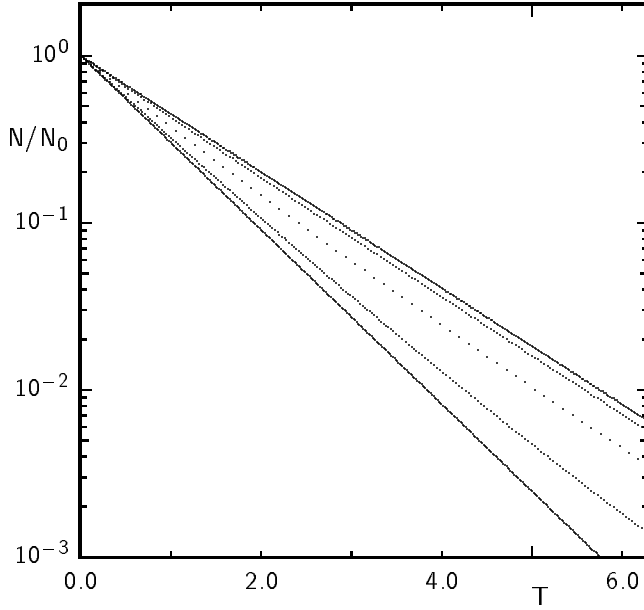
$$a(T) = \frac{\dot{N}(\bar{B}_s \rightarrow X) - \dot{N}(B_s \rightarrow X)}{\dot{N}(\bar{B}_s \rightarrow X) + \dot{N}(B_s \rightarrow X)} \Big|_T = \frac{\Theta_0 \cos xT + A_0 \sin xT}{\cosh yT + \Omega_0 \sinh yT} \quad (2.63)$$

where  $\delta_s = 0$  is used, which is believed to be a very good approximation, and

$$\Theta_0 = \frac{|r|^2 - 1}{|r|^2 + 1}, \quad A_0 = \frac{2\mathcal{I}m r}{1 + |r|^2} = D_P \sin \arg r, \quad \Omega_0 = \frac{2\mathcal{R}e r}{1 + |r|^2} = D_P \cos \arg r$$

with  $A_0^2 + \Theta_0^2 + \Omega_0^2 = 1$ . For the simpler case  $|r| = 1$  the asymmetry is

$$a(T) = \frac{\dot{N}(\bar{B}_s \rightarrow X) - \dot{N}(B_s \rightarrow X)}{\dot{N}(\bar{B}_s \rightarrow X) + \dot{N}(B_s \rightarrow X)} \Big|_T = \frac{A_0 \sin xT}{\cosh yT + \Omega_0 \sinh yT} \quad (2.64)$$



**Fig. 2.9** Time dependent rate of  $B_s + \bar{B}_s \rightarrow X$  for  $\arg r = 0$  or  $\pi$  (—), for  $\arg r = \pi/4$  or  $3\pi/4$  (-----), and for  $\arg r = \pi/2$  (.....), using  $y = -0.2$ .

with  $A_0 = \sin \arg r$  and  $\Omega_0 = \cos \arg r$ . This opens an alternative way to measure CP violation parameter  $\arg r$ . The time evolution of an equal, untagged mixture of  $B_s$  and  $\bar{B}_s$  mesons is given by

$$|\mathcal{M}|^2 + |\bar{\mathcal{M}}|^2 = 2e^{-T}|A|^2 \frac{1+|r|^2}{2} \left\{ \cosh yT + \Omega_0 \sinh yT \right\} \quad (2.65)$$

For decays into CP eigenstates  $|r| = 1$ , and the time dependence of the decay probability is simply

$$\begin{aligned} |\mathcal{M}|^2 + |\bar{\mathcal{M}}|^2 &= 2e^{-T}|A|^2 \left\{ \cosh yT + \cos \arg r \cdot \sinh yT \right\} \\ &= |A|^2 \left\{ (1 + \Omega_0)e^{-t/\tau_L} + (1 - \Omega_0)e^{-t/\tau_H} \right\} \end{aligned} \quad (2.66)$$

i. e. it is a sum of two exponential distributions with weights  $(1 \pm \Omega_0) = (1 \pm \cos \arg r)$ . This case is illustrated in figure 2.9 on a logarithmic scale. The upper and lower solid curve correspond to the CP conserving case  $r = \pm 1$ , where e. g.  $B_{sL}$  decays into either CP = +1 or CP = -1 eigenstates exclusively, and  $B_{sH}$  into the opposite one. The central curve corresponds to maximum CP violation, i. e.  $\mathcal{R}e r = 0$ , where both  $B_{sL}$  and  $B_{sH}$  decay into CP = +1 and CP = -1 eigenstates with the same probability, The other two curves correspond to  $\cos \arg r = \pm 0.7$ .

If  $\arg r = 2\phi_{\text{CKM}}$  is a large angle, a measurement of  $\cos 2\phi_{\text{CKM}}$  via the mixture of short and long lived states is complementary to a measurement of  $\sin 2\phi_{\text{CKM}}$  via an oscillating asymmetry function (2.64). Due to the large value of  $x_s$ , the latter requires a very precise measurement of the individual lifetimes and flavour tagging, while the decomposition of the short and long lived fractions can be done with untagged events and a modest resolution, but requires a large data sample.

### 2.3.2.2 Final CP Eigenstates from $B^0$ or $B_s$ Decays

Weak decay amplitudes can be described by (2.12) and (2.13). For CP eigenstates with eigenvalue  $\eta_X$  their ratio is then given by

$$\frac{\bar{A}}{A} = \eta_X e^{-i(\phi_{\text{CPB}} + 2 \arg V)} \quad (2.67)$$

where  $\arg V$  is the phase angle of the CKM elements involved in  $A$  (i. e. the  $B^0$  or  $\bar{b}$  decay amplitude). Using the CKM representation (2.9) with  $\eta_m = e^{i(\phi_{\text{CPB}} - 2\tilde{\beta})}$  results in

$$r = \eta_X e^{-2i(\arg V + \tilde{\beta})} \quad (2.68)$$

which is a convention independent phase factor of a product of four or more CKM elements. It can be transformed into an  $\epsilon$  parameter

$$\epsilon_X := \frac{1-r}{1+r} \quad (2.69)$$

which is, in contrast to  $\epsilon$  defined by (2.22), convention independent, but is specific to a final state  $X$ . A measurement of the angle  $\beta = \arg(-V_{td}^* V_{tb} V_{cd} V_{cb}^*)$  in the CKM triangle (figure 2.1a) requires a decay with  $\bar{b} \rightarrow \bar{c} + c\bar{d}$ . Examples for final states with this quark content are  $J/\psi \pi^0$  or  $D^+ D^-$ . In these decays one has  $r = \eta_X e^{-2i\beta}$ .

Similarly, for other final states common to  $B$  and  $\bar{B}$  the rephasing invariant net product of CKM elements in the combined amplitude/mixing phase ratio  $r$  is easily extracted using (2.9). A summary of common final states of  $B^0$  and  $\bar{B}^0$  is given in table 2.7. Since the spectator with a  $b$  quark is a  $\bar{d}$  quark, the decay products of the  $b$  must have the net flavour of a  $d$  quark, accompanied by one or more quark anti-quark pair.

<b>Table 2.7</b> Examples of CP eigenstates as final states of $B^0$ and $\bar{B}^0$ , and their sensitivity to the CKM phases. The asymmetry (2.62) has an amplitude $A_0 = -\eta_X \sin 2\phi_{\text{CKM}}$ .			
$b$ decay	$\prod$ CKM elements	angle $\phi_{\text{CKM}}$	some final states
$b \rightarrow c\bar{c}d$	$V_{tb}^* V_{td} V_{cd}^* V_{cb}$	$\beta$	$(J/\psi, \psi', \eta_c \dots) + (\pi^0, \eta, \rho^0 \dots), D^{(*)+} D^{(*)-}$
$b \rightarrow c\bar{c}s, s \rightarrow u\bar{u}d$	$V_{tb}^* V_{td} V_{cs}^* V_{cb} V_{ud}^* V_{us}$	$\beta - \phi_4 - \phi_6$	$(J/\psi, \psi', \eta_c \dots) + (K_S^0, K_L^0 \pi^0 \dots)$
$b \rightarrow c\bar{c}s, s\bar{d} \rightarrow K_L^0$	$V_{tb}^* V_{td} V_{cs}^* V_{cb} V_{cd}^* V_{cs}$	$\beta$	$(J/\psi, \psi', \eta_c \dots) + K_L^0$
$b \rightarrow u\bar{u}d$	$V_{tb}^* V_{td} V_{ud}^* V_{ub}$	$-\alpha$	$\pi\pi, \rho\rho \dots$
$b \rightarrow d$	$V_{tb}^* V_{td} V_{tb}^* V_{tb}$	0	$\pi^0 \eta', \dots$
$b \rightarrow s, s \rightarrow u\bar{u}d$	$V_{tb}^* V_{td} V_{ts}^* V_{tb} V_{ud}^* V_{us}$	$\beta'$	$(K_S^0, K_L^0 \pi^0 \dots) + (\pi^0, \eta, \eta', \rho^0, \omega, \phi \dots)$
$b \rightarrow s, s\bar{d} \rightarrow K_L^0$	$V_{tb}^* V_{td} V_{ts}^* V_{tb} V_{cd}^* V_{cs}$	$\beta' + \phi_4 + \phi_6$	$K_L^0 + (\pi^0, \eta, \eta', \rho^0, \omega, \phi \dots)$

Only the dominant contribution to the box diagram for  $B^0 \bar{B}^0$  mixing and to the penguin transitions  $b \rightarrow d$  and  $b \rightarrow s$  are considered in table 2.7. Very small modifications to the phase angles  $\phi_{\text{CKM}}$  will emerge from corrections to this approximation.

A special case are final states with a  $K_S^0$  or  $K_L^0$ . If it decays subsequently into a  $\text{CP} = \pm 1$  eigenstate, the whole system can still be taken as a CP eigenstate, and used to extract unitarity angles. In the tables, the tree level decay  $s \rightarrow u + \bar{u}d$  is used to determine the CKM phase angles. There may be penguin contributions as well, which modify the asymmetry. For a  $c$  quark in the loop, the relevant unitarity angle for  $B^0 \rightarrow c\bar{c}K_{S,L}$  is exactly  $\beta$ , for a  $u$  quark it is the same as for the tree diagram, and for a  $t$  quark it is the small angle  $\phi_2 + \phi_6$ .

A more precise treatment of the whole system includes oscillation and decay of the kaons as well, leading to four amplitudes which all interfere:

$$\begin{aligned} A_1 &:= A(B \rightarrow B|t_B) \cdot A(B \rightarrow c\bar{c}K) \cdot A(K \rightarrow K|t_K) \cdot A(K \rightarrow \pi\pi) \\ A_2 &:= A(B \rightarrow B|t_B) \cdot A(B \rightarrow c\bar{c}K) \cdot A(K \rightarrow \bar{K}|t_K) \cdot A(\bar{K} \rightarrow \pi\pi) \\ A_3 &:= A(B \rightarrow \bar{B}|t_B) \cdot \bar{A}(\bar{B} \rightarrow c\bar{c}\bar{K}) \cdot A(\bar{K} \rightarrow \bar{K}|t_K) \cdot A(\bar{K} \rightarrow \pi\pi) \\ A_4 &:= A(B \rightarrow \bar{B}|t_B) \cdot \bar{A}(\bar{B} \rightarrow c\bar{c}\bar{K}) \cdot A(\bar{K} \rightarrow K|t_K) \cdot A(K \rightarrow \pi\pi) \end{aligned}$$

Here the oscillation amplitudes  $A(K \rightarrow K)$  etc. depend on the kaon lifetime  $t_K$ . For  $t_K = 0$  we have  $A(\bar{K} \rightarrow K) = A(K \rightarrow \bar{K}) = 0$  and an oscillation  $A_0 \sin \Delta m_B t_B$  with an amplitude  $A_0 = \sin 2(\tilde{\beta} - \phi_6)$  as given in table 2.7. For other times  $t_K$ , the argument  $\tilde{\beta} - \phi_6 \approx \tilde{\beta}$  changes by a phase angle of  $\mathcal{O}(\lambda^4)$ . This is small compared to  $\tilde{\beta}$ , so it still measures  $\tilde{\beta}$  to that precision for any kaon lifetime.

If the final kaon is a  $K_L^0$ , it will usually be detected via its strong interaction—of a strangeness flavour component—with the detector material. Since the cross section for its  $\bar{K}^0$  part is considerably larger

than that of the  $K^0$  part, only two amplitudes need to be considered:

$$\begin{aligned} A_2 &:= A(B \rightarrow B|t_B) \cdot A(B \rightarrow c\bar{c}K) \cdot A(K \rightarrow \bar{K}|t_K \rightarrow \infty) \\ A_3 &:= A(B \rightarrow \bar{B}|t_B) \cdot \bar{A}(\bar{B} \rightarrow c\bar{c}\bar{K}) \cdot A(\bar{K} \rightarrow \bar{K}|t_K \rightarrow \infty) \end{aligned}$$

Their ratio is

$$\frac{A_3}{A_2} = \frac{A(B \rightarrow B|t_B)}{A(B \rightarrow \bar{B}|t_B)} \cdot \frac{V_{cb}V_{cs}^*}{V_{cb}^*V_{cs}} e^{i\phi_{\text{CP}K}} \cdot \frac{1}{-\eta_{mK}}$$

The last factor for the  $K^0/\bar{K}^0$  system is obtained using the limits  $T \rightarrow \infty$  of (2.27) as

$$\begin{aligned} A(K \rightarrow \bar{K}) &= e^{-imt-T/2} \left[ -i\eta_{mK} \sin(x-iy) \frac{T}{2} \right] \\ &= e^{-imt} e^{-T/2} \left[ -i\eta_{mK} \frac{e^{(ix+y)T/2} - e^{-ix-y)T/2}}{2i} \right] \rightarrow -e^{-imt} \frac{\eta_{mK}}{2} e^{(ix+y-1)T/2} \end{aligned} \quad (2.70)$$

and (2.28) as

$$A(\bar{K} \rightarrow \bar{K}) = e^{-imt-T/2} \left[ \cos(x-iy) \frac{T}{2} \right] \rightarrow -e^{-imt} \frac{1}{2} e^{(ix+y-1)T/2} \quad (2.71)$$

For the leading term in the box diagram it is given by

$$\eta_{mK} = e^{i(\phi_{\text{CP}K} + 2 \arg V_{cs}^{*2} V_{cd}^2)}$$

which yields

$$\frac{A_3}{A_2} \approx \frac{A(B \rightarrow B|t_B)}{A(B \rightarrow \bar{B}|t_B)} \cdot \frac{V_{cb}V_{cd}^*}{V_{cb}^*V_{cd}} \cdot (-1)$$

i.e. it behaves indeed as a  $b \rightarrow c\bar{c}d$  state with  $\text{CP} = -1$ .

The angles to be measured via oscillation/decay interference include all the factor  $V_{tb}^*V_{td}$  from mixing, which is one side in the triangle 2.7k. Hence only the adjacent angles  $\alpha$  and  $\beta$  can be measured this way. Similarly, interference in  $B_s$  oscillation can be used to measure the angles in the flat triangle 2.7l (see table 2.8). One of them,  $\gamma' = \tilde{\gamma} - \phi_2$ , is identical to an angle in (2.7h), and differs from the third angle  $\gamma$  in (2.7k) only at order  $\lambda^2$ . This would allow a test of  $\alpha + \beta + \gamma = 1$  to  $\mathcal{O}(\lambda^2)$ .

<b>Table 2.8</b> Examples of CP eigenstates as final states of $B_s$ and $\bar{B}_s$ , and their sensitivity to the CKM phases. The asymmetry (2.62) has an amplitude $A_0 = -\eta_X \sin 2\phi_{\text{CKM}}$ .			
$b$ decay	$\prod$ CKM elements	angle $\phi_{\text{CKM}}$	some final states
$b \rightarrow c\bar{c}s$	$V_{tb}^*V_{ts}V_{cs}^*V_{cb}$	$\phi_2 + \phi_6$	$(J/\psi, \psi', \eta_c \dots) + (\eta, \phi \dots), D_s^{(*)+} D_s^{(*)-}$
$b \rightarrow u\bar{u}s$	$V_{tb}^*V_{ts}V_{us}^*V_{ub}$	$\gamma'$	$\phi + (\pi^0, \rho^0 \dots), K^{(*)+} K^{(*)-}$
$b \rightarrow u\bar{u}d, \bar{s} \rightarrow \bar{u}d\bar{d}$	$V_{tb}^*V_{ts}V_{ud}^*V_{ub}V_{us}^*V_{ud}$	$\gamma'$	$(\pi^0, \eta, \rho^0 \dots) + (K_S^0, K_S^0 \pi^0 \dots)$
$b \rightarrow u\bar{u}d, \bar{s}d \rightarrow K_L^0$	$V_{tb}^*V_{ts}V_{ud}^*V_{ub}V_{cs}^*V_{cd}$	$\gamma' - \phi_4 - \phi_6$	$(\pi^0, \eta, \rho^0 \dots) + K_L^0$
$b \rightarrow s$	$V_{tb}^*V_{ts}V_{ts}^*V_{tb}$	0	$(\phi, \eta \dots) + (\pi^0, \eta' \dots)$
$b \rightarrow d, \bar{s} \rightarrow \bar{u}d\bar{d}$	$V_{tb}^*V_{ts}V_{td}^*V_{tb}V_{ud}^*V_{us}$	$-\beta'$	$(K_S^0, K_S^0 \pi^0 \dots) + (\eta' \dots)$
$b \rightarrow d, \bar{s}d \rightarrow K_L^0$	$V_{tb}^*V_{ts}V_{td}^*V_{tb}V_{cd}^*V_{cs}$	$-\beta' - \phi_4 - \phi_6$	$K_L^0 + (\eta' \dots)$

<b>Table 2.9</b> Examples of CP eigenstates relevant for $B^0$ decays, dependent on their relative orbital angular momentum $L$ .			
channel	$L$	CP	remarks
$J/\psi$		+1	
$\psi'$		+1	
$\chi$		+1	
$\eta_c$		-1	
$K_S^0$		+1	
$K_L^0$		-1	
$K^{*0} \rightarrow K_S^0 \pi^0$	1	+1	
$K^{*0} \rightarrow K_L^0 \pi^0$	1	-1	
$J/\psi K_S^0$	1	-1	
$J/\psi (K^{*0} \rightarrow K_S^0 \pi^0)$	0, 2	+1	helicities: $J_z = 0, \pm 1$
$J/\psi (K^{*0} \rightarrow K_L^0 \pi^0)$	1	-1	helicities: $J_z = \pm 1$
$\eta_c (K^{*0} \rightarrow K_S^0 \pi^0)$	1	+1	
$D^+ D^-$	0	+1	
$D^{*+} D^{*-}$	0, 2	+1	
$D^{*+} D^{*-}$	1	-1	
$\pi^+ \pi^-$	0	+1	
$\rho^+ \rho^-$	0, 2	+1	
$\rho^+ \rho^-$	1	-1	

If the given quark level transitions are the only contributions to a final state, the asymmetry with time is a simple  $\sin 2\phi_{\text{CKM}} \sin xT$  behaviour. However, many of the final states can be reached via loop graphs as well, often with different CKM elements involved. Many details can be found in a recent review [23]. In this case, both direct CP violation via the interfering amplitudes and the oscillation/decay interference lead to more complex asymmetries with the matrix elements (2.59) and both a  $\cos xT$  and  $\sin xT$  term.

The most promising examples are for  $\text{CP}(X) = -1$   $B \rightarrow J/\psi K_S^0$  with  $A_0 = \sin 2\beta$ , and for  $\text{CP}(X) = +1$   $B \rightarrow \pi^+ \pi^-$  with  $A_0 = \sin 2\alpha$  up to corrections from the penguin amplitude. The CP eigenvalues of related channels can be constructed from the data listed in table 2.9.

States with several possible angular momenta, like vector vector final states, are typically a mixture of  $\text{CP} = +1$  and  $-1$  eigenstates. Helicity 0 dominance would simplify these analyses, since it is forbidden for  $L = 1$  final states, and hence indicates a pure CP eigenstate. In general, though, these states have to be deconvoluted via a partial wave analysis.

### 2.3.2.3 Mixtures of CP Eigenstates

An example for a mixture of CP eigenstates is the final state  $D^{*+} D^{*-}$  which is  $\text{CP} = -1$  for  $L = 1$  and  $\text{CP} = +1$  for  $L = 0$  or 2. Other vector anti-vector decays like  $B_s \rightarrow D_s^{*+} D_s^{*-}$  or  $B^0 \rightarrow \rho^+ \rho^-$  or vector vector decays with two CP eigenstates like  $B_s \rightarrow J/\psi \phi$  or  $B^0 \rightarrow J/\psi (K_S^0 \pi^0)_{K^{*0}}$  show the same properties. In these cases the amplitude is

$$A = (V) \cdot (A_+ + A_-)$$

where  $(V)$  denotes the common CKM factors, and the subscripts of the residual factors are the CP eigenvalues, e.g.  $A(B^0 \rightarrow D^{*+} D^{*-}, L = 1) = V_{cb}^* V_{cd} A_-$  and  $A(B^0 \rightarrow D^{*+} D^{*-}, L = 0, 2) = V_{cb}^* V_{cd} A_+$ . They correspond to different helicities of the vector mesons, therefore the factors  $A_+$  and  $A_-$  have different phases changing with the angles of the decay products, e.g.  $D^{*+} \rightarrow D^0 \pi^+$  or  $J/\psi \rightarrow l^+ l^-$ .

Their ratio  $r_A := A_-/A_+$  depends on the decay angles, conveniently described as  $\theta_1, \theta_2$  and  $\phi_1 - \phi_2$  in the two helicity frames. The amplitude ratio observable in CP violation experiments is

$$r = e^{i\phi} \frac{1 - r_A}{1 + r_A}$$

where  $\phi$  is the invariant phase from the CKM elements in mixing and decay, which leads for  $B^0 \rightarrow D^{*+}D^{*-}$  to

$$e^{i\phi} = \eta_m \frac{V_{cb} V_{cd}^*}{V_{cb}^* V_{cd}} = e^{-2i\beta}$$

and the coefficients in the time evolution (2.58) are

$$\begin{aligned} \frac{1 + |r|^2}{2} &= \frac{1 + |r_A|^2}{1 + |r_A|^2 + 2 \operatorname{Re} r_A} \\ \frac{1 - |r|^2}{2} &= \frac{2 \operatorname{Re} r_A}{1 + |r_A|^2 + 2 \operatorname{Re} r_A} \\ \operatorname{Re} r &= |r| \cos \arg r = \frac{(1 - |r_A|^2) \cos \phi + 2 \operatorname{Im} r_A \sin \phi}{1 + |r_A|^2 + 2 \operatorname{Re} r_A} \\ \operatorname{Im} r &= |r| \sin \arg r = \frac{(1 - |r_A|^2) \sin \phi - 2 \operatorname{Im} r_A \cos \phi}{1 + |r_A|^2 + 2 \operatorname{Re} r_A} \end{aligned}$$

It has been emphasized in [85] that interference in mixed CP eigenstates like these can be used to observe a small phase angle  $\phi$  in untagged  $B_s$  decays. This is possible since the sum of both initial flavours is given by (2.65), being proportional to

$$|\mathcal{M}|^2 + |\overline{\mathcal{M}}|^2 = 2e^{-T} |A|^2 \left\{ \frac{1 + |r|^2}{2} \cosh yT - \operatorname{Re} r \sinh yT \right\}$$

and the coefficient of the  $\sinh yT$  term,  $\operatorname{Re} r$ , has a component  $\operatorname{Im} r_A \sin \phi$  which becomes dominant in regions of decay angle space where  $\operatorname{Im} r_A \gg 1 - |r_A|^2$ .

While helicity 0 corresponds to a pure CP eigenstate, the helicities  $\pm 1$  are mixtures of both eigenstates. However, states of definite transverse spin projections with respect to the decay plane of the second particle are pure CP eigenstates, too [86], and may be used to decompose the angular distribution into states with even and odd CP eigenvalue.

### 2.3.2.4 Non-Eigenstates

CP violation in oscillation/decay interference can also be observed in final states that are not CP eigenstates, as long as they can be reached by both  $B$  and  $\overline{B}$ . As an example [87], the channel shown in figure 2.7 has the decays  $b \rightarrow c(s\bar{u})$  leading to the final state  $D^0 K_s^0$  from a  $\overline{B}^0$  meson (a), and  $\bar{b} \rightarrow \bar{u}(\bar{s}c)$  leading to the same final state from a  $B^0$  meson (b). The amplitudes are

$$\begin{aligned} A &\propto V_{ub}^* V_{cs} \approx A\lambda^3 (\rho + i\eta) \\ \overline{A}' &\propto V_{cb} V_{us}^* \approx A\lambda^3 \end{aligned}$$

which are of the same order of magnitude. Using  $V_{cs}^* V_{cd}$  for the  $K^0 \rightarrow K_s^0$  amplitude and ignoring small CKM phase angles  $\mathcal{O}(\lambda^4)$  the observable ratio is

$$r = \eta_m \frac{\overline{A}'}{A} = \eta_m \exp \left( i \arg \frac{V_{cb} V_{us}^* V_{cs} V_{cd}^*}{V_{ub}^* V_{cd}} \right) e^{-i\delta_{AA'}} \frac{|A'|}{|A|} = e^{-i(2\beta + \gamma + \delta_{AA'})} \frac{|A'|}{|A|}$$



where  $\delta_{AA'}$  is the strong interaction phase difference. Similarly, for the final state  $\bar{D}^0 K_s^0$

$$r = \eta_m \frac{\bar{A}}{A'} = e^{-i(2\beta+\gamma-\delta_{AA'})} \frac{|A|}{|A'|}$$

From an observation of the time-dependent asymmetry (2.60) both the absolute values and the phases of these numbers can be determined, and the three unknown parameters  $\delta_{AA'}$ ,  $2\beta + \gamma$  and  $|A|/|A'|$  be extracted. Measuring separately  $D^0/\bar{D}^0$  decays into CP eigenstates like  $\pi\pi$  or  $KK$ , where both amplitudes interfere, the angle  $\gamma$  can be extracted from the rate measurement, which becomes simpler if the non-mixing charged  $B$  decay ( $\rightarrow D^0/\bar{D}^0 K^\pm$ ) [88] or the self-tagging decay  $B^0 \rightarrow D^0/\bar{D}^0 (K^+ \pi^-)_{K^{*0}}$  [89] are used.

A similar self-tagging decay  $B_s \rightarrow D_s^+ K^-$  has as weak phase  $\tilde{\gamma} + 2\phi_2 - \phi_6 \approx \gamma$  and has been suggested [90] to determine this angle.

### 2.3.2.5 The Total Decay Rate

The total decay rate of an initially pure  $B^0$  sample can be calculated as

$$\frac{dN}{dt} = N_0 \sum_X \int d\text{PS} |\mathcal{M}|^2 \delta(m_B - E_X)$$

using  $|\mathcal{M}|^2$  from equation (2.58) with  $A = A(B \rightarrow X)$ . This results in an expression like (2.58) with the replacements  $\sum_X |A|^2 \rightarrow \Gamma$ ,  $\sum_X |\bar{A}|^2 \rightarrow \Gamma$ ,  $|r|^2 \rightarrow |\eta_m|^2$  and  $\sum_X A^* \bar{A} \rightarrow \sum_X \langle B^0 | \mathbf{H}_w | X \rangle \langle X | \mathbf{H}_w | \bar{B}^0 \rangle = \Gamma_{12}$ . From (2.23) one can write

$$\begin{aligned} \sum_X \eta_m A^* \bar{A} &= \eta_m \Gamma_{12} = i\eta_m (H_{12} - H_{21}^*) \\ &= \frac{\Gamma}{2} [-ix(1 - |\eta_m|^2) - y(1 + |\eta_m|^2)] \\ &\approx \Gamma(1 - \delta) [-ix\delta - y] \end{aligned}$$

where the last line is an approximation for  $\delta \ll 1$ , which is good for all four meson pairs. This yields a total rate

$$\frac{dN}{dt} = N_0 \Gamma \frac{1 + |\eta_m|^2}{2} e^{-T} \left\{ \cosh yT + \delta \cos xT - y \sinh yT + x\delta \sin xT \right\} \quad (2.72)$$

In the approximation  $y = 0$  this is

$$\frac{dN}{dt} = N_0 \Gamma e^{-T} [1 + \delta \cdot (-1 + \cos xT + x \sin xT)] + \mathcal{O}(\delta^2) \quad (2.73)$$

with  $\int \frac{dN}{dt} dt = N_0$ . An initially pure  $\bar{B}^0$  sample gives the same rates with the replacement  $\eta_m \leftrightarrow 1/\eta_m$  and  $\delta \leftrightarrow -\delta$ . The asymmetry (where the  $B$  flavour is understood as the one at  $T = 0$ ) is therefore

$$\begin{aligned} a(T) &= \frac{\dot{N}(\bar{B}^0 \rightarrow \text{anything}) - \dot{N}(B^0 \rightarrow \text{anything})}{\dot{N}(\bar{B}^0 \rightarrow \text{anything}) + \dot{N}(B^0 \rightarrow \text{anything})} \Big|_T \\ &= \delta (1 - \cos xT - x \sin xT) \\ &= 2\delta \left( -\frac{x}{2} \sin xT + \sin^2 \frac{xT}{2} \right) \end{aligned} \quad (2.74)$$

A first measurement of the total asymmetry at LEP gave the preliminary result  $\delta = -0.011 \pm 0.015 \pm 0.005$  [91]. This is an alternative way to measure CP violation in  $B^0/\bar{B}^0$  oscillation, and gives a limit  $|2\delta| < 0.07$  (90%CL), but it implies the danger of a possible bias due to the  $B^0$  event selection.

### 2.3.2.6 CP Violation at the $\Upsilon(4S)$

$B$  meson pairs from  $\Upsilon(4S)$  decay are initially in a  $CP = +1, P = -1, C = -1$  eigenstate

$$|B^0(1)\bar{B}^0(2)\rangle - |B^0(2)\bar{B}^0(1)\rangle$$

with angular momentum  $L = 1$ . Their time evolution is described by (2.52a), where the two scaled times  $T_1$  and  $T_2$  may be taken as the decay times of the two mesons. By multiplying this state function with  $\langle X(1)X(2)|\mathbf{H}(1)\mathbf{H}(2)\rangle$  where

$$\langle X(1)X(2)|\mathbf{H}(1)\mathbf{H}(2)|B^0(1)B^0(2)\rangle = \langle X(1)|\mathbf{H}|B^0(1)\rangle \langle X(2)|\mathbf{H}|B^0(2)\rangle = A_1 A_2$$

are the decay amplitudes of two  $B^0$  mesons and amplitudes of other mixtures of  $B(i)$  and  $\bar{B}(j)$  yield products of  $A_i$  and  $\bar{A}_j$  accordingly, one obtains an amplitude

$$\mathcal{M}_- := e^{i\phi_0} e^{\frac{1}{2}(T_1+T_2)} \left[ C_- \cos(x-iy) \frac{T_1-T_2}{2} + iS_- \sin(x-iy) \frac{T_1-T_2}{2} \right] \quad (2.75)$$

where  $\phi_0$  is a common, unobservable phase including the *imt* phases of two free  $B$  mesons, and the coefficients are

$$C_- = A_1 \bar{A}_2 - \bar{A}_1 A_2, \quad S_- = \eta_m \bar{A}_1 \bar{A}_2 - \frac{A_1 A_2}{\eta_m}$$

There can be always two non-zero amplitude factors separated, leaving coefficients like

$$\frac{C_-}{A_1 \bar{A}_2} = 1 - \frac{\bar{A}_1 A_2}{A_1 \bar{A}_2}, \quad \frac{S_-}{A_1 \bar{A}_2} = \frac{\eta_m \bar{A}_1}{A_1} - \frac{A_2}{\eta_m \bar{A}_2}$$

These coefficients are **convention independent** factors similar to  $r$ : CP phases common to  $A/\bar{A}$  and  $\eta_m$  cancel, and the exchange of quarks with antiquarks ensure that the product of CKM elements has each quark index in as many  $V$  as  $V^*$  (or, with the same phase,  $1/V$ ) factors. From the general amplitude, we can derive various special cases listed in table 2.10.

The square  $|\mathcal{M}_-|^2$  leads to a general formula [92], which reads on the  $\Upsilon(4S)$  with the final states  $X_1, X_2$  from the two  $B^0$  mesons

$$\dot{N}(B\bar{B} \rightarrow X_1 X_2) \propto e^{-2\Gamma t_1} e^{-T} (g_1 \cosh yT + g_2 \sinh yT + h_1 \cos xT + h_2 \sin xT) \quad (2.76)$$

with  $T = T_2 - T_1 = \Gamma(t_2 - t_1)$  and

$$\begin{aligned} g_1 &= |C_-|^2 + |S_-|^2 \\ g_2 &= 2 \operatorname{Re}(S_-^* C_-) \\ h_1 &= |C_-|^2 - |S_-|^2 \\ h_2 &= 2 \operatorname{Im}(S_-^* C_-) \end{aligned}$$

For  $B^0$  mesons, we can assume  $\delta = 0$  and  $y = 0$ , which corresponds to the simpler equation

$$\dot{N}(B\bar{B} \rightarrow X_1 X_2) \propto e^{-2\Gamma t_1} e^{-T} (g_1 + h_1 \cos xT + h_2 \sin xT) \quad (2.77)$$

This includes the case of  $B\bar{B}$  oscillation, if we set e.g.  $\bar{A}_1 = A_2 = 0$ . Then  $C_- = A_1 \bar{A}_2$ ,  $S_- = 0$ ,  $g_1 = h_1 = |A_1 \bar{A}_2|^2$ , and  $g_2 = h_2 = 0$ . For a mixed mode we use e.g.  $\bar{A}_1 = \bar{A}_2 = 0$ . Then  $C_- = 0$ ,  $S_- = -A_1 A_2 / \eta_m$ ,  $g_1 = -h_1 = |A_1 A_2|^2$ , and  $g_2 = h_2 = 0$ . The corresponding asymmetry is

$$a(T) = \frac{\dot{N}(X_1 \bar{X}_2) - \dot{N}(X_1 X_2)}{\dot{N}(X_1 \bar{X}_2) + \dot{N}(X_1 X_2)} = \frac{\dot{N}(\bar{X}_1 X_2) - \dot{N}(\bar{X}_1 \bar{X}_2)}{\dot{N}(\bar{X}_1 X_2) + \dot{N}(\bar{X}_1 \bar{X}_2)} = \cos xT \quad (2.78)$$

<b>Table 2.10</b> Coefficients for $B\bar{B} \rightarrow X_1 X_2$ decays from $\Upsilon(4S)$ . $\eta_{1,2}$ are the CP eigenvalues of final states 1, 2, respectively, and $\eta_{12} = \eta_1 \eta_2$ . $d\bar{d}$ denotes a penguin mode with a $t$ quark in the loop, “com.” denotes a final state that can be reached from both $B^0$ and $\bar{B}^0$ and needs not to be a CP eigenstate. In this case, also strong phases are involved, which can be resolved using the charged conjugate final state, too. The coefficients of the time-dependent rate according to (2.77) are also given for $\delta = 0$ .							
$X_1$	$X_2$	$AA$	$C_-/AA$	$S_-/AA$	$g_1/ AA ^2$	$h_1/ AA ^2$	$h_2/ AA ^2$
$B$ -tag	$B$ -tag	$A_1 A_2$	0	$-1/\eta_m$	1	-1	0
$\bar{B}$ -tag	$\bar{B}$ -tag	$\bar{A}_1 \bar{A}_2$	0	$\eta_m$	1	-1	0
$B$ -tag	$\bar{B}$ -tag	$A_1 \bar{A}_2$	1	0	1	1	0
$\bar{B}$ -tag	$B$ -tag	$\bar{A}_1 A_2$	-1	0	1	1	0
com.	$B$ -tag	$\bar{A}_1 A_2$	-1	$-\frac{1}{r} = -\frac{A'_1}{\eta_m A_1}$	$\frac{1+ r ^2}{ r ^2}$	$\frac{1- r ^2}{ r ^2}$	$\frac{2\mathcal{I}m r}{ r ^2}$
com.	$\bar{B}$ -tag	$A'_1 \bar{A}_2$	1	$r = \frac{\eta_m A_1}{A'_1}$	$1 +  r ^2$	$1 -  r ^2$	$-2\mathcal{I}m r$
$c\bar{c}$	$B$ -tag	$\bar{A}_1 A_2$	-1	$-\eta_1 e^{2i\beta}$	2	0	$-2\eta_1 \sin 2\beta$
$c\bar{c}$	$\bar{B}$ -tag	$A_1 \bar{A}_2$	1	$\eta_1 e^{-2i\beta}$	2	0	$2\eta_1 \sin 2\beta$
$u\bar{u}$	$B$ -tag	$\bar{A}_1 A_2$	-1	$-\eta_1 e^{-2i\alpha}$	2	0	$2\eta_1 \sin 2\alpha$
$u\bar{u}$	$\bar{B}$ -tag	$A_1 \bar{A}_2$	1	$\eta_1 e^{2i\alpha}$	2	0	$-2\eta_1 \sin 2\alpha$
$d\bar{d}$	$B$ -tag	$\bar{A}_1 A_2$	-1	$-\eta_1$	2	0	0
$d\bar{d}$	$\bar{B}$ -tag	$A_1 \bar{A}_2$	1	$\eta_1$	2	0	0
$c\bar{c}$	$c\bar{c}$	$2A_1 \bar{A}_2$	$\frac{1-\eta_{12}}{2}$	$\frac{\eta_1}{2} e^{2i\beta} + \frac{\eta_2}{2} e^{-2i\beta}$	$1 - \eta_{12} \cos^2 2\beta$	$-\eta_{12} \sin^2 2\beta$	0
$c\bar{c}$	$u\bar{u}$	$2A_1 \bar{A}_2$	$\frac{1}{2} - \frac{\eta_{12}}{2} e^{2i(\beta+\alpha)}$	$\frac{\eta_1}{2} e^{2i\beta} + \frac{\eta_2}{2} e^{2i\alpha}$	$1 - \eta_{12} \cos 2\beta \cos 2\alpha$	$\eta_{12} \sin 2\beta \sin 2\alpha$	0
$c\bar{c}$	$d\bar{d}$	$2A_1 \bar{A}_2$	$\frac{1}{2} - \frac{\eta_{12}}{2} e^{2i\beta}$	$\frac{\eta_1}{2} e^{2i\beta} + \frac{\eta_2}{2}$	$1 - \eta_{12} \cos 2\beta$	0	0

corresponding to figure 2.4 for positive  $T$  as well as for negative  $T$  with  $T \rightarrow -T$ .

For a CP eigenstate with eigenvalue  $\eta_1 = \pm 1$  as meson (1),  $\bar{A}_1/A_1 = \eta_1 e^{-2i\tilde{\phi}}$ , where  $\tilde{\phi}$  is the phase of the CKM matrix elements involved. If the state (2) is a tagging mode, e.g.  $A_2 \neq 0$ ,  $\bar{A}_2 = 0$  we have the situation of a tagged decay with

$$\begin{aligned}
C_- &= \bar{A}_1 A_2 \cdot (-1) \\
S_- &= \bar{A}_1 A_2 \cdot (-\eta_1 e^{2i(\tilde{\phi}+\tilde{\beta})}) \\
g_1 &= 2|\bar{A}_1|^2 |A_2|^2 \\
h_1 &= 0 \\
h_2 &= -2|\bar{A}_1|^2 |A_2|^2 \eta_1 \sin 2(\tilde{\phi} + \tilde{\beta})
\end{aligned}$$

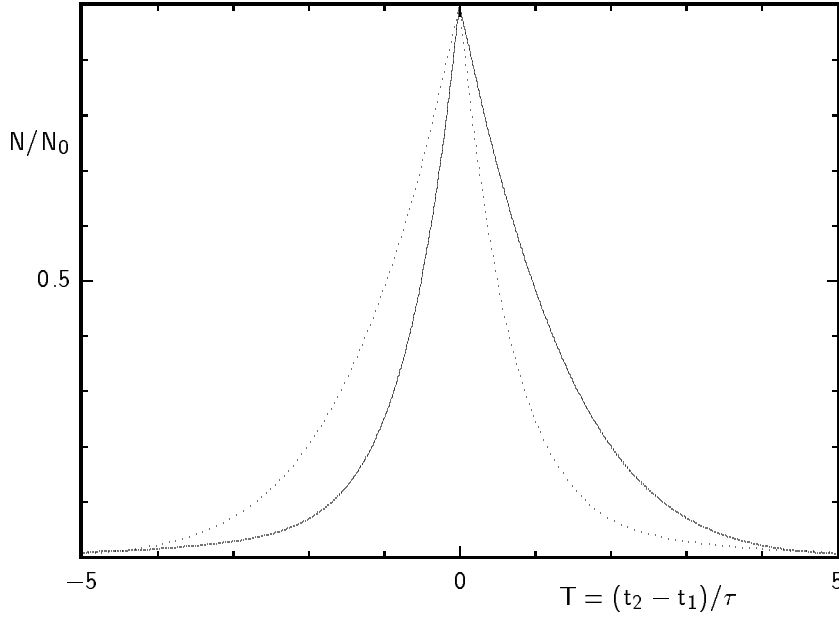
which is the typical situation of CP violation in the oscillation/decay interference, with a  $T$  dependence as shown in figure 2.10. The dotted curve corresponds to a  $\bar{B}$  tag  $A_2 = 0$ ,  $\bar{A}_2 \neq 0$  with

$$\begin{aligned}
C_- &= A_1 \bar{A}_2 \\
S_- &= A_1 \bar{A}_2 \cdot (\eta_1 e^{-2i(\tilde{\phi}+\tilde{\beta})}) \\
g_1 &= 2|A_1|^2 |\bar{A}_2|^2 \\
h_1 &= 0 \\
h_2 &= 2|A_1|^2 |\bar{A}_2|^2 \eta_1 \sin 2(\tilde{\phi} + \tilde{\beta})
\end{aligned}$$

and the asymmetry of both is described by equation (2.62) with  $A_0 = -\eta_1 \sin 2(\tilde{\phi} + \tilde{\beta})$ . The flavour of the signal- $B$  meson (1) is uniquely defined at the time of decay  $t_2$  of the second  $B$  meson, since the flavour of the latter can be identified by its final state.

If both final states are CP eigenstates with eigenvalues  $\eta_{1,2} = \pm 1$ ,  $\bar{A}_{1,2}/A_{1,2} = \eta_{1,2} e^{-2i\tilde{\phi}_{1,2}}$ , where  $\tilde{\phi}_{1,2}$  are the phases of the CKM matrix elements involved, the coefficients are

$$C_- = A_1 \bar{A}_2 (1 - \eta_1 \eta_2 e^{2i(\tilde{\phi}_1 - \tilde{\phi}_2)})$$



**Fig. 2.10** Time dependent rate of  $\Upsilon(4S) \rightarrow B^0 + J/\psi K_S^0$  (—) and  $\Upsilon(4S) \rightarrow \bar{B}^0 + J/\psi K_S^0$  (····) for  $\sin 2\beta = 0.5$  and  $x = 0.7$ .

$$\begin{aligned}
 S_- &= A_1 \bar{A}_2 (\eta_1 e^{-2i(\tilde{\phi}_1 + \tilde{\beta})} - \eta_2 e^{2i(\tilde{\phi}_2 + \tilde{\beta})}) \\
 g_1 &= 4|A_1|^2 |A_2|^2 [1 - \eta_1 \eta_2 \cos 2(\tilde{\phi}_1 + \tilde{\beta}) \cos 2(\tilde{\phi}_2 + \tilde{\beta})] \\
 h_1 &= -4|A_1|^2 |A_2|^2 \eta_1 \eta_2 \sin 2(\tilde{\phi}_1 + \tilde{\beta}) \sin 2(\tilde{\phi}_2 + \tilde{\beta}) \\
 h_2 &= 0
 \end{aligned}$$

which leads to a rate

$$\dot{N}(B\bar{B} \rightarrow X_1 X_2) \propto 4|A_1|^2 |A_2|^2 e^{-\Gamma t_1} e^{-T} [1 - \eta_1 \eta_2 (\cos 2\phi_1 \cos 2\phi_2 - \sin 2\phi_1 \sin 2\phi_2 \cos xT)]$$

where the observable phase angles are  $\phi_1 = \tilde{\phi}_1 + \tilde{\beta}$  and  $\phi_2 = \tilde{\phi}_2 + \tilde{\beta}$ . If CP were conserved throughout the decay chain, the eigenvalues are  $\eta_1 = -\eta_2$  since the total CP eigenvalue +1 is achieved via another factor (-1) from the relative  $L = 1$  angular momentum of both  $B$  mesons. This corresponds to

$$\dot{N}(B\bar{B} \rightarrow X_{1\pm} X_{2\mp}) \propto 4|A_1|^2 |A_2|^2 e^{-\Gamma(t_1+t_2)} [1 + \cos 2\phi_1 \cos 2\phi_2 + \sin 2\phi_1 \sin 2\phi_2 \cos xT] \quad (2.79)$$

while the forbidden rate is

$$\dot{N}(B\bar{B} \rightarrow X_{1\pm} X_{2\pm}) \propto 4|A_1|^2 |A_2|^2 e^{-\Gamma(t_1+t_2)} [1 - \cos 2\phi_1 \cos 2\phi_2 - \sin 2\phi_1 \sin 2\phi_2 \cos xT] \quad (2.80)$$

If both decays proceed via the same flavour changing transitions, the CKM angles are the same for both  $B$  mesons,  $\phi_1 = \phi_2 = \phi$ , and the forbidden rate is

$$\dot{N}(B\bar{B} \rightarrow X_{1\pm} X_{2\pm}) \propto 4|A_1|^2 |A_2|^2 e^{-\Gamma t_1} e^{-T} \sin^2 2\phi (1 - \cos xT)$$

This rate should be 0. It does actually vanish for  $T = 0$ , i.e. equal decay times of both. Only if their lifetimes differ CP violation builds up in the interference term of oscillation and decay processes. For different CKM angles, even at  $T = 0$  there is a CP violating rate  $\propto (1 - \cos(\phi_1 - \phi_2))$  which can be called consistently a special case of direct CP violation. The interference term is here, in contrast to the example (2.55), not between two amplitudes for one  $B$  decay, but between two amplitudes for two different  $B$  decays, which are in a coherent  $BB$  state. All these interesting cases will, however, not be observed in the first generation experiments on the  $\Upsilon(4S)$ , since they involve a product of two small branching ratios which are typically below  $10^{-4}$  and corresponds to less than one event per year at the presently envisaged luminosities.

### 2.3.3 CP Violation in $K$ Decays

CP Violation has first been observed in 1964 [3] in  $K^0$  decays. As shown in figure 2.2, the neutral kaon system is characterized by all parameters  $x$ ,  $y$  and  $|\eta_m|$  having non-trivial values. This makes it much more complicated than the  $B$  meson system. The light  $K_S^0$  decays to about 99.9% into the CP = +1 eigenstates  $\pi\pi$  and can therefore be identified with a CP = +1 eigenstate  $K_+^0$ , while  $K_L^0 \approx K_-^0$ . Using the convention  $K_+^0 = \frac{1}{\sqrt{2}}(K^0 + \bar{K}^0)$ , i.e.  $\phi_{\text{CPK}} = 0$ , this can be written as

$$K_S^0 = \frac{1}{\sqrt{1+|\epsilon|^2}}(K_+^0 + \epsilon K_-^0)$$

$$K_L^0 = \frac{1}{\sqrt{1+|\epsilon|^2}}(K_-^0 + \epsilon K_+^0)$$

up to an arbitrary common phase factor. For the standard parametrization of the CKM matrix (2.9), the leading term for  $m_{12}$  from the box graph for  $K^0/\bar{K}^0$  oscillation with a  $c$  quark in the loop yields

$$\eta_m \approx e^{i\phi_{\text{CPK}}} \frac{V_{cs}^{*2} V_{cd}^2}{|V_{cs}^2 V_{cd}^2|} = e^{i\phi_{\text{CPK}}} e^{2i(\phi_4 + \phi_6)}$$

which is for this choice of the CP phase  $\eta_m \approx 1 + 2i(\phi_4 + \phi_6)$  and corresponds to  $\epsilon \approx -i(\phi_4 + \phi_6)$  with  $|\epsilon| \ll 1$ . However, to this order, contributions from  $\Gamma_{12}$  become important, and eventually dominate the value of  $\epsilon$ . Within the same convention, the CKM elements in the dominant tree decay  $s \rightarrow u + \bar{u}d$  are real, hence the invariant phases including this decay are identical to the phases put into  $\eta_m$ . A convention independent definition of  $\epsilon$  similar to (2.69) is

$$\epsilon_0 = \frac{1 - \eta_m \bar{A}_0/A_0}{1 + \eta_m \bar{A}_0/A_0} \quad (2.81)$$

where

$$A_0 = \langle \pi^+ \pi^-, I=0 | \mathbf{H} | K^0 \rangle, \quad \bar{A}_0 = \langle \pi^+ \pi^-, I=0 | \mathbf{H} | \bar{K}^0 \rangle$$

are the decay amplitudes into the  $\pi^+ \pi^-$  final state with isospin 0. This quantity is identical to

$$\epsilon_0 = \frac{\langle \pi^+ \pi^-, I=0 | \mathbf{H} | K_L^0 \rangle}{\langle \pi^+ \pi^-, I=0 | \mathbf{H} | K_S^0 \rangle}$$

defined as  $\epsilon_K$  in [23].

There are again three possibilities for CP violation.

- 1) Direct CP violations have only been observed for neutral kaon decays to  $\pi\pi$ , where they constitute a component in the asymmetries observed in interference of oscillation and decay. The effects are much smaller than the expected ones in  $B$  decays. The phenomenology is in complete analogy with equation (2.55), and will be discussed in more detail below.
- 2) CP violation in the oscillation can be observed using flavour specific decays like  $K^0 \rightarrow \pi^- l^+ \nu$ . The oscillation asymmetry (2.42) starting with an initial  $K^0$  meson is dominated by the damped  $\cos xT$  oscillation term seen in the lower diagram in figure 2.2. The expansion of the asymmetry in  $\delta$  according to (2.56) approaches  $a(T) \rightarrow \delta$  at large times  $T \gg 1$  where the long-lived state  $K_L^0$  is the only remaining one. It is the same for an initial  $\bar{K}^0$ . Hence, there are more  $\bar{K} \rightarrow K$  oscillations than  $K \rightarrow \bar{K}$ , leaving a net excess of  $K^0$  mesons  $a(\infty) = \delta = (3.27 \pm 0.12) \cdot 10^{-3}$  [9] which has first been observed in 1967 [93].
- 3) A big fraction of neutral kaons decay not as a flavour specific state but as one of the CP eigenstates, e.g.  $K_+^0 \rightarrow \pi^+ \pi^-$  and  $K_-^0 \rightarrow \pi^+ \pi^- \pi^0$ . The asymmetry from interference of oscillation and decay has rates determined by (2.58), and has been observed in all these modes.

The CP asymmetry in the  $\pi^+\pi^-$  final state is a complex interplay between CP violation in oscillation ( $1 - |r|$ ) and a small phase angle  $\arg r$ . Therefore, a more pragmatic terminology has been introduced, based on the amplitudes for the two eigenstates using the complex parameter

$$\eta_{+-} = \frac{\langle \pi^+\pi^- | \mathbf{H} | K_L^0 \rangle}{\langle \pi^+\pi^- | \mathbf{H} | K_S^0 \rangle}$$

with a phase  $\phi_{+-} = \arg \eta_{+-}$ . If the formalism used for the  $B$  system is applied defining  $r_{+-} = \eta_m \bar{A}/A$  by the  $K^0$  and  $\bar{K}^0$  amplitudes as above, this parameter is an  $\epsilon$  parameter for the final state  $\pi^+\pi^-$  according to (2.69) and we get  $\langle \pi^+\pi^- | \mathbf{H} | K_S^0 \rangle = pA(1 + r_{+-})$  and  $\langle \pi^+\pi^- | H | K_L^0 \rangle = pA(1 - r_{+-})$  and

$$\eta_{+-} = \frac{1 - r_{+-}}{1 + r_{+-}}, \quad r_{+-} = \frac{1 - \eta_{+-}}{1 + \eta_{+-}}$$

Since  $r_{+-}$  is an observable, this holds also for  $\eta_{+-}$ . The coefficients for (2.58) are

$$\begin{aligned} 1 - |r_{+-}|^2 &= 4 \frac{\mathcal{R}e \eta_{+-}}{|1 + \eta_{+-}|^2} \\ 1 + |r_{+-}|^2 &= 2 \frac{1 + |\eta_{+-}|^2}{|1 + \eta_{+-}|^2} \\ \mathcal{R}e r_{+-} &= |r_{+-}| \cos(\arg r_{+-}) = \frac{1 - |\eta_{+-}|^2}{|1 + \eta_{+-}|^2} \\ \mathcal{I}m r_{+-} &= |r_{+-}| \sin(\arg r_{+-}) = -2 \frac{\mathcal{I}m \eta_{+-}}{|1 + \eta_{+-}|^2} \end{aligned}$$

Furthermore, we have direct CP violation from

$$\bar{A} = \langle \pi^+\pi^- | \mathbf{H} | \bar{K}^0 \rangle = \langle \pi^+\pi^- | \text{CP}(\text{CP} \mathbf{H} \text{CP}) \text{CP} | \bar{K}^0 \rangle = e^{i\phi_{\text{CPK}}} \langle \pi^+\pi^- | (\text{CP} \mathbf{H} \text{CP}) | K^0 \rangle = e^{i\phi_{\text{CPK}}} A \frac{1 - \epsilon'}{1 + \epsilon'}$$

where  $\epsilon'$  describes the small difference in the amplitudes. Its origin within the Standard Model lies in the interference of tree and penguin diagrams, where hadronic penguins contribute only to the isospin 0 final state, while the tree graph and electromagnetic penguins have also a small isospin 2 component. The two isospin amplitudes have different strong phases, and penguin and tree have a different weak phase. Therefore there is a small direct CP violation according to (2.55), which would be observed even without oscillation. If we choose an overall phase to make the isospin 0 amplitude  $A_0$  real, we may write the isospin 2 amplitude as  $A_2 e^{i\phi} e^{i\delta_{20}}$  with  $\delta_{20}$  being the strong phase difference, and  $\phi$  the weak phase difference. Then the ratio of amplitudes is

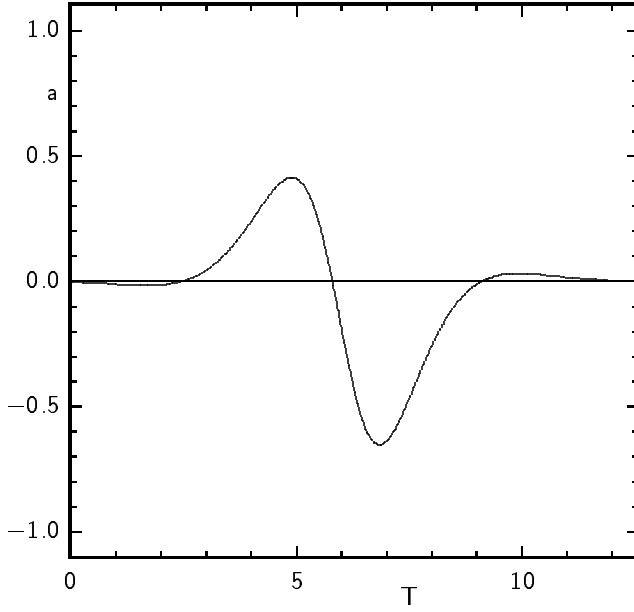
$$\begin{aligned} A(K^0 \rightarrow \pi^+\pi^-) &= \sqrt{\frac{1}{6}} A_2 e^{i\phi} e^{i\delta_{20}} + \sqrt{\frac{1}{3}} A_0 \\ \bar{A}(\bar{K}^0 \rightarrow \pi^+\pi^-) &= e^{i\phi_{\text{CPK}}} \left( \sqrt{\frac{1}{6}} A_2 e^{-i\phi} e^{i\delta_{20}} + \sqrt{\frac{1}{3}} A_0 \right) \\ \frac{\bar{A}}{A} &\approx e^{i\phi_{\text{CPK}}} \left( 1 + \sqrt{\frac{1}{2}} \frac{A_2}{A_0} e^{i\delta_{20}} (e^{-i\phi} - e^{i\phi}) \right) = e^{i\phi_{\text{CPK}}} \left( 1 - \sqrt{2} \frac{A_2}{A_0} e^{i\delta_{20}} i \sin \phi \right) \end{aligned}$$

and

$$\epsilon' = \sqrt{\frac{1}{2}} i \frac{A_2}{A_0} e^{i\delta_{20}} \sin \phi$$

Correspondingly we obtain

$$r_{+-} = \frac{\eta_m \bar{A}}{A} = \frac{1 - \epsilon_0}{1 + \epsilon_0} \cdot \frac{1 - \epsilon'}{1 + \epsilon'} \approx 1 - 2\epsilon_0 - 2\epsilon'$$



**Fig. 2.11** Time dependent rate asymmetry  $a(T)$  of  $\bar{K}^0 \rightarrow \pi^+ \pi^-$  and  $K^0 \rightarrow \pi^+ \pi^-$ .  $T = t/\bar{\tau}$  is the lifetime in units of  $\bar{\tau} \approx 2\tau_S$ , the inverse of the average width of  $K_L^0$  and  $K_S^0$ .

and

$$\eta_{+-} \equiv \epsilon_{\pi^+\pi^-} \approx \epsilon_0 + \epsilon'$$

Using the present world average [94], these numbers are

$$\begin{aligned} \phi_{+-} &= (43.56 \pm 0.56)^\circ \\ |\eta_{+-}| &= (2.290 \pm 0.020) \cdot 10^{-3} \\ |r_{+-}| &= 0.996687 \pm 0.000042 \\ \sin(\arg r_{+-}) &= -(3.156 \pm 0.043) \cdot 10^{-3} \\ r_{+-} &= 0.996682 - 0.003146 i \end{aligned}$$

Expressed in these variables, the squared matrix elements are

$$\begin{aligned} |\mathcal{M}|^2 &= e^{-T} \frac{|A|^2}{|p|^2 |1 + \eta_{+-}|^2} \left\{ (1 + |\eta_{+-}|^2) \cosh yT + (1 - |\eta_{+-}|^2) \sinh yT \right. \\ &\quad \left. + 2 \operatorname{Re} \eta_{+-} \cos xT + 2 \operatorname{Im} \eta_{+-} \sin xT \right\} \\ |\bar{\mathcal{M}}|^2 &= e^{-T} \frac{|A|^2}{|q|^2 |1 + \eta_{+-}|^2} \left\{ (1 + |\eta_{+-}|^2) \cosh yT + (1 - |\eta_{+-}|^2) \sinh yT \right. \\ &\quad \left. - 2 \operatorname{Re} \eta_{+-} \cos xT - 2 \operatorname{Im} \eta_{+-} \sin xT \right\} \end{aligned} \quad (2.82)$$

which corresponds to the asymmetry function

$$\begin{aligned} a(T) &= \frac{\dot{N}(\bar{K}^0 \rightarrow \pi^+ \pi^-) - \dot{N}(K^0 \rightarrow \pi^+ \pi^-)}{\dot{N}(\bar{K}^0 \rightarrow \pi^+ \pi^-) + \dot{N}(K^0 \rightarrow \pi^+ \pi^-)} = -\frac{2|\eta_{+-}| \cos(xT - \phi_{+-}) - \delta[|\eta_{+-}|^2 e^{yT} + e^{-yT}]}{|\eta_{+-}|^2 e^{yT} + e^{-yT} - 2\delta|\eta_{+-}| \cos(xT - \phi_{+-})} \\ &\approx -\frac{2|\eta_{+-}| \cos(xT - \phi_{+-})}{|\eta_{+-}|^2 e^{yT} + e^{-yT}} \end{aligned} \quad (2.83)$$

shown in figure 2.11, where the  $K$  flavour is understood to be the one at  $T = 0$ . The approximation in (2.83) is for  $|\eta_m| = 1$ .

The phenomenology for the  $\pi^0\pi^0$  state is similar, with a small change due to the different interference between

$$\begin{aligned}
 A(K^0 \rightarrow \pi^0\pi^0) &= \sqrt{\frac{2}{3}}A_2e^{i\phi}e^{i\delta_{20}} - \sqrt{\frac{1}{3}}A_0 \\
 \bar{A}(\bar{K}^0 \rightarrow \pi^0\pi^0) &= e^{i\phi_{\text{CPK}}} \left( \sqrt{\frac{2}{3}}A_2e^{-i\phi}e^{i\delta_{20}} - \sqrt{\frac{1}{3}}A_0 \right) \\
 \frac{\bar{A}}{A} &\approx e^{i\phi_{\text{CPK}}} \left( 1 - \sqrt{2}\frac{A_2}{A_0}e^{i\delta_{20}}(e^{i\phi} - e^{-i\phi}) \right) = e^{i\phi_{\text{CPK}}} \left( 1 + 2\sqrt{2}\frac{A_2}{A_0}e^{i\delta_{20}}i\sin\phi \right)
 \end{aligned}$$

and

$$\epsilon'_{00} = -\sqrt{2}i\frac{A_2}{A_0}e^{i\delta_{20}}\sin\phi = -2\epsilon'$$

which finally leads to  $\eta_{00} = \epsilon_{\pi^0\pi^0} \approx \epsilon_0 - 2\epsilon'$ .

A more general description of the kaon system waiving CPT invariance can be found in the literature [21] and is discussed in [22]. Recent results on the kaon system [94] have reached an amazing precision on many parameters, but are all well compatible with the Standard Model.



### 3. Measurement of CP Violation at $B$ Meson Factories

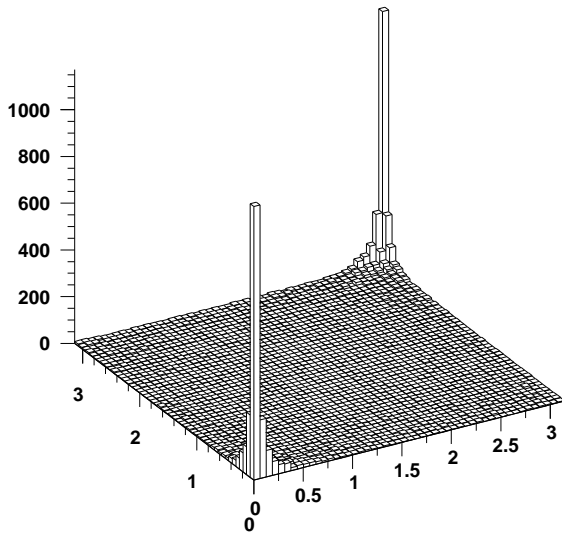
There are two experimental environments suitable to measure CP violation:

- $e^+e^-$  storage rings operating at a cms energy of the  $\Upsilon(4S)$  resonance mass, where about 1nb cross section is available for exclusive  $B\bar{B}$  production, almost at rest. At luminosities between  $1 \cdot 10^{33}$  and  $1 \cdot 10^{34}/\text{cm}^2/\text{s}$ , they accumulate roughly  $10^7 \dots 10^8$   $B^0$  mesons and the same number  $B^\pm$  mesons per year.

There have been many places proposed for such machines in the past [95–99], of which recently the storage ring PEP-II at SLAC (USA) and the storage ring KEKB in the TRISTAN tunnel at KEK (Japan) evolved into real projects, which both aim at data taking early in 1999 with one detector each.

- Hadron collision experiments at energies far above the  $b\bar{b}$  threshold, which provide a substantially higher rate of incoherent  $b\bar{b}$  pairs, but need dedicated triggers to select those from a tremendous background.

The most promising place is LHC, which provides both a high  $B$  production cross section and a high luminosity. There have been several proposals for dedicated experiments, which are either fixed target experiments at LHC [100,101], or—as a special case—use the  $pp$  collider mode with a detector sensitive in the very forward direction [102,103] where the cross section has a pronounced maximum (see figure 3.1). This setup selects parton interactions, where one parton has much higher momentum than the other, and comes therefore close to a fixed target setup, with the advantage of using the high luminosity provided in beam–beam collisions. In all proposals, the setup has been chosen to provide a large boost, which allows the separation of  $B$  mesons via their lifetime.



**Fig. 3.1**  $b\bar{b}$  cross section  $d^2\sigma/d\theta_B d\theta_{\bar{B}}$  at 14 TeV  $pp$  collisions versus  $\theta_B$  and  $\theta_{\bar{B}}$  (cross section scale arbitrary, angles in rad) [103]. The distribution shows that  $B$  meson production peaks in the very forward direction, and that  $B$  mesons are accompanied by their partner  $b$ -jet at close angular distance there.

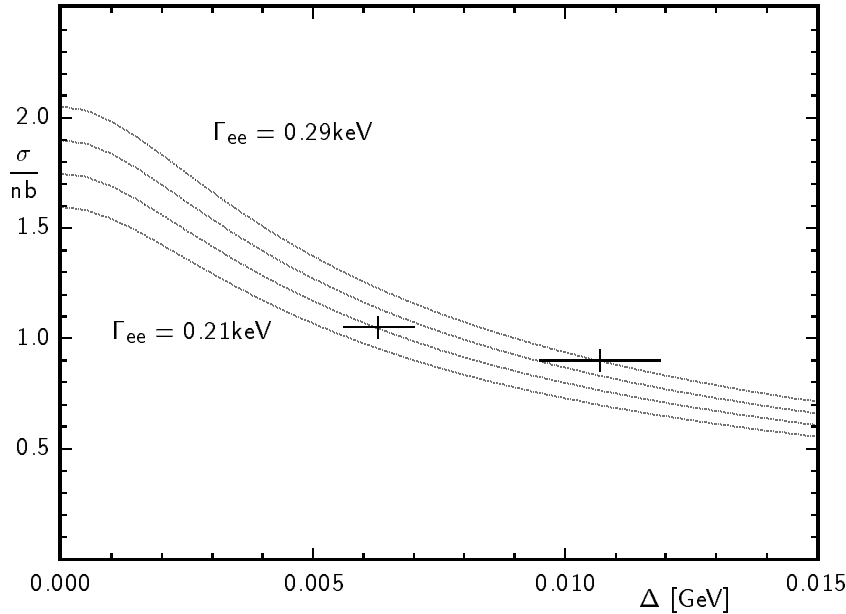
The number of produced  $B$  mesons within a reasonable data taking period is substantially lower at any envisaged  $e^+e^-$  collider than at hadronic  $B$  factories. On the other hand, there is a much better signal-to-background ratio, and without any sophisticated trigger every  $B$  meson can be recorded. Experiments at the  $\Upsilon(4S)$  with only  $B$  and  $\bar{B}$  in one event make also much better use of statistical methods compared to an already restrictive event selection used at hadron machines. Therefore, the  $e^+e^-$  colliders will most likely be able to establish CP violating effects in the  $B$  system unambiguously, given their clean

systematics. An high energy hadron experiment will be required, however, to supply the statistics needed to determine the parameters with precision.

While the LHC will start as a  $B$  factory not before 2005, there are also hadron experiments at lower energies foreseen in near future: HERA-B [104], a fixed target experiment using the halo of the HERA 820 GeV proton storage ring at DESY, and the experiments at Fermilab, the most promising being an upgraded CDF experiment [105] with improved performance in  $B$  physics for the next run at the Tevatron, a 2 TeV  $p\bar{p}$  collider.

All experiments are summarized in table 3.1. The asymmetric  $e^+e^-$  storage rings PEP-II and KEKB are both designed to run with two separate rings and many bunches (1658 and 5000 per ring, respectively). At KEKB the bunches cross at an angle of 22 mrad in parallel orientation (crab crossing), while the more conservative PEP-II design aims at head-on collision. This allows a closer bunch spacing and slightly higher focussing at KEKB, resulting in a gain in luminosity by a factor of 3. If this option proves viable, also PEP-II can be upgraded to nonzero crossing angle. Another factor of 2 seems possible if one goes more close to the limits of machine design, so that by the start of the second generation CP experiments at LHC-B a luminosity of  $2 \cdot 10^{34}/\text{cm}^2/\text{s}$  at  $e^+e^-$   $B$  factories will be reached.

<b>Table 3.1</b> Proposed $B$ factories (most of them being rejected, the approved ones are typed in <b>bold</b> ) [95–109]. The cms energy of $b\bar{b}$ , median $B$ momentum $\langle p(B) \rangle_5$ , estimated $b\bar{b}$ cross section and expected $b\bar{b}$ pair rate are compared.				
machine	type (beam energies [GeV])	$E_{b\bar{b}\text{CMS}}$ [GeV]	$\langle p(B) \rangle_5$ [GeV]	$N(b\bar{b})/a$
<b>CESR (Cornell)</b>	$e^+e^-$	10.58	0.32	$4 \cdot 10^6$
BETA (PSI) symm.	$e^+e^-$	10.58	0.32	$1 \cdot 10^7$
ISR-B (CERN) symm.	$e^+e^-$	10.58	0.32	$1 \cdot 10^8$
CESR III (Cornell)	$e^+e^-$	10.58	0.32	$1 \cdot 10^7$
BETA (PSI) asym.	$e^+e^- (7+4)$	10.58	1.5	$1 \cdot 10^7$
VEPP-5 (Novosibirsk)	$e^+e^- (7+4)$	10.58	1.5	$5 \cdot 10^7$
ISR-B (CERN) asym.	$e^+e^- (8+3.5)$	10.58	2.25	$6 \cdot 10^7$
CESR-B (Cornell)	$e^+e^- (8+3.5)$	10.58	2.25	$3 \cdot 10^7$
<b>KEKB (KEK)</b>	$e^+e^- (8+3.5)$	10.58	2.25	$1 \cdot 10^8$
<b>PEP II (SLAC)</b>	$e^+e^- (9+3.1)$	10.58	2.95	$3 \cdot 10^7$
HELENA (DESY)	$e^+e^- (9.3+3)$	10.58	3.15	$3 \cdot 10^7$
<b>HERA-B (DESY)</b>	$p(820) \rightarrow C$	$< 39$	100	$3 \cdot 10^8$
HERA-B'	$p(1000) \rightarrow C$	$< 43$	140	$6 \cdot 10^8$
LHB (CERN)	$p(7000) \rightarrow \text{Be}$	$< 114$	400	$1 \cdot 10^{10}$
GAJET (CERN)	$p(7000) \rightarrow \text{H}$	$< 114$	400	$1 \cdot 10^{10}$
BTEV (FNAL)	$p\bar{p}$ forw.	$\ll 2000$	$\sim 30$	$1 \cdot 10^{11}$
COBEX (CERN)	$pp$ forw.	$\ll 14000$	$\sim 50$	$5 \cdot 10^{11}$
LHC-B (CERN)	$pp$ forw.	$\ll 14000$	$\sim 50$	$5 \cdot 10^{11}$
<b>CDF Run 2 (FNAL)</b>	$p\bar{p}$	$< 2000$	15	$2 \dots 10 \cdot 10^{10}$
<b>D0 Run 2 (FNAL)</b>	$p\bar{p}$	$< 2000$	15	$2 \dots 10 \cdot 10^{10}$
<b>ATLAS, CMS (LHC)</b>	$pp$	$< 14000$	$\sim 20$	$5 \cdot 10^{12}$
SSC	$pp$	$< 40000$	$\sim 20$	$5 \cdot 10^{11}$



**Fig. 3.2** Peak cross section of the  $\Upsilon(4S)$ , using  $\Gamma_{\text{tot}} = 10 \text{ MeV}$  [110] and various  $\Gamma_{ee}$  values from  $0.21 \text{ keV}$  to  $0.29 \text{ keV}$ , versus the machine resolution  $\Delta = \sigma(E_{\text{CMS}})$  [111]. The crosses are the ARGUS/DORIS data (right) and CLEO/CESR (left, errors guessed).

### 3.0.4 $B$ Production Cross Sections

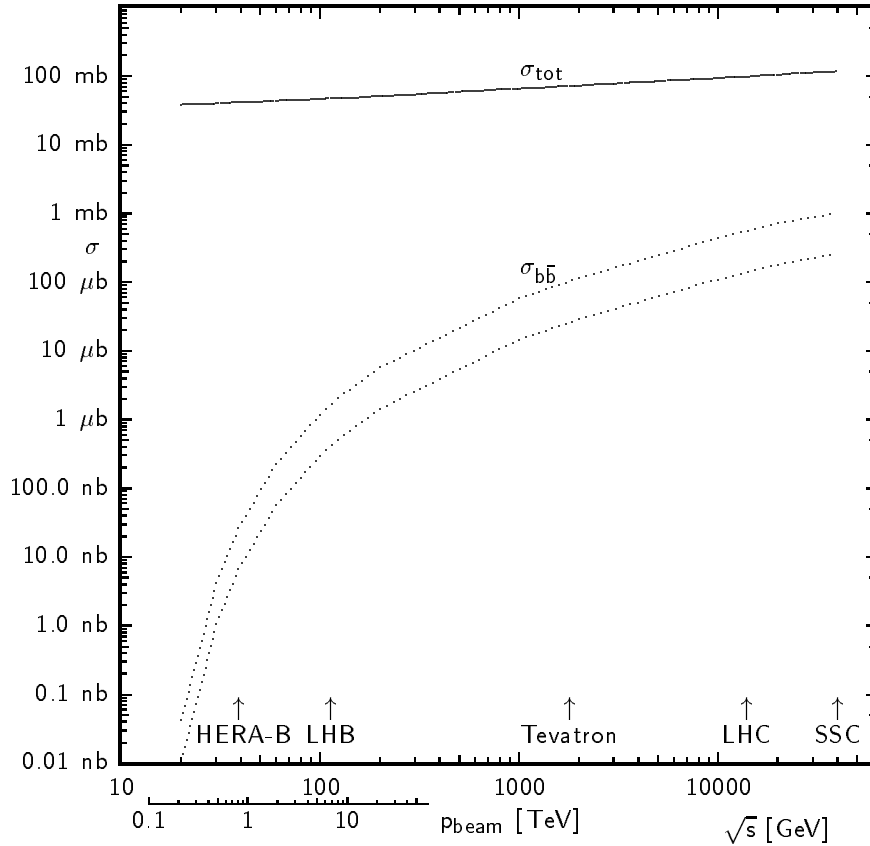
The cross section on top of the  $\Upsilon(4S)$  resonance is proportional to the width  $\Gamma_{ee}$  of  $\Upsilon(4S) \rightarrow e^+e^-$ , and varies with the machine energy spread and the total width of the  $\Upsilon(4S)$ . Using the ARGUS result  $\Gamma_{\text{tot}} = (10.0 \pm 2.8 \pm 2.7) \text{ MeV}$  [110], the predicted peak cross section is given by the diagram in figure 3.2 for different  $\Gamma_{ee}$ . Unfortunately, the resonance parameters have big errors. Previous measurements by CUSB and CLEO have used a parametrization valid for narrow resonances and can therefore not be combined with the ARGUS results. The approximation  $\Delta \gg \Gamma_{\text{tot}}$  used for its derivation is not valid for the broad  $\Upsilon(10580)$  and increases the resulting width artificially.

For the machine spread of a typical  $B$  factory of  $6 \dots 6.5 \text{ MeV}$ , the range is in the  $1 \dots 1.2 \text{ nb}$  region. A better estimate is the observed peak cross section at CESR, which has a similar width in cms energy ( $\sigma_E = 6.3 \text{ MeV}$ ). CLEO observed a cross section  $\sigma = (1.05 \pm 0.02) \text{ nb}$  [112], therefore a value of  $1 \text{ nb}$  seems to be a conservative number for rate estimates.

For  $pp$  scattering, the cross section of  $b\bar{b}$  production is dominated by gluon gluon fusion, and depends on the gluon structure function of the proton. QCD calculations are very uncertain close to threshold, but more reliable at higher energies. Precise data exist at  $1.8 \text{ TeV}$  from CDF [113] for a limited phase space region, and can be used to check QCD calculations. For the proposed machines and detector acceptance volumes, the uncertainties are still large. Figure 3.3 gives an idea of  $b\bar{b}$  production compared to the  $pp$  total cross section.

The low fraction of  $b\bar{b}$  events from all interactions at the low cms energies of fixed target experiments can be somewhat compensated by the use of heavy nuclear targets. While the rare  $b\bar{b}$  production cross section per nucleon remains about constant and is  $\propto A$ , the number of nucleons per nucleus, the total cross section feels shielding by the densely packed nucleons, and scales approximately with the cross section area of the nucleus  $\propto A^{2/3}$ . This brings a gain in the ratio of cross sections  $\propto A^{1/3}$ . The scaling of  $\sigma_{b\bar{b}}$  with  $A$  is supported by measurements of the  $c\bar{c}$  production cross section at high beam energies [115]. A disadvantage of heavy elements is, however, the increased multiplicity due to secondary interactions in the nucleus, and experiments have to balance the increase in relative rate with the increase in detector occupancy.

The asymmetric  $gg$  collisions dominate the  $b\bar{b}$  production process, producing jets peaked both in forward



**Fig. 3.3** Estimated range for the cross section of  $pN \rightarrow b\bar{b}X$  (between dotted curves) using the PYTHIA 5.6 parametrization [114] as a lower limit and an estimated upper limit 4 times larger, compared to the total  $pp$  cross section (solid line [9]).

or in backward direction, and the  $b$  and  $\bar{b}$  jets are close together in these events. This is illustrated in figure 3.1, where

$$\frac{d^2\sigma}{d\theta_b d\theta_{\bar{b}}} = \sin\theta_b \sin\theta_{\bar{b}} \frac{d^2\sigma}{d\Omega_b d\Omega_{\bar{b}}}$$

is shown versus  $\theta_b$  and  $\theta_{\bar{b}}$ . This fact is exploited by LHC-B [103], which is designed to operate at an LHC  $pp$  collision point, with an acceptance limited to the forward region, but coming as close as some 10 mrad to the beam axis.

### 3.0.5 $B$ Meson Fractions

At the  $\Upsilon(4S)$ , the only final states are  $B^+B^-$  and  $B^0\bar{B}^0$ , which are produced at the same rate, i. e. 50% each. While unequal fractions due to phase space were discussed in the 80s, with more precise mass measurements [9] moving the world average mass difference

$$m(B^0) - m(B^+) = (0.20 \pm 0.28) \text{ MeV}/c^2$$

close to zero, and with new theoretical insights on the size of the Coulomb correction for charged  $B$  mesons [116], the production ratio is narrowed down to

$$\frac{f_+}{f_0} = \frac{\mathcal{B}(\Upsilon(4S) \rightarrow B^+B^-)}{\mathcal{B}(\Upsilon(4S) \rightarrow B^0\bar{B}^0)} = 1.00 \pm 0.04$$

At hadron machines, the  $B$  meson fractions depend on fragmentation, and vary with target and cms energy. An estimate for 8TeV protons on a  $p$  or  $n$  target using the Lund fragmentation model [114] is given in table 3.2. Experimental ratios obtained at LEP are included in this table, and indicate an underestimated baryon production in the Monte Carlo model. Little is known, however, on the effects of the initial  $u$  and  $d$  quarks in  $pp$  or  $pn$  collisions. Consequently, the model predictions should be taken as nothing more but an educated guess, which should be correct within better than 10%.

<b>Table 3.2</b> $b$ hadron production rates per event predicted by the Lund Monte Carlo (8TeV $p \rightarrow p/n$ ). The fractions on the $Z^0$ [64] give the best present experimental knowledge for $b\bar{b}$ jets without further quarks from the initial state.						
$\bar{b}$	$pp$	$pn$	$b$	$pp$	$pn$	$Z^0$
$B^0$	0.408	0.430	$\bar{B}^0$	0.409	0.402	$0.39 \pm 0.02$
$B^+$	0.454	0.428	$B^-$	0.405	0.410	$0.39 \pm 0.02$
$B_s$	0.091	0.093	$\bar{B}_s$	0.118	0.122	$0.11 \pm 0.02$
$\bar{\Lambda}_b$	0.041	0.043	$\Lambda_b$	0.060	0.058	} $0.11 \pm 0.04$
other	0.006	0.006	other	0.008	0.008	

From these estimates, the expected fraction of  $B^0$  per  $\bar{b}$  jet is about 38%, while studies at the  $B_s$  meson must build on samples which are almost a factor four smaller. The expected rates per year are estimated for five experiments in table 3.3. Although the LHB project is no longer pursued, it is included in the table as an example for a true fixed target experiment, with the advantage of a very close vertex detector.

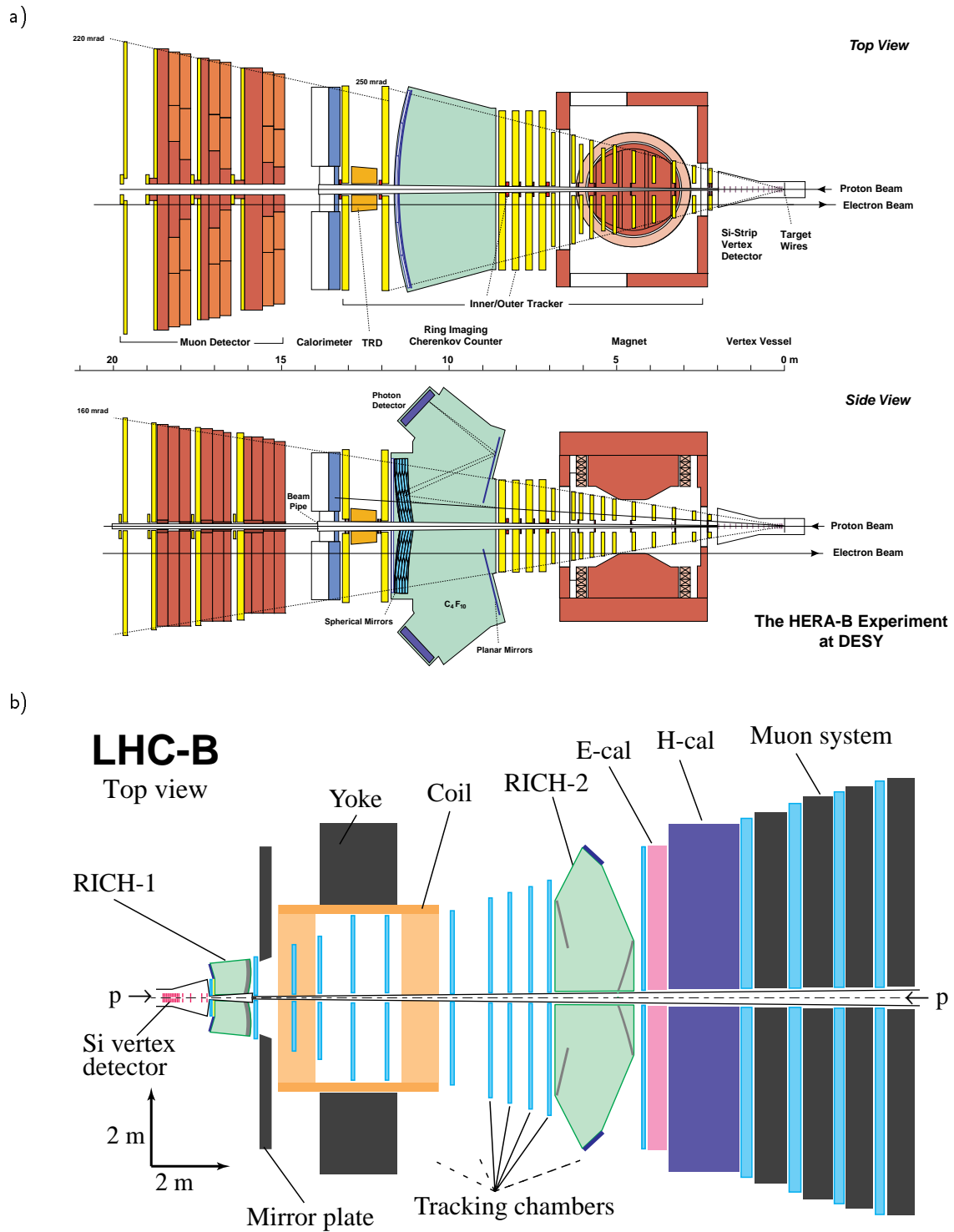
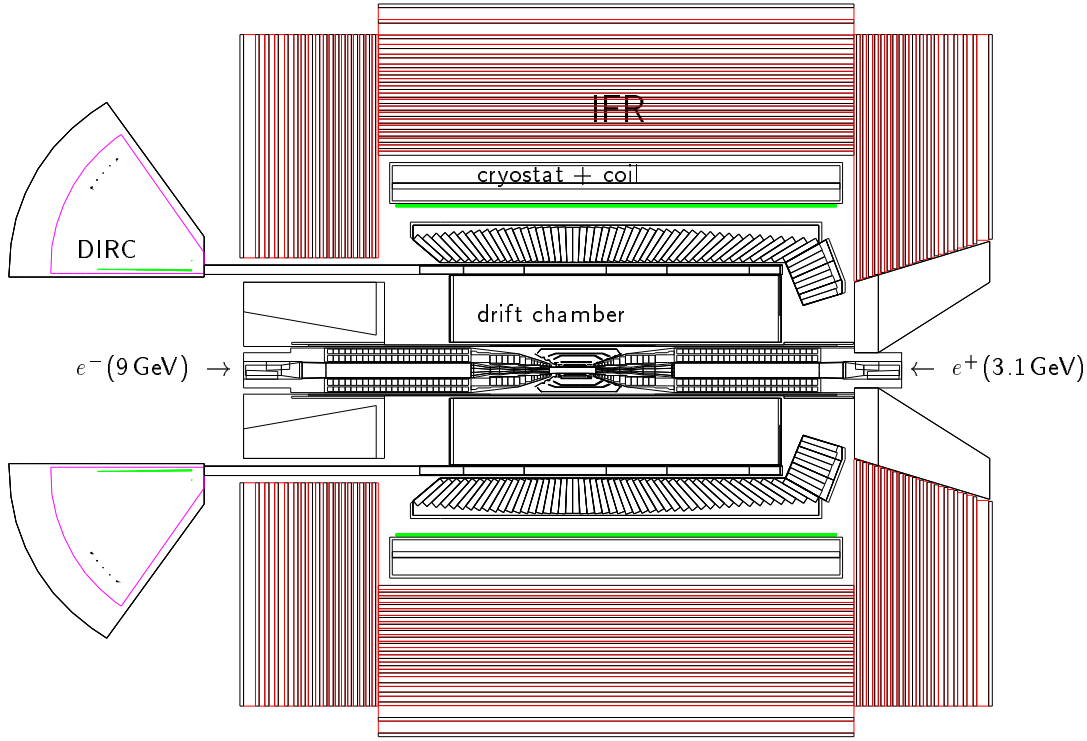


Fig. 3.4 The proposed HERA-B (a) and LHC-B (b) detectors.



**Fig. 3.5** Schematic view of the BABAR detector cut along the beam axis. The focusing quadrupoles and the beam separation dipoles are inside the detector, leaving only limited space for the silicon vertex detector. Both are surrounded by a cylindrical drift chamber, followed in radial direction by the DIRC, the CsI calorimeter, the superconducting magnet coil and the instrumented flux return (IFR).

### 3.1 Flavour Tagging

Any oscillation or CP asymmetry observation requires a tag of the initial flavour at  $T = 0$ . Starting with the most popular example, the initial flavour is tagged with a charged lepton ( $e$  or  $\mu$ ) from the semileptonic decay of the partner  $b$ -hadron. The final states are

$$\begin{aligned} b &\rightarrow \bar{B}^0 \rightarrow J/\psi K_s^0, & \bar{b} &\rightarrow l^+ X \\ \bar{b} &\rightarrow B^0 \rightarrow J/\psi K_s^0, & b &\rightarrow l^- X \end{aligned}$$

Similarly, for other tags there exists always a correlation between a charge  $Q$ —in most cases the electric charge of the tagging particle, but e.g. for  $\Lambda$  hyperons the baryon number—and the beauty flavour of the tag.

The asymmetry  $a$  is in an ideal case, where the flavour  $B^0$  or  $\bar{B}^0$  at  $T = 0$  is known unambiguously from the lepton charge,

$$a(T) = \frac{\dot{N}(\bar{B}^0 \rightarrow J/\psi K_s^0) - \dot{N}(B^0 \rightarrow J/\psi K_s^0)}{\dot{N}(\bar{B}^0 \rightarrow J/\psi K_s^0) + \dot{N}(B^0 \rightarrow J/\psi K_s^0)} = \frac{\dot{N}(J/\psi K_s^0 + l^+) - \dot{N}(J/\psi K_s^0 + l^-)}{\dot{N}(J/\psi K_s^0 + l^+) + \dot{N}(J/\psi K_s^0 + l^-)}$$

### 3.1.1 Observed Versus True Asymmetry

In the real experiment, there are additional asymmetries involved. These are few at  $\Upsilon(4S)$  decays, and many more at hadron  $B$  factories using  $pp$  collisions:

- 1) The number of  $B^0$  and  $\bar{B}^0$  produced in  $pp$  collisions are not equal, due to the fact that an excess of 4  $u$ -quarks and 2  $d$ -quarks is present from the beginning. There are four different fragmentation probabilities:

$$\begin{aligned} f_0 &= N(B^0)/N(\bar{b}) & \bar{f}_0 &= N(\bar{B}^0)/N(b) \\ f_s &= N(B_s)/N(\bar{b}) & \bar{f}_s &= N(\bar{B}_s)/N(b) \end{aligned}$$

This introduces an intrinsic asymmetry, which is not present at  $e^+e^-$  colliders operating at the  $\Upsilon(4S)$ .

- 2) The second  $b$ -hadron used for tagging can have oscillated into its anti-particle with probability

$$\begin{aligned} \chi &= \frac{N(\bar{b} \rightarrow l^-)}{N(\bar{b} \rightarrow l)} = f_0 \chi_0 + f_s \chi_s \\ \bar{\chi} &= \frac{N(b \rightarrow l^+)}{N(b \rightarrow l)} = \bar{f}_0 \chi_0 + \bar{f}_s \chi_s \end{aligned}$$

Here  $\chi$  is the average probability for  $\bar{b} \rightarrow b$ , and  $\bar{\chi}$  for  $b \rightarrow \bar{b}$  through mixing;  $\chi_0$  and  $\chi_s$  denote the mixing probabilities of  $B^0$  and  $B_s$ , respectively. Due to the coherent  $B\bar{B}$  state in  $\Upsilon(4S)$  decays, this effect is absent at  $B$  factories operating at the  $\Upsilon(4S)$ .

- 3) The lepton can be from semileptonic charm decay in the  $b \rightarrow c$  cascade. Likewise, almost all tags—except fully reconstructed  $b$ -hadrons—have a chance to occur at the “wrong” charge. Part of this effect is even due to wrong particle identification of  $b$  decay products. This mistag probability  $w$  is present at all experiments, but is reduced if determined as a function of discriminating variables, as described below.
- 4) The lepton can be faked by  $\pi$  or  $K$ , with absolute multiplicities  $m_+$  and  $m_-$  for faked positive and negative tag leptons, with

$$\begin{aligned} m_+ &= N(\pi^+) \cdot \delta_\pi \cdot \varepsilon_{\pi^+} + N(K^+) \cdot \delta_K \cdot \varepsilon_{K^+} \\ m_- &= N(\pi^-) \cdot \delta_\pi \cdot \varepsilon_{\pi^-} + N(K^-) \cdot \delta_K \cdot \varepsilon_{K^-} \end{aligned}$$

Here  $\varepsilon_X$  is the kinematic tagging acceptance and  $\delta_X$  the misidentification probability for hadron  $X$ . Two sources of hadrons contribute in two different ways:

- At hadronic machines, the charged hadron production through fragmentation yields  $m_+ \neq m_-$  due to the initial quarks from the  $pp$  or  $pn$  state, with no correlation to the  $b$  flavour.
- The charged hadron production through  $b$ -hadron decays may show a substantial charge asymmetry, which is correlated to the  $b$  flavour and therefore has also effective tagging power and mistag probability. This case is absorbed in the mistag probability  $w$ , which includes mistags from true and faked tag leptons.

- 5) Two  $b$ -hadrons with the same beauty may have been produced simultaneously.

At LHB, the rate of  $b\bar{b}$  events is approximately  $2 \cdot 10^{-5}$  per bunch crossing, i.e. 2 in 100 000 events have two separate interactions leading both to a  $b\bar{b}$  pair. According to the Lund model (as simulated in the PYTHIA program) single interactions with  $pp \rightarrow b\bar{b}b\bar{b}X$  have a frequency  $\sim 2 \cdot 10^{-5}$  compared to all  $pp \rightarrow b\bar{b}X$  events. The total rate of  $4 \cdot 10^{-5}$  can safely be neglected. The rate gets slightly higher with increasing cms energy, but stays always below the level to become a significant source of mistag.

- 6) A  $c\bar{c}X$  event occurs together with a  $b\bar{b}$  event, producing additional leptons from charmed hadron decays with no relation to the beauty flavour. At LHB this occurs with a frequency  $\sim 4 \cdot 10^{-3}$ .



Although it may lead to a small amount of additional uncorrelated mistags, which are included in Monte Carlo simulations, it is negligible compared to the contribution from secondary charmed particles in  $b\bar{b}X$  events.

For  $b$  and  $\bar{b}$  flavours as tags at  $T = 0$  we have two event rates  $\dot{N} = dN/dT$  as a function of the proper scaling lifetime  $T$

$$\begin{aligned}\dot{N}(J/\psi K_s^0 + \bar{b}) &= f_0(1+a) \cdot N \\ \dot{N}(J/\psi K_s^0 + b) &= \bar{f}_0(1-a) \cdot N\end{aligned}$$

for given true asymmetry  $a = a(T)$ . Tagging the  $b$  or  $\bar{b}$  with an electron or muon at a hadron machine, the effects mentioned above give the following rates:

$$\begin{aligned}\dot{N}_1 = \dot{N}(J/\psi K_s^0 + l^+) &= (1-a) \cdot \bar{f}_0 \cdot [B(1-\chi) + C\chi + m_+] \cdot N \\ &\quad + (1+a) \cdot f_0 \cdot [B\bar{\chi} + C(1-\bar{\chi}) + m_+] \cdot N \\ \dot{N}_2 = \dot{N}(J/\psi K_s^0 + l^-) &= (1+a) \cdot f_0 \cdot [B(1-\bar{\chi}) + C\bar{\chi} + m_-] \cdot N \\ &\quad + (1-a) \cdot \bar{f}_0 \cdot [B\chi + C(1-\chi) + m_-] \cdot N\end{aligned}\tag{3.1}$$

with the visible branching fractions  $B$  for  $b \rightarrow l^- X$  and  $C$  for  $b \rightarrow l^+ X$  being

$$\begin{aligned}B &\approx 2 [\mathcal{B}(b \rightarrow l^- \nu X) + 0.18\mathcal{B}(B \rightarrow \tau^- \nu X) + 0.08\mathcal{B}(B \rightarrow D_s^- X)] \cdot \varepsilon_B \approx 0.24\varepsilon_B \\ C &\approx \mathcal{B}(b \rightarrow cX) \cdot 2\mathcal{B}(c \rightarrow l^+ \nu X) \cdot \varepsilon_C \approx 0.20\varepsilon_C\end{aligned}$$

Here  $\varepsilon_B$  is the tagging acceptance for ‘‘right sign’’ leptons from the second  $b$ -hadron,  $\varepsilon_C$  the tagging acceptance for ‘‘wrong sign’’ leptons, mainly from secondary charmed hadron decays. The given branching fractions illustrate the main contributions to both classes. Both fractions get additional contributions from right- and wrong-sign pions and kaons, with an amount depending on the lepton identification capability of the detector. Note that the resulting event numbers are about equal, if the efficiency is uniform over the whole phase space, and tagging power has to come from the use of kinematic differences of both lepton samples.

$m_-$  and  $m_+$  are the fake rates from misidentification of hadrons originating not from  $b$  decays. Double tags, e.g. by a true plus a fake lepton, have been ignored in these formulae.

The normalization constant is

$$N = N(b\bar{b}) \cdot \mathcal{B}(B^0 \rightarrow J/\psi K_s^0 \rightarrow l^+ l^- \pi^+ \pi^-) \cdot \varepsilon(T) \cdot e^{-|T|}$$

where  $\varepsilon$  is the reconstruction and trigger efficiency. It will cancel in all ratios.

The observed asymmetry  $a_{\text{obs}}$  is then

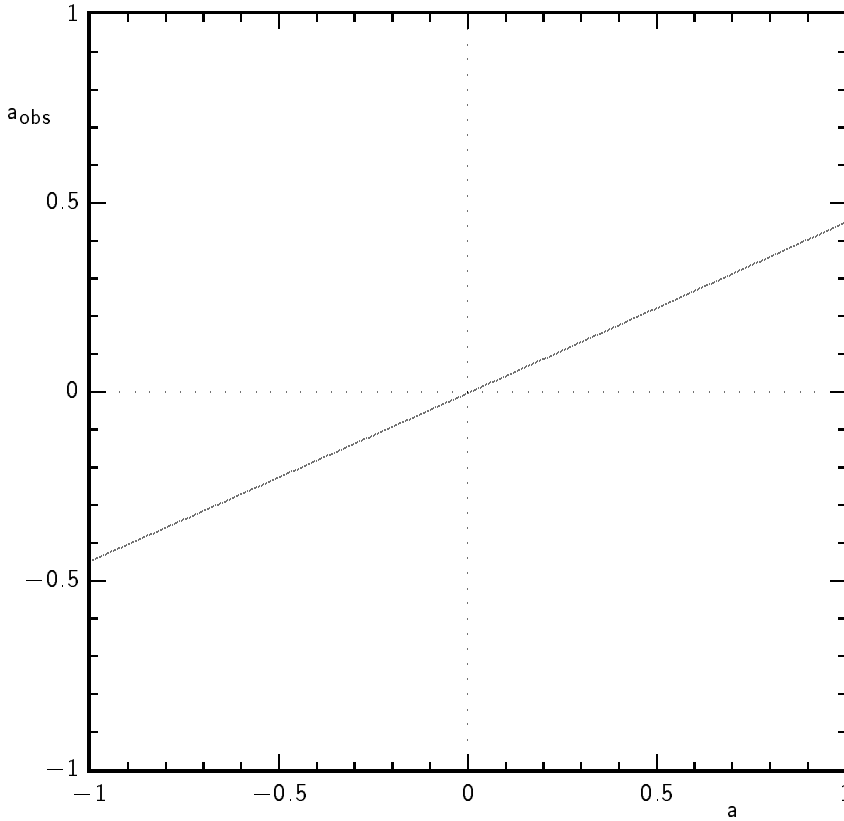
$$\begin{aligned}a_{\text{obs}} &= \frac{\dot{N}_1 - \dot{N}_2}{\dot{N}_1 + \dot{N}_2} \\ &= \frac{I_0(1-2w) + 2\Delta_\chi(1-2w) + I_m}{(1+(1-w)\frac{m_-+m_+}{B})(1+I_0a)} + a \cdot \frac{(1-2w)[1-2\chi_{\text{eff}}] + I_0\Delta_m}{(1+(1-w)\frac{m_-+m_+}{B})(1+I_0a)}\end{aligned}\tag{3.2}$$

with

$$\begin{aligned}w &= \frac{C}{B+C}, & \Delta_\chi &= \frac{f_0\bar{\chi} - \bar{f}_0\chi}{\bar{f}_0 + f_0}, & \chi_{\text{eff}} &= \frac{f_0\bar{\chi} + \bar{f}_0\chi}{\bar{f}_0 + f_0}, \\ I_m &= \frac{m_+ - m_-}{B}(1-w), & I_0 &= \frac{\bar{f}_0 - f_0}{f_0 + \bar{f}_0}\end{aligned}$$

or approximately, ignoring terms  $\mathcal{O}(a^2)$ ,

$$a_{\text{obs}} \approx I + D \cdot a$$



**Fig. 3.6** Observed asymmetry  $a_{\text{obs}}$  versus physical asymmetry  $a$  for a cut on the tag lepton at  $p_{\perp} = 1 \text{ GeV}/c$ , using  $f_0 = 0.404$ ,  $\bar{f}_0 = 0.410$ ,  $f_s = 0.091$ ,  $\bar{f}_s = 0.119$ ,  $N(K^+) = 0.8$ ,  $N(K^-) = 1.12$ ,  $N(\pi^+) = 9.3$  and  $N(\pi^-) = 8.1$  (without those from  $K_S^0$ ) from the PYTHIA/JETSET Monte Carlo programs,  $\mathcal{B}(b \rightarrow l^- X) = 23\%$  and a lepton tagging acceptance of 57%,  $\mathcal{B}(b \rightarrow c \rightarrow l^+ X) = 19\%$  and a tagging acceptance for leptons from charm of 15% (corresponding to  $p_{\perp} > 1 \text{ GeV}/c$ ), a misidentification probability of 2% for  $K$  and 1% for  $\pi$ , and a tagging acceptance for fake pions of 8% and for kaons of 12% ( $K^+$ ) and 17% ( $K^-$ ). In the linear approximation, these parameters give  $I = -0.003$  and  $D = 0.45$ . The deviation from linearity is below visibility in this plot.

with an “intrinsic” asymmetry

$$I = I_0 + 2\Delta_{\chi} + I_m$$

and a “dilution factor”

$$D = \frac{(1 - 2w)(1 - I_0^2)}{1 + (1 - w)\frac{m_- + m_+}{B}} \cdot (1 - \chi - \bar{\chi}) = D_t \cdot D_m$$

where the dilution factor has been split into a tagging component  $D_t$  and a mixing component  $D_m = 1 - \chi - \bar{\chi} \approx 0.78$ . The linear approximation holds very well for all practical purposes, as can be seen in fig. 3.6 from a Monte Carlo simulation using the event parameters for the LHB experiment. The next order approximation is

$$a_{\text{obs}} = I + Da + DI_0 a^2$$

which will only be important at large production asymmetries between  $B^0$  and  $\bar{B}^0$ .

The rate number of reconstructed tagged events is

$$\dot{N}_{\text{tot}} = \dot{N}_1 + \dot{N}_2 = (B + C + m_+ + m_-) \cdot [f_0 + \bar{f}_0 + a(\bar{f}_0 - f_0)] \cdot N$$

On the  $\Upsilon(4S)$ , where a  $B\bar{B}$  pair is produced exclusively and  $T = 0$  is the decay time of the tag- $B$ , the relation (3.2) simplifies considerably, with  $m_- = m_+ = 0$ ,  $\chi = \bar{\chi} = 0$ , and  $f_0 = \bar{f}_0 = 0.5$  to

$$a_{\text{obs}} = (1 - 2w)a \quad (3.3)$$

There is no intrinsic asymmetry ( $I = 0$ , unless the detector has different acceptances for positive and negative particles, which is not considered in the relations above), there is no mixing dilution,  $D_m = 1$ , and the dilution factor is related to the mistag probability simply as  $D = D_t = 1 - 2w$ . This tagging dilution, which is also a good first approximation in more complicated jet environments, can be expressed in the simple form

$$D_t = 1 - 2w = \frac{\text{right-sign} - \text{wrong-sign}}{\text{right-sign} + \text{wrong-sign}} \quad (3.4)$$

where “right-sign” and “wrong-sign” refers to the number of correct and wrong tags, respectively.

As will be shown in detail below, the error on the observed asymmetry amplitude is  $\sigma_a \propto 1/\sqrt{N_1 + N_2}$ . Therefore, the error on the asymmetry amplitude  $A_0$  is approximately

$$\sigma(A_0) = \frac{1}{D\sqrt{N_1 + N_2}} = \frac{1}{\sqrt{\varepsilon_t D^2 N_s}}$$

where  $N_s$  is the number of signal events and  $\varepsilon_t$  is the tagging efficiency, i.e.  $\varepsilon_t N_s$  is the fraction of signal events with a flavour tag. The performance of tagging can therefore be defined by the factor  $(\varepsilon_t D_t^2)_{\text{eff}}$  which gives the effective reduction in number regarding statistical precision. It is also called **separation**, since it is 1 if  $b$  and  $\bar{b}$  can be separated perfectly event by event, and 0 if they cannot be distinguished.

### 3.1.2 Statistical Tagging

Flavour tagging exploits always a correlation between the beauty flavour of the parent  $b$ -hadron and a charge  $Q$ —in most cases the electric charge of the tagging particle, but e.g. for  $\Lambda$  hyperons the baryon number or strangeness and for  $D^0$  mesons the charm. This correlation is perfect for fully reconstructed beauty mesons or baryons.

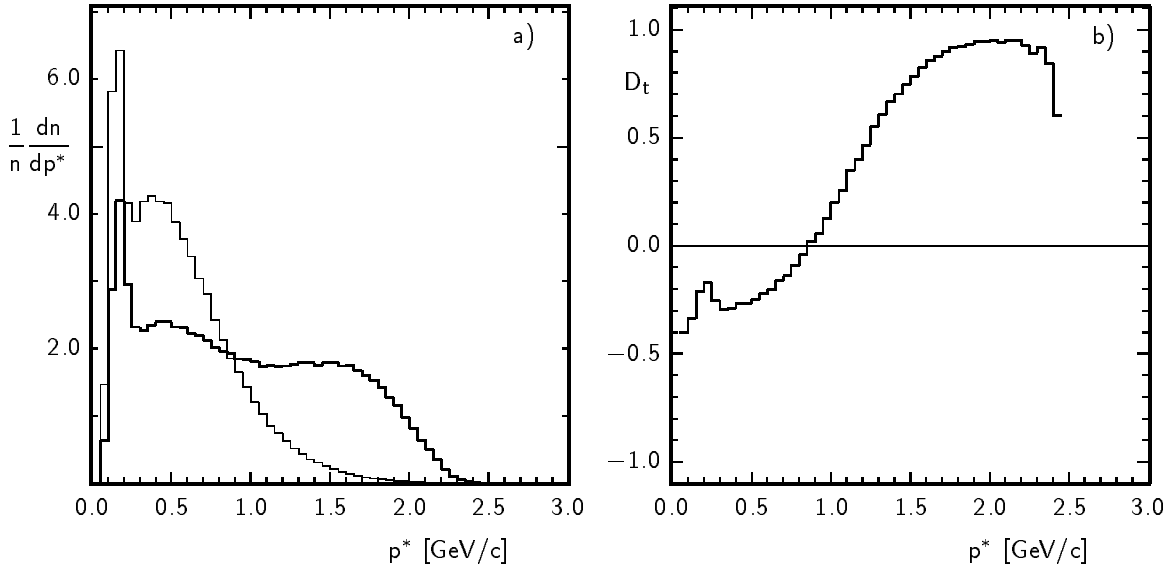
However, a complete reconstruction of  $B$  decays will only be possible in a very limited number of events. A more universal approach is to collect this information via certain characteristics of the particles which are able to identify the flavour. In the example above, only leptons have been used, with a charge correlated to the beauty flavour via semileptonic decays  $b \rightarrow l^- \bar{\nu} c$ . This tagging method suffers from two problems:

- only about 20% of all  $b$  hadrons decay semileptonically, and
- a substantial fraction of leptons from other sources have the “wrong” charge.

A more complete exploitation of the secondaries from  $B$  decays can be achieved in a statistical analysis. The flavour tagging power of these decay products (like charged leptons) is determined by the values of a small number of discriminating variables  $X_1, X_2, \dots$  which help to identify their role in the decay process [117,118,119]. Thus, instead of fitting  $a_{\text{obs}}(T) = D A_0 \sin xT + I$ , we may fit a two-dimensional distribution

$$a_{\text{obs}}(T, D) = D A_0 \sin xT + I \quad (3.5)$$

to obtain the parameter  $A_0$ . Here the mistag contribution to  $D$  is not a constant average dilution factor, but a **function** of the discriminating variables  $X_1, X_2, \dots$ , and varies between  $-1$  and  $+1$ . Negative values mean that in the kinematic range defined by  $\{X_1, X_2, \dots\}$  there are more “wrong-sign” tags with opposite sign of charge and flavour than “right-sign” (or same-sign) tags. In other words, the correlation between the charge and the beauty flavour has flipped.  $D$  is evaluated event by event in addition to the scaled lifetime (difference)  $T$ .



**Fig. 3.7** Distributions of muons in the  $\Upsilon(4S)$  cms momentum for “right-sign” (—) and “wrong-sign” (---) tags (a), and the corresponding dilution factor (b). The simulation has been done for the BABAR detector; the peak at low momentum is due to  $K$  and  $\pi$  decays and particle misidentification.

While this concept should be applied to all dilution factors, e.g. to mixing dilution as a function of the lifetime of a  $B$  meson in the second jet or to the dilution due to limited precision in the determination of the oscillation time  $T$  as a function of vertex precision, in the following sections only the application to the tagging dilution will be discussed. The relevant information for the fit is the tagging dilution coefficient  $D_t(X_1, X_2, \dots)$  itself. It is given by all tag particles, i.e. particles with a nonzero charge-like quantum number  $Q$  that can be correlated to the beauty flavour. The discriminating variables for each particles have to be chosen in a way to differentiate maximally between kinematic situations with different correlation strength. An obvious variable is the momentum of the particle in the parent’s rest frame, if this can be reconstructed. This is illustrated in figure 3.7, where the momentum of muons in the  $\Upsilon(4S)$  rest frame—which comes close to the  $B$  rest frame—is used as discriminator: Above a value of about  $1.5 \text{ GeV}/c$ , almost all muons are from semileptonic  $B$  decays, and show therefore an almost perfect correlation with the beauty flavour. This is indicated by a dilution factor close to 1 in figure 3.7b, which is calculated from the distributions in figure 3.7a using (3.4). At values below  $0.7 \text{ GeV}/c$  there is an opposite correlation due to  $b \rightarrow c \rightarrow l^+ \nu X$ , though diluted to about one fifth. The flip of the correlation is at  $0.9 \text{ GeV}/c$ , where the mistag probability is  $w = \frac{1}{2}$ , and no flavour information is obtained.

Other discriminating variables can be e.g. the impact parameter to the beam axis or the angle to the closest track from the same  $B$ . Often information on the environment may have even better or at least complementary discriminating power, e.g. the energy of a neutrino as missing momentum in the case of a charged lepton tag.

In the statistical approach one considers the distributions of the variables  $X_{11}, X_{12} \dots$  of daughter particle 1 with charge  $Q_1$ , the variables  $X_{21}, X_{22} \dots$  of daughter particle 2 with charge  $Q_2$ , and so on, i.e.

$$f_B(X_{11}, X_{12} \dots, X_{21}, X_{22}, \dots, \dots | Q_1, Q_2 \dots)$$

if the parent was a  $B$  meson (or  $\bar{b}$ -hadron), and

$$f_{\bar{B}}(X_{11}, X_{12} \dots, X_{21}, X_{22}, \dots, \dots | Q_1, Q_2 \dots)$$

if the parent was a  $\bar{B}$  meson (or  $b$ -hadron). The mostly continuous variables  $X_{ij}$  and the charges  $Q_i$  may both be considered random variables. The flavour of this event is assigned by maximum likelihood,

i. e. if  $f_B > f_{\bar{B}}$  the beauty of the event is taken to be +1 and vice versa. This assignment is unique, and depends on the  $X$  and  $Q$  variables together. The signed dilution factor is then

$$D_t(X \dots, Q \dots) = \frac{f_B(X \dots | Q \dots) - f_{\bar{B}}(X \dots | Q \dots)}{f_B(X \dots | Q \dots) + f_{\bar{B}}(X \dots | Q \dots)}$$

where the sign gives the estimated beauty quantum number, and its absolute value gives the dilution factor corresponding to this flavour assignment.

For one-dimensional distributions, the true flavour is statistically related to  $Q$  by the densities  $f_B(X_j|Q)$  of tags with a  $\bar{b}$  quark, and  $f_{\bar{B}}(X_j|Q)$  of tags with a  $b$  quark. The average beauty flavour of a sample with a certain value  $X_j$  and  $Q$  is then

$$\hat{B}_i = \frac{f_B(X_j|Q) - f_{\bar{B}}(X_j|Q)}{f_B(X_j|Q) + f_{\bar{B}}(X_j|Q)} \quad (3.6)$$

For the opposite charge, the densities are  $f_B(X_j|-Q) = f_{\bar{B}}(X_j|Q)$  and  $f_{\bar{B}}(X_j|-Q) = f_B(X_j|Q)$  up to negligible explicit CP violations. This reduces four functions in the general ansatz to only two functions. Instead of treating  $Q = +1$  and  $-1$  as two values of an additional random variable, the flavour of the parent  $b$ -hadron may be a priori assigned to be  $Q$ . This assignment is arbitrary, and could be opposite, as long as it is uniquely defined. Then the flavour estimator can be written as

$$\hat{B}_i = D_t(X_j) \cdot Q \quad (3.7)$$

The absolute value of the signed factor

$$D_t(X_j) = \frac{f_B(X_j|+) - f_{\bar{B}}(X_j|+)}{f_B(X_j|+) + f_{\bar{B}}(X_j|+)} = \frac{f_B(X_j|+) - f_B(X_j|-)}{f_B(X_j|+) + f_B(X_j|-)}$$

is the tagging dilution factor for all tags with a value  $X_j$ . It is  $|D_t| = 1$  if the flavour is perfectly correlated with  $Q$ . The sign is a flavour corrector: It is negative if the arbitrary a priori assignment from  $Q$  is more often wrong than right:

$$D_t = \frac{\text{right-sign} - \text{wrong-sign}}{\text{right-sign} + \text{wrong-sign}}$$

It is typically a smooth function of  $X_j$ , and can be obtained from a Monte Carlo simulation or from real data measuring the  $B\bar{B}$  oscillation amplitude as described below.

The flavour estimator  $\hat{B}$  defined in (3.7) is the average flavour of events in a sample with tagging particles of charge  $Q$  and discriminating variable  $X_j$ , e. g. of positive leptons at a given cms momentum:

$$\hat{B} = (+1) \cdot \frac{f_B(X_j|Q)}{f_B(X_j|Q) + f_{\bar{B}}(X_j|Q)} + (-1) \cdot \frac{f_{\bar{B}}(X_j|Q)}{f_B(X_j|Q) + f_{\bar{B}}(X_j|Q)}$$

The coefficients are the fractions (or *a posteriori* probabilities) of events from  $B$  and  $\bar{B}$ , respectively. This variable is itself a discriminating variable comprising all used information in the event. It can be split into its sign—used as flavour guess—and its absolute value  $|\hat{B}|$ , which is the tagging dilution factor

$$D_t(\hat{B}) = |\hat{B}|$$

All informations  $X_{ij}$  from one or several tags in an event are combined to estimate the flavour of the tag hadron more reliably.

A full exploitation of this tagging method is, however, impossible since the detailed information required to determine the innumerable multidimensional functions cannot be achieved within the statistical precision of any experiment. Several approximations are proposed to overcome the technical problems.

One approach is to use only one-dimensional distributions and to assume factorization [117,119]

$$f_B(X_{11}, X_{12} \dots, X_{21} \dots | Q_1, Q_2 \dots) = f_B(X_{11} | Q_1) \cdot f_B(X_{12} | Q_1) \cdots f_B(X_{21} | Q_2) \cdots$$

With this ansatz, one can add all flavour estimators of the same event like relativistic velocities. For two tagging particles with variables  $X_1, Q_1$  and  $X_2, Q_2$ , inserting (3.7) into the result

$$\hat{B} = \hat{B}_1 \oplus \hat{B}_2 := \frac{\hat{B}_1 + \hat{B}_2}{1 + \hat{B}_1 \hat{B}_2} \quad (3.8)$$

leads immediately to

$$\hat{B} = \frac{f_B(X_1 | Q_1) f_B(X_2 | Q_2) - f_{\bar{B}}(X_1 | Q_1) f_{\bar{B}}(X_2 | Q_2)}{f_B(X_1 | Q_1) f_B(X_2 | Q_2) + f_{\bar{B}}(X_1 | Q_1) f_{\bar{B}}(X_2 | Q_2)}$$

Repeated addition of the estimators from all tagging particles and discriminating variables yields the total flavour estimator of the event.

Although factorization is not valid, the approximation is usually quite good and can be tested by determining  $D_t(\hat{B})$ . The deviation  $D_t(\hat{B}) - |\hat{B}|$  is a measure of the correlations; if it is small, the approximation is a good one, if it is large, a different way to combine tagging information may improve the result.

A very promising approach for this improvement is to **combine** many discriminating variables for one particle into one output variable, which is an optimum representation of the flavour information including the correlations. A linear combination of carefully chosen variables is used in a Fisher discriminant analysis. Even better results are achieved with the help of learning neural networks [120]. A combination of both methods, or more flexible neural networks which allow input of a variable number of tag particles and their corresponding parameters, can finally give a maximum of information.

In a statistical tagging method, the effective performance or separation  $(\varepsilon_t D_t^2)_{\text{eff}}$  can no longer be split into two factors. In fact,  $\varepsilon_t$  is one in the ultimate realization, where every event is used as a tag. The product, on the other hand, can still be evaluated as

$$(\varepsilon_t D_t^2)_{\text{eff}} = \int_0^1 \frac{d\varepsilon_t}{ds} D_t^2(s) ds$$

where

$$\frac{d\varepsilon_t}{ds} = f(s)$$

is the probability density of  $s = |\hat{B}|$ . In the general concept, a flavour estimator is constructed for every event—with a value close to 0 if no good tagging information is available—and the performance number

$$(\varepsilon_t D_t^2)_{\text{eff}} = \langle D_t^2 \rangle = \langle s^2 \rangle$$

is the average tagging dilution of all events.

The idea to calculate a flavour estimator for every event is especially promising on the  $\Upsilon(4S)$ , where  $B^0 \bar{B}^0$  are produced exclusively. After removing the signal CP channel (e.g.  $J/\psi K_s^0$ ), the whole residual event is from the other  $B$ , so every charged particle can be used for statistical tagging.

## 3.2 Estimating the Performance

The performance of an experiment can be estimated by the expected error within one year of data taking. Complications due to penguin amplitudes (“penguin pollution”) are shortly discussed below. The error on an asymmetry amplitude  $A_0$  (or likewise  $\Theta_0$ ) is approximated as

$$\sigma(A_0) = \frac{1}{S_0 \sqrt{N_{\text{eff}}}} \quad (3.9)$$

where the “effective number of events” is

$$N_{\text{eff}} = D_r^2 D_c D_m^2 (\varepsilon_t D_t^2)_{\text{eff}} \varepsilon_s \mathcal{B}(B^0 \rightarrow X) \cdot 2f_0 \sigma(b\bar{b}) \cdot L \cdot 10^7 \text{ s}$$

with the following factors:

$10^7 \text{ s}$  is the assumed duty time of any dedicated experiment at design luminosity in a year.

$L$  is the luminosity of the machine.

$\sigma(b\bar{b})$  is the cross section for  $b$  quark pair production.

$f_0$  is the fraction of  $b$  quarks turned into  $B^0$  mesons.

$\mathcal{B}(B^0 \rightarrow X)$  is the product branching fraction of  $B^0$  into the final state investigated, e.g.  $\mathcal{B}(B^0 \rightarrow J/\psi K_s^0) \cdot \mathcal{B}(K_s^0 \rightarrow \pi^+ \pi^-) \cdot [\mathcal{B}(J/\psi \rightarrow e^+ e^-) + \mathcal{B}(J/\psi \rightarrow \mu^+ \mu^-)]$ .

$\varepsilon_s$  is the signal reconstruction efficiency, including the geometric acceptance and the trigger efficiency. This may be correlated with  $\varepsilon_t$ , if a trigger uses information from the tag.

$\varepsilon_t$  is the tagging efficiency. It goes always with the tagging dilution factor  $D_t$  as the product  $\varepsilon_t D_t^2$ . Exploiting statistical tagging to its fullest,  $\varepsilon_t = 1$  while all loss from ambiguous tags is moved into the effective average  $\langle D_t^2 \rangle = (\varepsilon_t D_t^2)_{\text{eff}}$ .

$D_m$  is the mixing dilution factor:  $D_m = 1$  at the  $\Upsilon(4S)$ ,  $D_m = 1 - \chi - \bar{\chi} \approx 0.78$  for incoherent  $b\bar{b}$  production and tags from the other  $b$ -hadron. Same-jet tagging techniques, like using a jet charge or the pion from  $B^{*+} \rightarrow B^0 \pi^+$ , are not subject to mixing dilution.

$D_c \approx 1 - c$  is a dilution factor induced by background to the signal channel. The total number of events is increased by background by a factor  $1/D_c$ , and at the same time the asymmetry amplitude is decreased by a factor  $D_c$ , giving rise to a reduction factor  $D_c^2$  for the effective number. This is the simplest way to incorporate background effects. A detailed study of the time evolution of background can further reduce its influence on the error.

$D_r$  is the dilution factor arising from lifetime resolution.

Comparing the various experimental proposals requires detailed information, since they use different assumptions for these numbers, and also different levels of realism in detector simulation. It is, however, fair to predict that—if the Standard Model is right—CP violation will be discovered around the year 2000.

## Acknowledgements

My understanding of heavy flavour physics and  $B/\bar{B}$  mixing has evolved during my long stay with the ARGUS collaboration, and I owe thanks to many colleagues there for having improved my knowledge in theory, data analysis and experimental techniques. During my work for LHB and BABAR, I have profited greatly from the common work with hundreds of physicists in these collaborations all around the world. Many ideas written in this paper have been evolved or clarified in very fruitful discussions with other colleagues, among them Giovanni Carboni, Robert Fleischer, Joachim Graf, Frank Krauss, Christof Kreuter, Francois Le Diberder, Ralph Müller, Dominic Pötschke, Helen Quinn, Klaus R. Schubert, Bernhard Spaan, and Jörg Urban. I thank the organizers of the Herbstschule Maria Laach for arranging this interesting school.



## References

- [1] T. D. Lee, C. N. Yang, *Phys. Rev.* **104**, 254 (1956).
- [2] C. S. Wu et al., *Phys. Rev.* **105**, 1413 (1957); R. L. Garvin et al., *Phys. Rev.* **105**, 1415 (1957); J. J. Friedman, V. L. Telegdi, *Phys. Rev.* **105**, 1681 (1957).
- [3] J. H. Christenson, J.W. Cronin, V.L. Fitch, R. Turlay, *Phys. Rev. Lett.* **13**, 138 (1964).
- [4] N. Cabibbo, *Phys. Rev. Lett.* **10**, 531 (1963).
- [5] M. Kobayashi, T. Maskawa, *Progr. Theor. Phys.* **49**, 652 (1973).
- [6] see e. g. chapter 20 in M. E. Peskin, D. V. Schroeder, “An Introduction to Quantum Field Theory”, Addison-Wesley Publ., Reading 1995.
- [7] C. Jarlskog, “Mysteries in the Standard Model”, *Proc. of the Int. Symp. on Production and Decay of Heavy Flavours, Heidelberg 1996*, p.331.
- [8] The Large Hadron Collider, Conceptual Design, CERN/AC/95-05; C. H. Llewellyn Smith, *Proc. of the 17th Int. Symp. on Lepton-Photon Interactions, Beijing 1995*, eds. Z.-P. Zheng, H.-S. Chen, World Scientific Publ., Singapore 1996, p. 370.
- [9] The Particle Data Group, *Phys. Rev.* **D54**, 1 (1996).
- [10] L.-L. Chau, W.-Y. Keung, *Phys. Rev. Lett.* **53**, 1802 (1984).
- [11] H. Harari, M. Leurer, *Phys. Lett.* **B181**, 123 (1986).
- [12] L. Wolfenstein, *Phys. Rev. Lett.* **51**, 1945 (1984).
- [13] Z. Z. Xing, *Phys. Rev.* **D51**, 3958 (1995).
- [14] M. Kobayashi, *Progr. Theor. Phys.* **92**, 287 (1994).
- [15] K. R. Schubert, *Proc. of the Int. Europhysics Conf. on High Energy Physics, Uppsala, Sweden*, ed. O. Botner, June 1987, vol. II, p. 791.
- [16] C. Hamzaoui, J. L. Rosner, A. I. Sanda, *Proc. of the Workshop on High Sensitivity Beauty Physics at Fermilab, Batavia IL, USA*, eds. N. Lockyerd, J. Slaughter, Nov. 1987, p. 215.
- [17] C. Jarlskog, *Phys. Rev. Lett.* **55**, 1039 (1985); *Z. Phys.* **C29**, 491 (1985).
- [18] A. Ali, D. London, *Nucl. Phys. Proc. Suppl.* **54A**, 297 (1997)
- [19] T. T. Wu, C. N. Yang, *Phys. Rev. Lett.* **13**, 380 (1964).
- [20] G. Lüders, *Dan. Mat. Fys. Medd.* **28**, 5 (1954); *Ann. Phys. N.Y.* **2**, 1 (1957).
- [21] e. g. E. D. Commins, P. H. Bucksbaum, “Weak Interactions of Leptons and Quarks”, Cambridge University Press, 1983.
- [22] T. Nakada, PSI-PR-91-02 (1991);  
T. Nakada, *Proc. of the XVIth Int. Symp. on Lepton-Photon Interactions, Ithaca 1993*, eds. P. S. Drell, D. L. Rubin, AIP, New York 1994, p. 425.
- [23] A. J. Buras, R. Fleischer, TUM-HEP-275/97, to appear in *Heavy Flavours II*, ed. by A. J. Buras, M. Lindner, World Scientific 1997.
- [24] V. F. Weisskopf, E. P. Wigner, *Z. Phys.* **63**, 54 (1930) and *Z. Phys.* **65**, 18 (1930). A detailed discussion is in O. Nachtmann, “Elementarteilchenphysik – Phänomene und Konzepte” (in German), Vieweg, Braunschweig 1986; see also [21,22].
- [25] A. J. Buras, W. Słominski, H. Steger, *Nucl. Phys.* **B245**, 369 (1984).
- [26] T. Inami, C. S. Lim, *Progr. Theor. Phys.* **65**, 297 (1981), and erratum *Progr. Theor. Phys.* **65**, 1772 (1981).

- [27] A. J. Buras, M. Jamin, P. H. Weisz, Nucl. Phys. **B347**, 491 (1990).
- [28] for recent reviews see e.g. H. Wittig, DESY 96-110 (1996);  
A. Patel, e-print hep-ph/9611279 (1996);  
V. Giménez, G. Martinelli, C. T. Sachrajda, Nucl. Phys. Proc. Suppl. **53**, 365 (1997).
- [29] Y. Nir, Phys. Lett. **B327**, 85 (1994).
- [30] OPAL Coll., Z. Phys. **C67**, 379 (1995).
- [31] DELPHI Coll., Z. Phys. **C68**, 13 (1995).
- [32] DELPHI Coll., Z. Phys. **C68**, 363 (1995).
- [33] ALEPH Coll., CERN-PPE/96-14.
- [34] DELPHI Coll., CERN-PPE/96-139.
- [35] SLD Coll., SLAC-PUB-7226 (1996).
- [36] SLD Coll., SLAC-PUB-7227 (1996).
- [37] T. Miao, CDF Coll., FERMILAB-CONF-96/268-E
- [38] H. Albrecht et al. (ARGUS), Phys. Lett. **B192**, 245 (1987).
- [39] ALEPH Collab., Phys. Lett. **B313**, 498 (1993).
- [40] M. Artuso et al. (CLEO), Phys. Rev. Lett. **62**, 2233 (1989).
- [41] H. Albrecht et al. (ARGUS), Z. Phys. **C55**, 357 (1992).
- [42] J. Bartelt et al. (CLEO), Phys. Rev. Lett. **71**, 1680 (1993).
- [43] H. Albrecht et al. (ARGUS), Phys. Lett. **B324**, 249 (1994).
- [44] H. Albrecht et al. (ARGUS), Phys. Lett. **B375**, 256 (1996).
- [45] ALEPH Collab., Phys. Lett. **B322**, 441 (1994).
- [46] ALEPH Collab., CERN-PPE/96-102.
- [47] DELPHI Collab., Phys. Lett. **B338**, 409 (1994).
- [48] DELPHI Collab., Z. Phys. **C72**, 17 (1996).
- [49] DELPHI Collab., CERN-PPE/97-51.
- [50] OPAL Collab., Phys. Lett. **B327**, 411 (1994).
- [51] OPAL Collab., CERN-PPE/96-074.
- [52] OPAL Collab., CERN-PPE/97-036.
- [53] OPAL Collab., CERN-PPE/97-064.
- [54] L3 Collab., Phys. Lett. **B383**, 487 (1996).
- [55] SLD Collab., SLAC-PUB-7230 (1996).
- [56] SLD Collab., SLAC-PUB-7228 (1996).
- [57] SLD Collab., SLAC-PUB-7229 (1996).
- [58] CDF Collab., FERMILAB-CONF-96/175-E, contributed paper pa08-032 to the 28th Int. Conf. on High Energy Physics, Warsaw 1996.
- [59] CDF Collab., FERMILAB-PUB-97/312-E.
- [60] F. DeJongh, G. Michail (CDF), FERMILAB-CONF-96/407-E (1996).
- [61] ALEPH Collab., Phys. Lett. **B356**, 409 (1995).
- [62] ALEPH Collab., Phys. Lett. **B377**, 205 (1996).
- [63] ALEPH Collab., contributed paper pa08-020 to the 28th Int. Conf. on High Energy Physics,

- Warsaw 1996.
- [64] O. Schneider, presentation at the 18th Int. Symp. on Lepton-Photon Interactions, Hamburg 1997.
  - [65] OPAL Coll., Phys. Lett. **B350**, 273 (1995).
  - [66] CDF Coll., FERMILAB-CONF-96/154-E, contributed paper pa05-098 to the 28th Int. Conf. on High Energy Physics, Warsaw 1996.
  - [67] CDF Coll., Phys. Rev. Lett. **77**, 1945 (1996).
  - [68] DELPHI Coll., Z. Phys. **C71**, 11 (1996).
  - [69] DELPHI Coll., DELPHI 96-60 CONF 19, contributed paper pa01-042 to the 28th Int. Conf. on High Energy Physics, Warsaw 1996.
  - [70] ALEPH Coll., Z. Phys. **C69**, 585 (1996).
  - [71] OPAL Collab., CERN-PPE/97-095.
  - [72] H. Wittig, OUTP-97-20P (1997), subm. to J. Mod. Phys. A.
  - [73] I. Bigi et al., CERN-TH-7132/94 (1994), published in “*B* Decays”, ed. S. Stone, World Scientific Publ., 1995.
  - [74] R. Aleksan, Phys. Lett. **B316**, 567 (1993).
  - [75] M. Beneke, G. Buchalla, I. Dunietz, Phys. Rev. **D54**, 4419 (1996).
  - [76] I. Dunietz, FERMILAB-PUB-94/36-T (1995);  
T. Browder, S. Pakvasa, UH-511-814-95 (1995).
  - [77] see e.g. H. Quinn, SLAC-PUB-95-7053 (1995).
  - [78] an experiment to measure CP violation in  $\Xi^-$  decays is E-871: J. Antos et al., FERMILAB Proposal P-871 (1994).
  - [79] for a recent review on neutrino oscillations see e.g. A. Yu. Smirnov, talk given at the 28th Int. Conf. on High Energy Physics, Warsaw 1996, e-print hep-ph/9611465 (1996);  
CP and T violation is discussed in M. Tanimoto, Phys. Rev. **D55**, 322 (1997); J. Arafune, J. Sato, Phys. Rev. **D55**, 1653 (1997).
  - [80] U. Kilian et al., Z. Phys. **C62**, 413 (1994); S. Y. Choi et al., Phys. Rev. **D52**, 1614 (1995);  
J. H. Kühn, E. Mirkes, TTP-96-43 (1996); Y. S. Tsai, Phys. Lett. **B378**, 272 (1996).
  - [81] for reviews see e.g. W. Grimus, Fortschr. Phys. **36**, 201 (1988); W. Bernreuther, M. Suzuki, Rev. Mod. Phys. **63**, 313 (1991); J. Bernabéu et al., FTUV/95-15 and Proc. of the Ringberg Workshop on Perspectives for Electroweak Interactions in  $e^+e^-$  Collisions, Feb 1995, ed. by B. A. Kniehl, World Scientific, 1995.
  - [82] M. Gronau et al., Phys. Rev. **D50**, 4529 (1994); Phys. Rev. **D52**, 6374 (1994); Phys. Lett. **B333**, 500 (1994); Phys. Rev. Lett. **73**, 21 (1994);  
L. Wolfenstein, Phys. Rev. **D52**, 537 (1995);  
N. G. Deshpande, X. G. He, Phys. Rev. Lett. **75**, 1705 (1995); Phys. Rev. Lett. **75**, 3064 (1995);  
A. J. Buras, R. Fleischer, Phys. Lett. **B360**, 138 (1995); Phys. Lett. **B365**, 390 (1996);  
G. Kramer, W. F. Palmer, Phys. Rev. **D52**, 6411 (1995);  
B. Grinstein, R. F. Lebed, Phys. Rev. **D53**, 6344 (1996).
  - [83] A. B. Carter, A. I. Sanda, Phys. Rev. Lett. **45**, 952 (1980); Phys. Rev. **D23**, 1567 (1981).
  - [84] I. I. Bigi, A. I. Sanda, Nucl. Phys. **B193**, 85 (1981); Nucl. Phys. **B281**, 41 (1987).
  - [85] R. Fleischer, I. Dunietz, Phys. Lett. **B387**, 361 (1996); Phys. Rev. **D55**, 259 (1997).
  - [86] I. Dunietz et al., Phys. Rev. **D43**, 2193 (1993).
  - [87] M. Gronau, D. London, Phys. Lett. **B253**, 483 (1991).
  - [88] M. Gronau, D. Wyler, Phys. Lett. **B265**, 172 (1991).

- [89] I. Dunietz, Phys. Lett. **B270**, 75 (1991).
- [90] R. Aleksan, I. Dunietz, B. Kayser, Z. Phys. **C54**, 653 (1992).
- [91] DELPHI Collab., M. Feindt et al., DELPHI 97-98 CONF 80, contributed paper to the 18th Int. Symp. on Lepton-Photon Interactions, Hamburg 1997.
- [92] Z.-Z. Xing, Phys. Rev. **D53**, 204 (1996)
- [93] D. E. Dorfan et al., Phys. Rev. Lett. **19**, 987 (1967);  
S. Bennett et al., Phys. Rev. Lett. **19**, 993 (1967).
- [94] for a recent review see T. Ruf, CERN-PPE/96-190 (1996).
- [95] Proposal for an Electron Positron Collider for Heavy Flavour Particle Physics and Synchrotron Radiation, PR-88-09, PSI Villigen, 1988.
- [96] Feasibility Study for a *B*-Meson Factory in the CERN ISR Tunnel, ed. T. Nakada, CERN 90-02 (1990).
- [97] HELENA - A Beauty Factory in Hamburg, DESY 92-041 (1992).
- [98] PEP II Conceptual Design Report, SLAC-372 (1991); BABAR Letter of Intent SLAC-443 (1994);  
J. T. Seeman, SLAC-Pub-7475 (1997);  
see also [121].
- [99] BELLE Collab., Letter of Intent for a Study of CP Violation in *B* Meson Decays, KEK Report 94-2 (1994); see also [122].
- [100] The LHB Collab., K. Kirsebom et al., CERN/LHCC/93-45 (Letter of Intent, 1993) and  
CERN/LHCC/94-11 (Addendum, 1994).
- [101] GAJET Collab., R. Arnold et al., CERN/LHCC/93-54 (Letter of Intent, 1993).
- [102] COBEX Collab., S. Erhan et al., CERN/LHCC/93-50 (Letter of Intent, 1993).
- [103] LHC-B Collaboration, K. Kirsebom et al., CERN/LHCC 95-5 (Letter of Intent, 1995).
- [104] T. Lohse et al., DESY-PRC 94/02 (HERA-B Proposal) and E. Hartouni et al., DESY-PRC 95/01  
(Design Report).
- [105] CDF Collab., The CDF Upgrade, CDF/DOC/3171 (1995); M. Paulini, FERMILAB-Conf-96/261-E  
(1996); see also [107].
- [106] CLEO collaboration, Detector for a B Factory, CLNS-91-1047-REV (1993).
- [107] R. Lipton, Il Nuovo Cim. **109A**, 1089 (1996).
- [108] D0 Collab., The D0 Upgrade, The Detector and Its Physics, FERMILAB-Pub-96/357-E (1996);  
see also [107].
- [109] J. N. Butler, FERMILAB-Conf-96/436 (1996); A. Santoro et al., BTeV: An Expression of Interest  
for a Heavy Quark Program at C0, May 1997.
- [110] ARGUS Coll., Z. Phys. **C65**, 619 (1995).
- [111] using a FORTRAN program of S. Werner.
- [112] CLEO Collab., Phys. Rev. **D50**, 43 (1994).
- [113] CDF Collab., Phys. Rev. Lett. **71**, 500 (1993); Phys. Rev. Lett. **71**, 2396 (1993); Phys. Rev. Lett.  
**75**, 1451 (1995).
- [114] T. Sjöstrand, PYTHIA 5.6 and JETSET 7.3 Physics and Manual, CERN-TH.6488/92 (1992).
- [115] H. Cobbaert et al. (WA78), Phys. Lett. **B191**, 456 (1987); M. Adamovich et al. (WA82), Phys.  
Lett. **B284**, 453 (1992); G. A. Alves et al. (E769), Phys. Rev. Lett. **70**, 722 (1993).
- [116] G. P. Lepage, Phys. Rev. **D42**, 3251 (1990); N. Byers, E. Eichten, Phys. Rev. **D42**, 3885 (1990).
- [117] D. E. Jaffe, F. Le Diberder, M. H. Schune, G. Wormser, BABAR note #132 (1994).

---

[118] R. Waldi, BABAR note #172 (1994).

[119] R. Waldi, BABAR note #190 (1994).

[120] A. Gaidot, C. Yèche, M. Zito, BABAR tagging notes #3 (1996) and #7 (1997).

\* \* \*